AD-A055 647 YALE UNIV NEW HAVEN CONN DEPT OF GEOLOGY AND GEOPHYSICS F/G 8/8
FIELD STUDY OF THE MECHANICS OF THE PLACEMENT OF DREDGED MATERI--ETC(U)
APR 78 H J BOKUNIEWICZ, J GEBERT, R B GORDON DACW39-76-C-0105
UNCLASSIFIED WES-TR-D-78-7-VOL-1 NL

1 OF 2
AD
A055 647

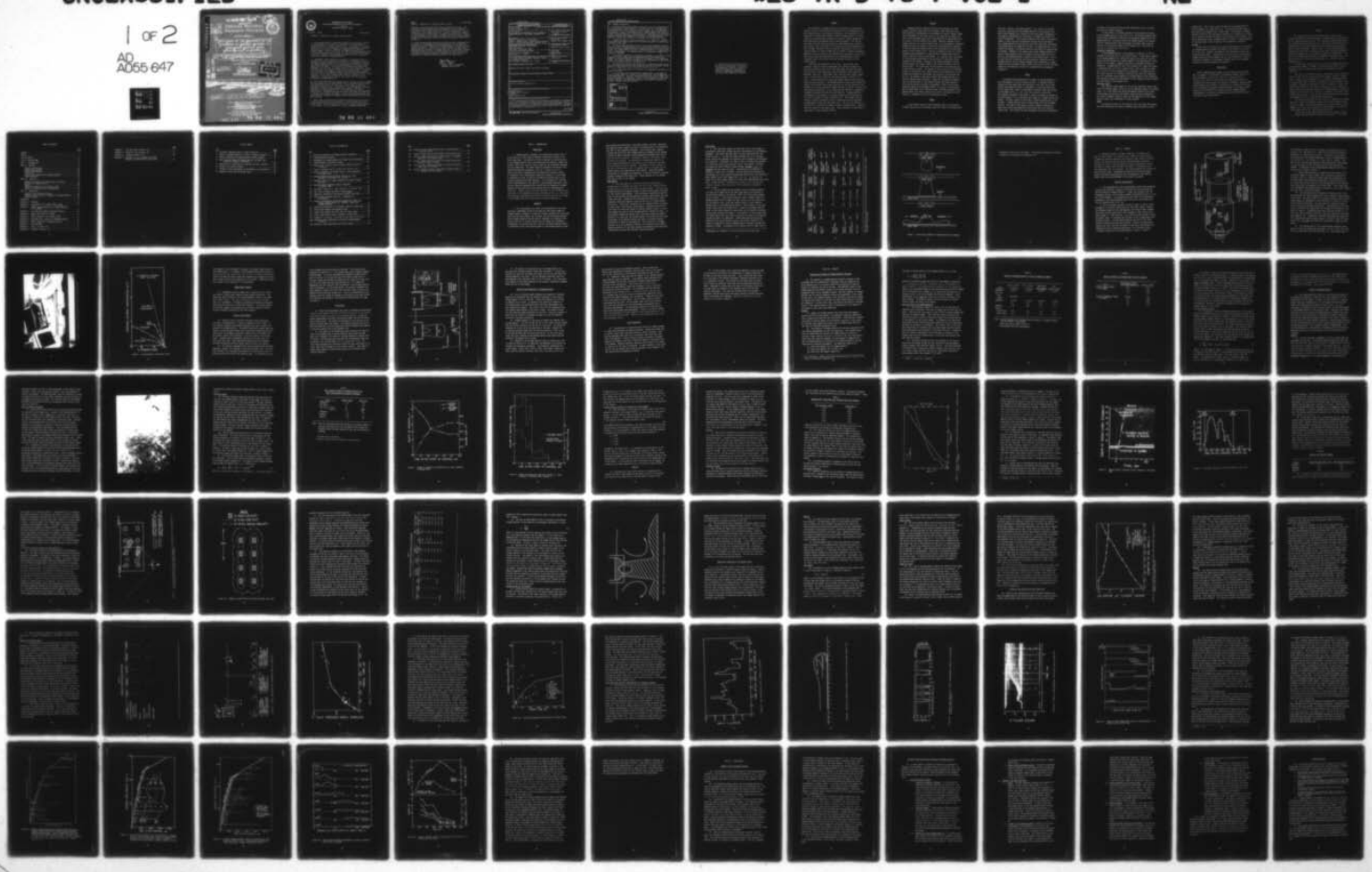

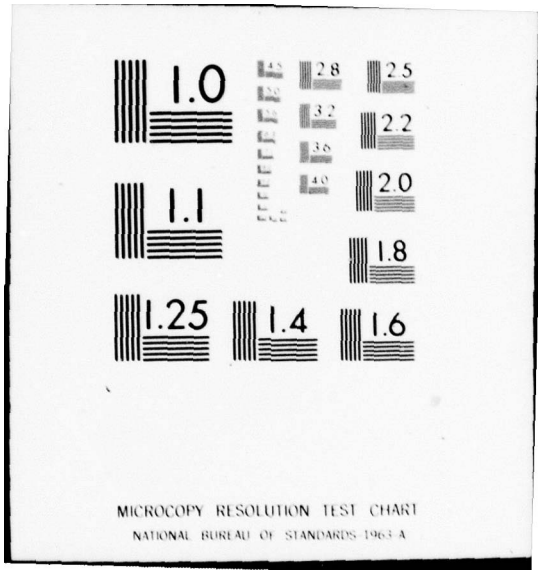
1.0
1.1
1.25
1.4
1.6
1.8
2.0
2.2
2.5
2.8
3.2
3.6
4.0
MICROCOPY RESOLUTION TEST CHART
NATIONAL BUREAU OF STANDARDS 1963-A

(12)

DREDGED MATERIAL RESEARCH PROGRAM

(7) TECHNICAL REPORT D-78-7

(6)

FIELD STUDY OF THE MECHANICS OF THE PLACEMENT OF DREDGED MATERIAL AT OPEN-WATER DISPOSAL SITES

VOLUME I: MAIN TEXT AND APPENDICES A-I

by

(10) Henry J. Bokuniewicz, Jeffrey Gebert, Robert B. Gordon, Jane L. Higgins
Peter Kaminsky, Carol C. Pilbeam, Matthew Reed, Catherine Tuttle

Department of Geology and Geophysics
Yale University
New Haven, Connecticut 06520

(12) 152 p.

(11) April 1978

(9) Final Report

Approved For Public Release; Distribution Unlimited

(18) WES (19) TR-D-78-7-VOL-I

Prepared for Office, Chief of Engineers, U. S. Army
Washington, D. C. 20314

Under (15) Contract No. DACW39-76-C-0105 Mod. P001
(DMRP Work Unit No. 1B09)

Monitored by Environmental Laboratory
U. S. Army Engineer Waterways Experiment Station
P. O. Box 631, Vicksburg, Miss. 39180

JOB

DEPARTMENT OF THE ARMY
WATERWAYS EXPERIMENT STATION, CORPS OF ENGINEERS
P. O. BOX 631
VICKSBURG, MISSISSIPPI 39180

IN REPLY REFER TO: WESYV

15 June 1978

SUBJECT: Transmittal of Technical Report D-78-7

1. The technical report transmitted herewith represents the results of an investigation to observe the mechanics of the placement of dredged material at aquatic disposal sites. This study is one of the major efforts to be accomplished under Task 1B (Movements of Dredged Material) of the Corps of Engineers' Dredged Material Research Program (DMRP). Task 1B is part of the DMRP Environmental Impacts and Criteria Development Project, which is a broad, multi-faceted investigation that includes the environmental impacts and other aspects of open-water disposal of dredged material.

2. Regardless of the location or character of a disposal site, an integral part of the problem of assessing the environmental impact of open-water disposal operations is an ability to determine the spatial and temporal distribution of the dredged material following its discharge into the water. The estuarine environment may include time-dependent currents that vary significantly in three dimensions, density stratification, and depths variable in both time and space. The material itself may be a composite ranging from slow-settling extremely fine particles to fast-falling coarse particles and may include a solute fraction. All of these and many other factors contribute to the complexity of water-quality impacts associated with the open-water discharge of dredged material.

3. This report describes the methods used to follow the path of dredged material disposed in an aquatic medium and to determine how much material reaches the bottom, in what form, and how long it takes for placement processes to go to completion. The investigation determined the nature of the controlling physical processes to develop a capability for predicting the fate of dredged material released at the water surface. Observations were made over a wide range of conditions to evaluate all relevant processes. Critical physical parameters that controlled the placement of dredged material were measured at all sites and locations.

4. These field evaluations have shown that disposal activity follows a three-step process at all localities: descent through the water column, impact with the bottom, and spread of a bottom surge generated by the impact. It was found that all of the dredged material was

confined to the zone where these three processes are active. The field observations demonstrated the dependence of the placement processes on water depth, the currents at the disposal site, and the properties of the dredged material. Accurate, controlled placement is possible under a wide range of disposal site conditions. Control of the placement can be attained through selection of dredging method, design of the containing vessel, and choice of disposal site characteristics.

5. These investigations supplied field data for the calibration and evaluation of the mathematical models developed for the DMRP for predicting what will happen to the dredged material during any given disposal operation. The results of these studies are important in determining the placement of dredged material for open-water disposal. Referenced studies as well as those reported on herein will aid in determining the optimum disposal conditions and site selection for dispersion or retention within the confines of a given site.

JOHN L. CANNON
Colonel, Corps of Engineers
Commander and Director

Unclassified

SECURITY CLASSIFICATION OF THIS PAGE (When Data Entered)

REPORT DOCUMENTATION PAGE		READ INSTRUCTIONS BEFORE COMPLETING FORM
1. REPORT NUMBER Technical Report D-78-7	2. GOVT ACCESSION NO.	3. RECIPIENT'S CATALOG NUMBER
4. TITLE (and Subtitle) FIELD STUDY OF THE MECHANICS OF THE PLACEMENT OF DREDGED MATERIAL AT OPEN-WATER DISPOSAL SITES		5. TYPE OF REPORT & PERIOD COVERED Final report (in two volumes) 6. PERFORMING ORG. REPORT NUMBER
7. AUTHOR(s) Henry J. Bokuniewicz, Jeffrey Gebert, Robert B. Gordon, Jane L. Higgins, Peter Kaminsky, Carol C. Pilbeam, Matthew Reed, Catherine Tuttle		8. CONTRACT OR GRANT NUMBER(s) Contract No. DACW-39-76-C-0105-Mod. P001
9. PERFORMING ORGANIZATION NAME AND ADDRESS Department of Geology and Geophysics Yale University New Haven, Connecticut 06520		10. PROGRAM ELEMENT, PROJECT, TASK AREA & WORK UNIT NUMBERS DMRP Work Unit No. 1B09
11. CONTROLLING OFFICE NAME AND ADDRESS Office, Chief of Engineers, U. S. Army Washington, D. C. 20314		12. REPORT DATE April 1978 13. NUMBER OF PAGES 318
14. MONITORING AGENCY NAME & ADDRESS(if different from Controlling Office) U. S. Army Engineer Waterways Experiment Station Environmental Laboratory P. O. Box 631, Vicksburg, Miss. 39180		15. SECURITY CLASS. (of this report) Unclassified 15a. DECLASSIFICATION/DOWNGRADING SCHEDULE

16. DISTRIBUTION STATEMENT (of this Report)

Approved for public release; distribution unlimited.

17. DISTRIBUTION STATEMENT (of the abstract entered in Block 20, if different from Report)

18. SUPPLEMENTARY NOTES

Volume II contains Appendices J-O.

ABSTRACT

19. KEY WORDS (Continue on reverse side if necessary and identify by block number)

Dredged material
Dredged material disposal
Dredging
Waste disposal sites

20. ABSTRACT (Continue on reverse side if necessary and identify by block number)

A field study has been made of the mechanics of the placement of dredged material at five locations, an estuarine site on the Atlantic and one on the Pacific coast, two sites in the Great Lakes, and one in the open ocean. The objective was to observe all of the processes by which dredged material is emplaced on the bottom at a disposal site.

CONT

(Continued)

DD FORM 1 JAN 73 1473 EDITION OF 1 NOV 65 IS OBSOLETE

Unclassified

SECURITY CLASSIFICATION OF THIS PAGE (When Data Entered)

20. ABSTRACT (Continued).

CONT

Instrument arrays were designed to define the transit of dredged material in time and space from the moment of its release until its final deposition. Close attention was given to accurate timing of events and to the placement of instruments close to the discharging vessel. Methods used included optical transmittance, acoustic pulse echo and water flow measurements with instrument arrays, and water sampling by continuous pumping. Additional observations were made to characterize the mechanical properties of the dredged material, its quantity, and the rate at which it is released into the receiving water.

Placement proceeds by a three-step process at all localities: descent through the water column, impact with the bottom, and spread of a bottom surge generated by the impact.

The descent phase proceeds by either or both of two processes. Cohesive blocks or clods of dredged material fall at their terminal speed and arrive at the bottom intact, whereas noncohesive dredged material falls as a jet of dense fluid. The descent speed of the jet is constant and there is a large entrainment of ambient water. The dredged material is diluted about seventyfold when descent is completed.

If the impact strength of clods reaching the bottom is large, they survive impact and form a compact mound of dredged material on the disposal site. Otherwise, they disintegrate and release their contained solids to the bottom surge. This surge is formed by deflection of the descending jet by the bottom. The jet may erode the bottom in the impact area.

The bottom surge spreads radially outwards at a decreasing speed and runs until the kinetic energy left after descent and impact is dissipated. Dredged material is deposited from the surge in the form of a flat ring.

All of the dredged material is confined to the zone where these three processes are active.

The field observations demonstrate the dependence of the placement processes on water depth, the currents at the disposal site, and the properties of the dredged material. Accurate, controlled placement is possible under a wide range of disposal site conditions. Control of the placement can be attained through selection of dredging method, design of the containing vessel, and choice of disposal site characteristics.

THE CONTENTS OF THIS REPORT ARE NOT TO BE USED FOR ADVERTISING, PUBLICATION, OR PROMOTIONAL PURPOSES. CITATION OF TRADE NAMES DOES NOT CONSTITUTE AN OFFICIAL ENDORSEMENT OR APPROVAL OF THE USE OF SUCH COMMERCIAL PRODUCTS.

SUMMARY

The placement of dredged material on the seafloor at open-water disposal sites has been observed during the course of dredging and disposal operations at a wide range of locations. The objectives of this study were to define the processes by which dredged material is transported to the bottom after release from a scow or hopper dredge and to fine what physical parameters control these processes. The results were used to define what observations or measurements must be made at any disposal site of interest to find the way in which dredged material will act when released at the site and the susceptibility of the resultant deposit to further dispersion by currents or other disturbances. Numerical values for some of the characteristic parameters of the placement process have been obtained for sites representative of those frequently used in the Great Lakes and northern estuaries of the United States.

Field data were obtained at five sites. Two of these were estuarine, those at Seattle, Washington, and Saybrook, Connecticut. Data were obtained at one site in the open ocean, the New York Bight, and two sites on the Great Lakes, one at Ashtabula, Ohio, and one at Rochester, New York. Among these study sites the water depths ranged from 15 to 67 m and currents in the receiving water, from 0 to 0.7 m/sec. A wide range of sea states and weather conditions were encountered during the studies. The dredged material being placed ranged from highly fluid riverine mud to dense marine silt, and the quantities discharged in any single operation ranged from 380 to 6120 m^3. Despite this wide range of conditions, it was found that the same basic sequence of placement processes took place at each locality. Dredged material is transported to the bottom in a narrowly defined jet of high density fluid and as blocks or clods of cohesive soil. Upon impact with the bottom, a radially expanding surge is formed that carries dispersed dredged material away from the impact area. This material deposits in the form of a ring having a radius of several hundred meters. Cohesive material remains at the impact area. These processes are described in more detail in the following sections.

Descent

Dredged material released into the receiving water as clods acquires terminal speed after fall through a small fraction of the water depth and then descends to the bottom at a nearly constant speed. The displacement of the impact point of the clods due to lateral current in the receiving water can be calculated by the same methods that are used to find the terminal fall speed. Material released in dispersed form falls in a jet of dense fluid. Any distribution of material between jet and clod descent is possible; the proportion of material in the two forms has a major effect on the structure of the resultant deposit at the disposal site. The jet is observed to fall at a nearly constant speed and entrains a large volume of ambient water during transit from the surface to the bottom. In a typical case, the volume of fluid reaching the bottom in the jet may be 70 times the volume released at the surface. Because of the large entrainment, the jet quickly attains the lateral speed of any current flowing in the receiving water. Its impact point can be predicted with good accuracy if the current is known. The descent of the jet sets up a circulation pattern in the ambient water inward toward the discharge point on the surface and outwards on the bottom; the resultant inflow around the hull of the dredge or scow helps contain the dredged material in a narrowly defined zone of descent. (There will be losses of material into the ambient water if the dredge releases additional material after the jet phase of descent is completed.) Much of the initial potential energy of the dredged material is used up in accelerating the entrained water and in setting up the circulation pattern in the ambient water; the kinetic energy of the jet in its impact with the bottom is, therefore, held to a relatively low value.

Impact

If the kinetic energy of the descending clods is sufficiently low when they arrive at the bottom, they will lodge in the impact area

and form a central, cone-shaped deposit. This results in the most effective containment of the dredged material on the disposal site both during placement and, because of the high erosion resistance of the deposit, subsequently as the deposit is exposed to currents or other disturbances. If the kinetic energy of the clods at the time of impact is high, they will disintegrate as they strike the bottom. The dredged material carried down as clods will then enter the bottom surge generated by the impact of the jet. The descending jet, as it reaches the bottom, is deflected laterally and starts to spread across the bottom. Sediment in the impact area--either dredged material or natural bottom material--may be eroded during the impact of the jet and join the dredged material in motion in the bottom surge. It will be seen from this discussion that the mechanical properties of the dredged material and the bottom sediments under conditions of impact loading are the principal factors controlling the form of the resultant deposit on the disposal site and its susceptibility to subsequent dispersion.

Surge

The bottom surge generated by the impact of the descending jet with the bottom is a form of density current. It spreads radially outward from the impact area and continues to run until its initial kinetic and potential energy is dissipated. As the surge moves out of the impact area, there is entrainment of ambient water and erosion of the bottom follows, as the surge loses energy by deposition. The greatest thickness of the surge is found to be about 15 percent of the water depth; it is a relatively thin layer as it spreads across the bottom. The upper surface of the surge is sharply defined and, as it spreads, it leaves behind a wake of turbid water from which sediment settles. The range of the surge at typical disposal operations is about 150 to 300 m and deposition starts about 100 m out from the impact area. The friction law that determines the rate of dissipation

of energy in the surge has not yet been determined; this is an important area for further research.

A large number of variables determine the quantitative aspects of the placement process at any given site. The present research shows that the most important of these are the mechanical properties of the dredged material, the speed at which the dredged material is inserted into the receiving water from the hoppers, the water depth, and the current in the receiving water at the disposal site. The effect of each may be summarized as shown below.

Mechanical properties

If the dredged material in the hoppers is cohesive, it will be released for the most part in the form of clods. If the impact strength of the dredged material is sufficiently great, the clods will survive impact with the bottom and a compact deposit of dredged material on the bottom will be formed, a deposit resistant to subsequent erosion and dispersion. Dredged material that lacks cohesion will reach the bottom in dispersed form, will form a deposit with a large surface-to-volume ratio, and will be more susceptible to dispersion. An important task for future research is to develop laboratory and field test procedures that will determine those properties of dredged material that determine its mechanical behavior during passage from the hoppers and during impact with the bottom at the disposal site.

Insertion speed

The insertion speed appears to be the most important factor determining the descent speed of the jet and the spreading speed of the bottom surge. It is one factor over which considerable control can be exercised through the design of the hopper shape and door configuration. The relation between insertion speed and the properties of the dredged material needs to be determined in future research.

Depth

The deeper the water at the disposal site, the longer the descent path and the greater the amount of ambient water entrained by the de-

scending jet. Thus, there is more dilution of the dredged material during placement on a deep water site. The resultant bottom surge is then thicker and probably has a longer range. The deposit of dredged material carried in the jet phase of descent will, therefore, be spread over a greater area when the water at the disposal site is deeper. This may be considered to be an argument against disposal of dredged material in the deep ocean, unless dispersion of the material is desired.

Current

Current over the disposal site causes displacement of the descending dredged material, whether the descent is by the fall of clods or by a fluid jet. However, the amount of the displacement can be predicted for both cases. Strong currents do not result in dispersion of dredged material during placement nor are they necessarily a cause of inaccurate placement on a designated disposal area if the placement operation is properly designed and executed.

Application

Several immediate applications of this research could be made. One, for example, is the design of containment disposal sites, i.e., sites designed to minimize the dispersal of dredged material. In such a site the run of the bottom surge would be minimized by increasing the rate at which its energy is dissipated. Several alternative methods are available. One would be to increase the friction over the bottom by increasing bottom roughness, as by placing rough stone on the site before it is used to receive dredged material. Alternatively, a pit could be designed that would confine the run of the surge to any desired limit.

PREFACE

This report describes work performed during a field study to observe the mechanics of the placement of dredged material on the bottom at five specified disposal sites. This study was performed under Work Unit 1B09 entitled "An Investigation of the Physical Characteristics of Dredged Material and the Effects of Dispersion Behavior During Open-Water Disposal Operations," between the U. S. Army Engineer Waterways Experiment Station (WES), Vicksburg, Mississippi, and the Department of Geology and Geophysics, Yale University, New Haven, Connecticut. The work was performed under Contract No. DACW39-76-C-0105-Mod. P001. Volume I contains the main text and Appendices A-I. Volume II contains Appendices J-O.

The study was conducted as part of the Corps Dredged Material Research Program (DMRP). The DMRP is sponsored by the Office, Chief of Engineers, and is assigned to WES under the Environmental Laboratory (EL).

This report was written by Henry J. Bokuniewicz, now at State University of New York at Stony Brook, Jeffrey Gebert, Robert B. Gordon, Jane L. Higgins, Peter Kaminsky, Carol C. Pilbeam, and Matthew Reed, all of the Department of Geology and Geophysics, Yale University. Measurements in Appendix M were made by Susan P. Giagnocavo. Many of the figures were drafted by Gail Mercer of New Haven, and the typing was done by Wanda Stark and Peggy Keating, of the Department of Geology and Geophysics, Yale University. Tom Ford, of Branford, Connecticut, read current meter records. Tidal data were obtained from the Tides Branch, Oceanographic Division of the National Ocean Survey.

The study was performed as part of Task 1b, "Movements of Dredged Material," in the Environmental Impacts and Criteria Development Project of the DMRP. The study was managed by Dr. Robert Engler, Project Manager, EL, and Mr. Barry Holliday, Contract Manager, EL, under the direct supervision of Dr. John Harrison, Chief, EL.

The Director of WES during the course of this contract was COL J. L. Cannon, and the Technical Director of WES was Mr. F. R. Brown.

TABLE OF CONTENTS

LIST OF TABLES

LIST OF ILLUSTRATIONS

PART I: INTRODUCTION

Objectives

1. Dredged material released at an open-water disposal site is at the mercy of a wide range of physical forces while moving to its final repository. The objective of this study was to follow the path of the dredged material and to determine how much material reaches the bottom in what form, and how long it takes for the placement processes to go to completion. The study sought to determine the nature of the controlling physical processes to develop a capability for predicting the fate of dredged material released at the water surface. To accomplish this, observations needed to be made over a wide range of conditions so that it might be confidently asserted that all the relevant processes have been observed. It was necessary to identify, from an understanding of the physics of the placement processes, those critical physical parameters that controlled the placement of dredged material at any given site and to measure these at representative localities. [These results supplied field data for the calibration and evaluation of the mathematical models developed at the U. S. Army Engineer Waterways Experiment Station (WES) for predicting what will happen to the dredged material during any given disposal operation.]

Approach

2. This investigation was based on data obtained in the field. Laboratory experiments could not be made with the large volumes of dredged material released in a typical disposal operation nor could they duplicate the water depths, the currents, and the interaction between moving dredged material and the natural sediments at a disposal site. Scaling laws for all these processes are not known with confidence. Consequently, the events that occur during a disposal operation should be identified in the field before models of the dredged material place-

ment process are constructed. Once these events are known, laboratory and numerical model studies can become a valuable means of investigating the steps of the placement processes. Field studies must, however, overcome the difficulty that dredged material placement occurs through a series of rapid, transient, three-dimensional processes that may be quite difficult to observe. Instruments capable of continuous, rapid recording are required. The temptation to concentrate attention on easily measured phenomena at the expense of more important, but more obscure processes, must be avoided. The amount of effort devoted to any one of the processes active in dredged material placement must be proportioned to the importance of that process. Even with optimum utilization of instruments and observers, it may be difficult to achieve adequate coverage of the study area. These problems will be evident from time to time in this report.

Measurements

3. The requirement for rapid and continuous observation of dredged material placement has been best met in this study by optical transmittance and acoustic and water flow measurements. Optical transmittance detects the sediment content of water with accuracy sufficient for this study's requirements. Both continuous transmittance observations at one location and transmittance profiles made through the water column were used. Comparison with concentration measured in simultaneously taken water samples assured reliability of transmissometer calibration. Since small concentrations of dredged material dispersed in water cause a sufficiently great acoustic impedance contrast with clear water to return good echos of 200-kHz acoustic pulses, a survey echo sounder was used to track dredged material through the water. If the boundary between the ambient water and water containing dredged material is a sharp one, the sounder permits flow velocities and layer thicknesses to be measured without the need to calibrate acoustic reflectance in terms of concentration. Flow velocities of dredged material can also be measured directly with standard current meters. Whenever possible all available methods of measurement have been used simultaneously during each disposal operation studied.

Field sites

4. The localities chosen for field work cover a wide range of hydrographic conditions, dredged material characteristics, and dredging equipment. The study sites and their principal characteristics are listed in Table 1. The New York Bight disposal site is in the open ocean, Seattle and Saybrook are estuarine, while Ashtabula and Rochester are lacustrine. (New Haven is listed in Table 1 because data obtained in an earlier study at this site are used in this report.) Studies were made with three different hopper dredges (Hoffman, Lyman, and Essayons) and four types of scows. (Examination of a pipeline discharge at a James River, Virginia, site was planned but dredging was terminated just as the requisite background observations were completed.) Water depths at the sites ranged from 18 to 67 m. At Saybrook the speed of the tidal stream reached 0.7 m/sec while measurements were being made. Dredged material included dense, cohesive silt-clay dug with clamshell buckets, sand, and dilute silt suspensions generated by hopper dredges.

5. For all localities and sediment types the dredged material was found to be deposited by the same three steps first observed at the New Haven disposal site (Gordon, 1974)* and illustrated schematically in Figure 1. Upon release from the scow or hopper dredge, the dredged material falls through the water column as a well-defined jet of high density fluid, which may contain blocks of solid material. Ambient water is entrained during descent. After transit of the water column, impact with the bottom occurs. Some of the dredged material comes to rest during impact and some enters the horizontally spreading bottom surge formed by the impact. This material is carried away from the impact point until the kinetic energy of the surge is sufficiently reduced to permit its deposition. Since these same processes were observed at all the localities studied, the results section of this report is organized to follow dredged material placement through this sequence of steps. A synthesis of the results from all study sites is

---

*References are included in a list at the end of the main text.

Table 1

Principal Characteristics of Study Localities

Site Name	Hydrographic Characteristic	Water Depth	Bottom Currents	Dredged Material	Dredge Type	Hopper or Scow Capacity
Ashtabula (Lake Erie)	Lake	15-18 m	0-0.20 m/sec	Cohesionless sandy silt	Hopper dredge (Hoffman)	690 m^3
New York Bight	Open Ocean	26 m	0.05-0.25 m/sec	Organic marine silt	Hopper dredge (Essayons)	6120 m^3
					Bucket dredge and scow	3060 m^3
Saybrook (Long Island Sound)	Estuary	52 m	0.2-0.7 m/sec	Organic marine silt	Clamshell bucket Bottom-dump scow	1150 m^3
Seattle (Duamish River)	Estuary	67 m	0-0.2 m/sec	Oily sandy-silt	Clamshell bucket - scow	380 or 535 m^3
Rochester (Lake Ontario)	Lake	17-46 m	0-0.2 m/sec	River silt	Hopper dredge (Lyman)	690 m^3
New Haven*	Estuary	18 m	0.1-0.4 m/sec	Organic marine silt-clay	Clamshell bucket scow	1530 m^3

* New Haven was not a field site during this study but data collected in an earlier study are used in this report.

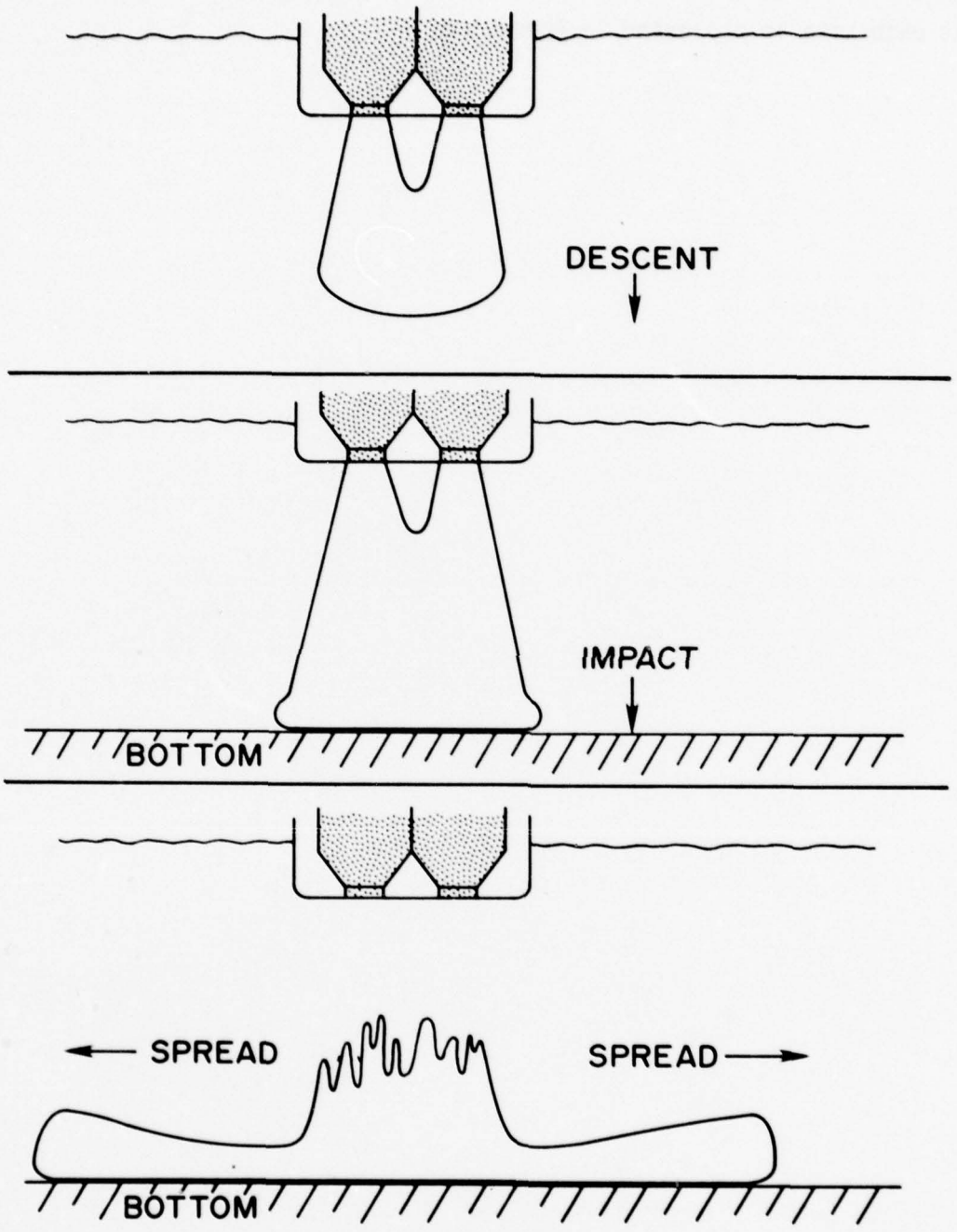

Figure 1. Three-step schematic of dredged material placement.

presented in the text of the report. The detailed information collected at each site is presented in Appendices J-O.

PART II: METHODS

6. Wherever possible, standard, commercial instruments were used in these studies. For the most part, simplicity and reliability in operation were more important considerations than technical sophistication. One exception was the optical transmissometer; operating successfully within a disposal operation required mechanical strength not found in commercially available instruments. Simultaneous pressure measurement was also required. The transmissometers were especially built for this study. Throughout the research the principal experimental difficulty encountered was with the adequacy of the sampling rather than with the performance of individual instruments.

Optical Transmittance

7. The requirements of the transmissometer design were mechanical rigidity and sufficient strength to withstand forces encountered during the release of dredged material. It was also necessary that the instruments operate at much higher sediment concentrations than are usual for optical methods. To accommodate the wide range of concentrations encountered, the transmissometers were built with a path length that could be adjusted from 10 to 1 cm.

8. One of the most important sources of error in optical transmissometers is variable light output from the light source. Because the radiation output of the lamp depends on the lamp filiment temperature raised to the fourth power, small changes in lamp current cause large changes in light intensity. This difficulty was avoided by using two optical paths, a reference path through air and a measurement path through the water. The instrument measured the ratio of the light intensity transmitted along the two paths. Pressure and temperature sensors were built into the instrument so that both transmittance and temperature could be measured continuously as a function of depth. A schematic diagram of the transmissometer is shown in Figure 2.

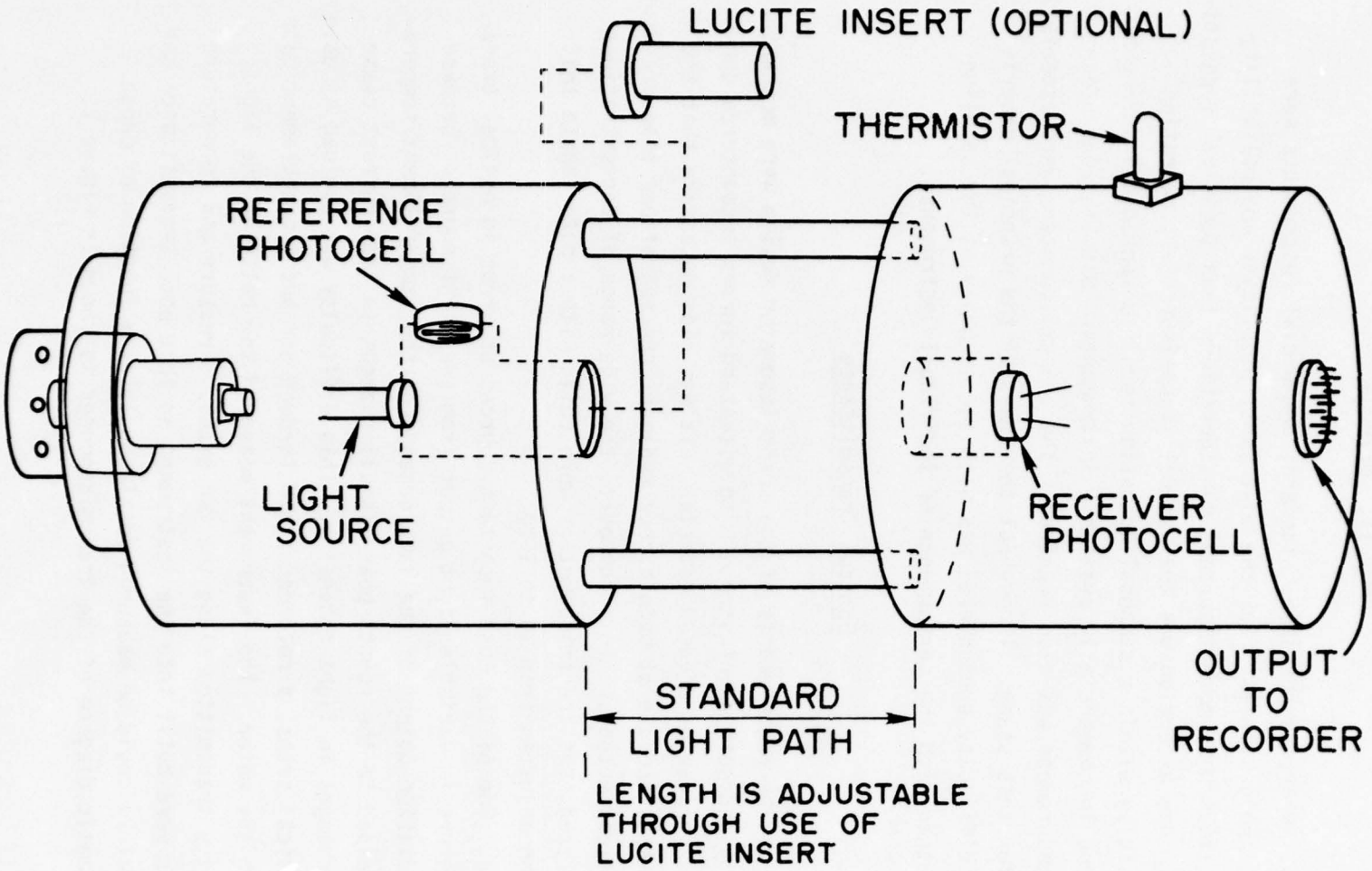

Figure 2. Transmissometer schematic.

The electronic system for this instrument was designed and built by Lutronix, Inc. (New Haven, CT). Both digital output and voltage to operate an X-Y recorder were provided. To protect the instrument from impact with the dredging equipment, blocks of dredged material, or the seafloor, it was housed in a large, plastic cylinder. The ends of this cylinder were open and large holes were drilled through its walls so that the flow of water past the light beam was not impeded. A photograph of the transmissometer removed from its protective case is shown in Figure 3.

9. Light attenuation due to scattering and absorption is described by Lambert's law (Williams, 1973), according to which the intensity ratio for a given path length should be proportional to the logarithm of the attenuation coefficient. When particle sizes are small, difficulties can arise from the dependence of the attenuation coefficient on wavelength of the light used. It was found that, for the sediments and concentrations encountered in this study, Lambert's law holds with a white light source.

10. The instruments were calibrated by immersing them in suspensions made with known concentrations of the sediment to be measured in the field. The water content of a sample of sediment taken from the dredge hopper was determined so that the weight of solids in a known volume could be determined. This was added to a measured volume of water to make the calibration suspension. Transmittance was then measured as a function of concentration to produce the calibration curves shown in Figure 4. Calibrations were made with path lengths of 2, 7, and 10 cm; the calibration curve for a 1-cm path length was calculated from Lambert's law. Comparison of sediment concentrations determined from transmittance and from water samples collected in the field were found to be in agreement to within the limitations of sampling sufficiency.

11. The response time of the transmissometer depended on the speed of fluid flow through the instrument. At all of the field sites this was sufficiently fast that there was only a few seconds delay in

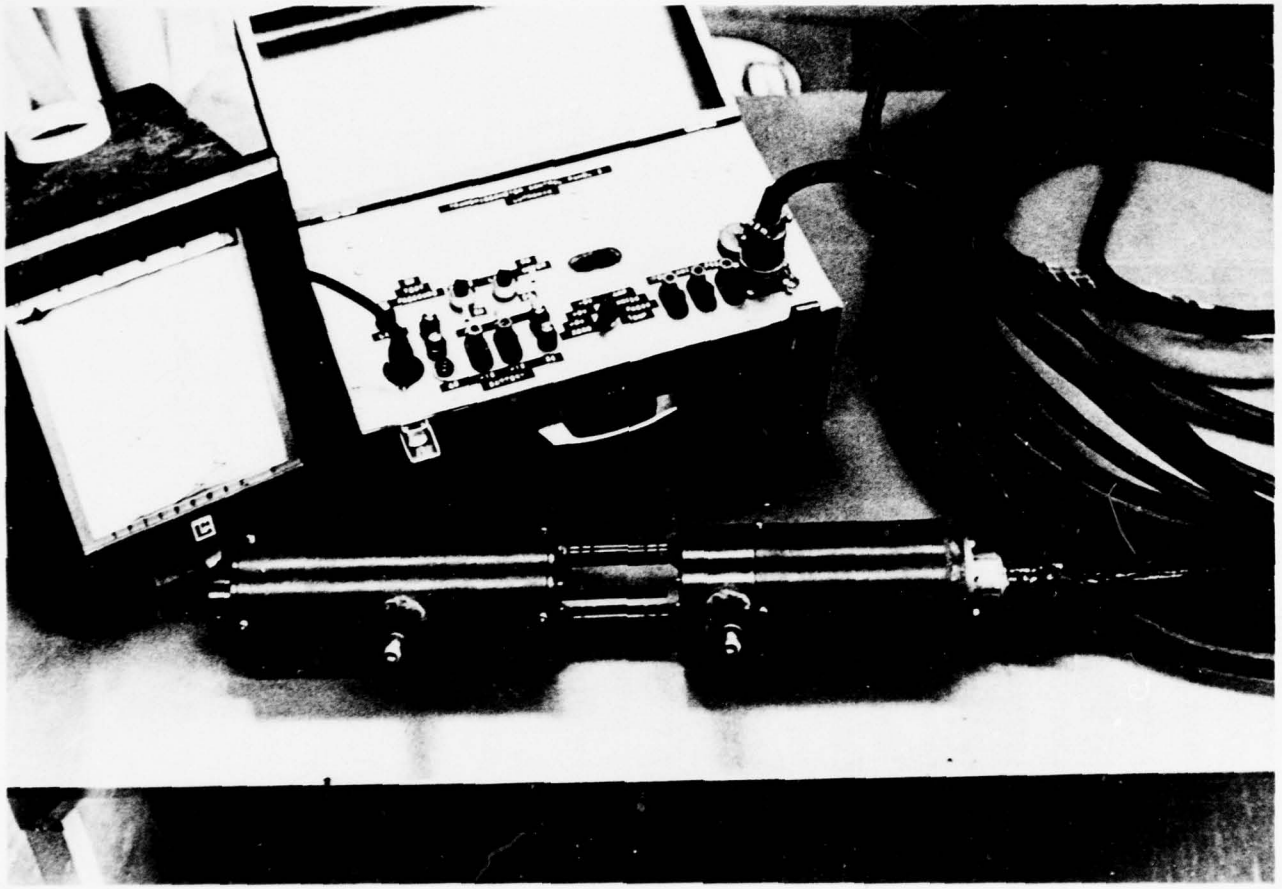

Figure 3. Photograph of transmissometer with panel box and recorder.

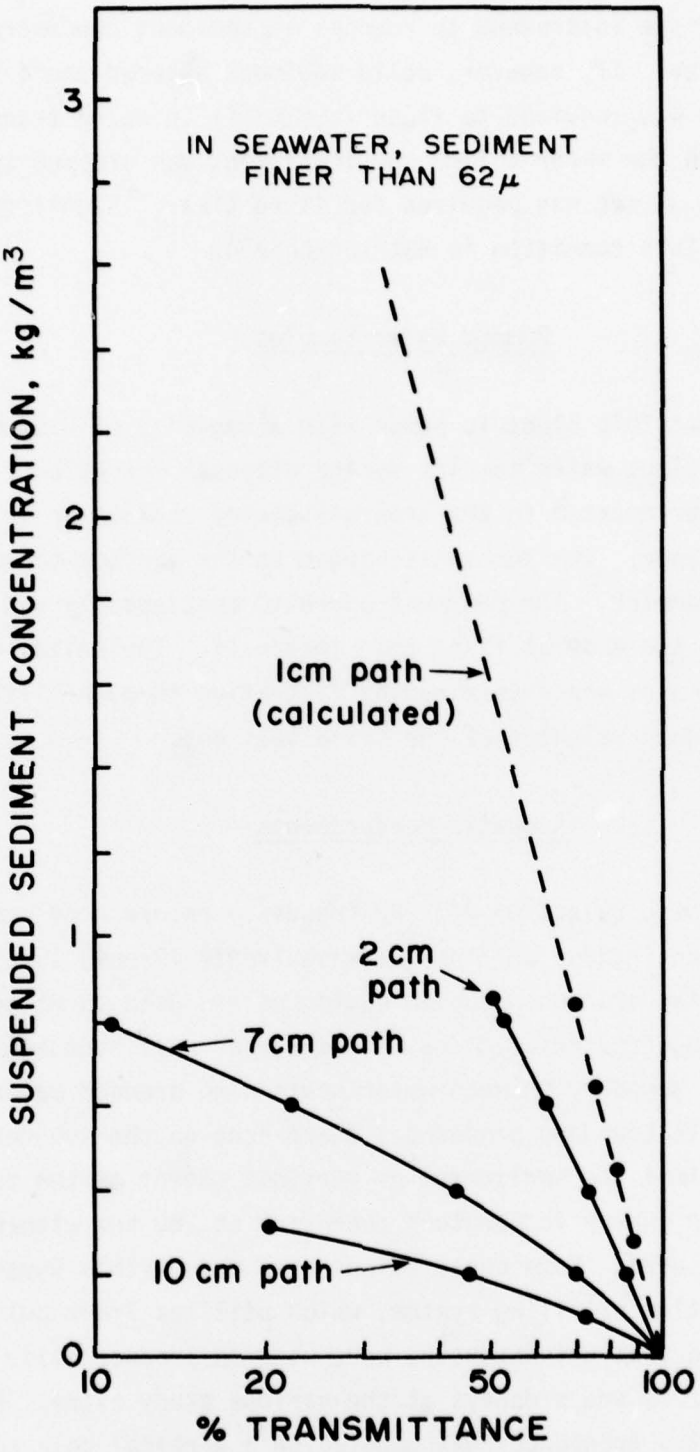

Figure 4. Transmissometer calibration curves.

the response of the instrument to changes in sediment concentration in the ambient water. If, however, solid sediment entered the transmissometer, some time was required to flush it out; if in doing transmittance profiles through the water column the instrument was dropped to the bottom, as much as 30 sec was required for it to clear. Significant errors may be made if this condition is not recognized.

Pumped Water Samples

12. Submersible electric pumps with a capacity of 0.01 m^3/min were used to collect water samples during disposal operations. The pumps were either mounted in the transmissometer casings or on frames set on the seafloor. The pumps discharged to the surface through hose of 2 cm diameter. The pump was operated continuously and samples were taken from the hose at fixed time intervals. The solids content of the water samples was determined by filtration through millipore filters followed by weighing of the dried sediment.

Acoustic Measurements

13. Acoustic pulses of 200-kHz frequency return good echos from small concentrations of fine-grain sediments (Proni, 1976). In this project, standard echo sounder equipment was used to detect the presence of dredged material. The method worked well because there was usually a sharp boundary between water containing dredged material and clear water; this boundary produced a sharp echo on the sounder that was used to delimit the horizontal or vertical extent of the turbid water. Raytheon survey fathometers operating at 200 kHz with a 8^o cone angle were used. Some observations were made with a Raytheon RTT-1000 reflection profiling system, which utilizes 7-kHz pulses.

14. The acoustic transducers were used to produce beams directed downwards, upwards, and sideways at the various study sites. For sideways scanning, the transducer was mounted on a vertical pole set in a bearing plate on the side of the observing boat. By rotating the pole,

a scan through the desired angle was obtained. This system proved practical for depths to 5 m. Two systems were used to produce upwards directed beams. In one the transducer was mounted in gimbals which were in turn set on a tripod that could be placed on the seafloor. The echo sounder was modified to permit use of a cable 50 m long; this was led to the observing boat some distance off. The dredge was maneuvered over the tripod so that the descent of the dredged material could be observed. In the second design, the acoustic transducer was again mounted in gimbals but this time the outer gimbal ring was suspended directly below the dredge hull. With this configuration it was necessary that the dredge be anchored or held dead in the water before the transducer was deployed. Both mounting configurations are shown in Figure 5.

Fluid Flow

15. Fluid flow measurements were made to determine the background current at the disposal sites and to record the velocity of the bottom surge and the speed of descent of the dredged material. Background current measurements were made with Braincon model 381 and 1381 histogram current meters. The meters were mounted on taut moorings at the desired distance above the bottom. The sampling interval was 20 min. After the data were read out, progressive vector diagrams were prepared to show the current flow at the disposal site.

16. Two types of flow meters were used to measure the speed of flow in the bottom surge, a General Oceanics model 2010 wand-type meter and a standard Price meter of the type designed to measure flow in rivers. The wand-type meter recorded the instantaneous speed and direction of the current every 15 sec on photographic film. The Price meter produced four electrical pulses for each revolution of its rotor; these were recorded on a strip chart recorder. Both types of meters were attached to heavy blocks placed on the bottom at the desired locations.

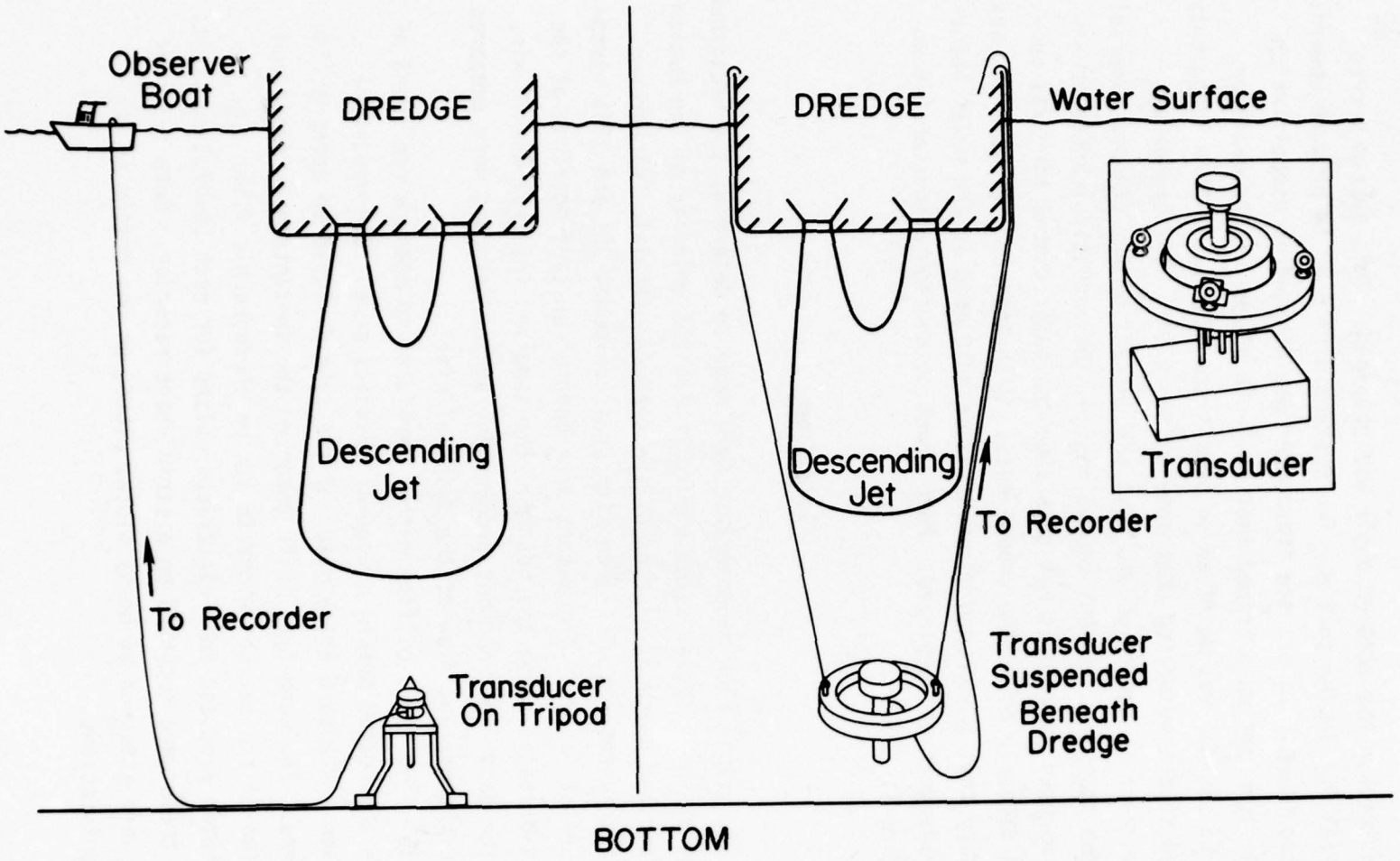

Figure 5. Methods used to deploy upward-looking, 200-kHz acoustic transducers.

17. The speed of the descending jet of dredged material was measured with a General Oceanics model 2031 flow meter. A strip chart recorder was used with the model 2031 meter to print out the electrical pulses produced by its rotor. The low threshold propeller which was used measures flow velocities from 0.03 to 1.00 m/sec. This flow meter was attached to the gimbal mounting of the acoustic transducer suspended below the hull of the dredge.

Quantity and Properties of Dredged Material

18. At all locations except Rochester the quantity of dredged material was determined from the reported dimensions of the scows or dredge hoppers in use at the site. These were observed to be filled to capacity in all cases. At Rochester the quantity of material in the dredge hoppers was determined both from draft measurements and from sampling the hoppers. The draft of the ship was determined from the standard gage mounted on the ship's bridge. The pressure sensor for this gage was mounted amidships on the keel. Since only changes in draft were of interest, no attempt was made to verify the absolute accuracy of the gage calibration.

19. Dredged material in the scows or hoppers was sampled with a syringe sampler. A 50-cm^3 syringe cut off at the closed end was mounted with the piston pointing up on the end of a long pole. The piston was withdrawn by a wire led to the upper end of the pole. Because the syringe was mounted upside down, no material entered it until it was at the desired depth and the piston was pulled. At the sites where scows were used, samples of the dredged material were taken from the surface of the deposit with a scoop.

20. Samples of the dredged material taken at Seattle were sent to Haley and Aldrich Inc. in Cambridge, Massachusetts, for analysis by standard soil mechanics procedures. The parameters determined were percent water, liquid limit, plastic limit, unit weight, organic content, specific gravity of solids, void ratio, and the particle-size

distribution by sieve and hydrometer analysis. Water content and density were determined for samples from the other sites in the laboratory at Yale University by the procedures described by Lambe (1951).

21. Mechanical tests were done on samples of the dredged material taken from the scows at Saybrook. Consolidation tests were made with a consolidometer fitted with a precision slidewire potentiometer to indicate piston displacement. During the first 10 to 15 min of the tests the potentiometer output was recorded so that a continuous consolidation curve was obtained. The settlement was then measured periodically over the next 24 hr. A drained triaxial test was done in a standard test cell and a series of unconfined compression tests, some with the sample submerged, was carried out. These were done over a very wide range of strain rates. For the slower rates an Instron testing machine was used. For the higher rates, force was measured with a WES soil pressure cell and displacement was measured with a slidewire potentiometer. The transducer outputs were displayed on a dual trace oscilloscope and photographed. Finally, a series of impact tests was conducted by allowing samples of the dredged material to fall onto a WES soil pressure cell. Again, an oscilloscope was used to display the impact forces.

Field Procedures

22. The positions of observing points around the hopper dredges or scows were determined by range and bearing. Ranges were taken with an optical range finder and were accurate to about 5 percent. Hand-bearing compasses were used to fix directions; the errors were less than a few degrees. Timing of events during a discharge of dredged material was based on the time at which the hopper or scow doors were first opened. Wherever possible, observers were placed on the dredge or scow to call the time of discharge. At some locations it was necessary to rely on signals given from the tow boat or the dredge to fix the time at which discharge was started.

23. At the Saybrook site a detailed bathymetric survey was made of the disposal area before the commencement of dredging operations. A Raytheon survey echo sounder was used. Tidal corrections were based on a tide gage at the Saybrook Breakwater Lighthouse operated by the U. S. Geological Survey. The position of the survey boat was taken from crosses of theodolite lines made from two observing stations on shore. Bathymetric surveys were also made by the Seattle District of the Army Corps of Engineers of the disposal area in Elliott Bay, Seattle, Washington. This area was surveyed before the disposal operation, and the same tracks were again surveyed on three occasions after the disposal was completed. Additional information on field methods can be found in Appendix I.

PART III: RESULTS

Quantity and Energy of Dredged Material Released

24. The quantity of dredged material actually released in each experiment had to be determined if subsequent loss by dispersion was to be detected and if an accurate record of the quantity of material placed on a disposal site was to be kept. The potential energy of the dredged material just before release is the energy available to drive subsequent steps of the placement process. Both the quantity of dredged material and its initial potential energy were determined in this study. In most cases, the dredged sediment is not uniformly distributed through the hoppers that contain it and does not have uniform density or mechanical properties. At most field sites, the density and physical characteristics of the dredged material, and its distribution in the hoppers of the dredge or scow, were also determined.

Methods

25. Samples of dredged material were taken from the hoppers, usually with the syringe sampler, for subsequent laboratory determination of density and particle-size distribution. Where possible, samples were taken at several depths and at different locations in each vessel. At Saybrook large samples were taken from the dredge bucket and from the scow for laboratory mechanical tests.

26. The quantity of dredged material in scows was determined from the density measurements and the scow dimensions. The standard procedure for determining the quantity of dredged material in Corps of Engineers hopper dredges involved a calculation from draft measurements. Draft data were taken at Rochester for the purpose of comparing the mass of dredged material calculated by the standard method to the mass determined by sampling the hoppers. The quantities required are

d_1, draft with hoppers full of dredged material,

d_2, draft with hoppers full of water, and

d_3, draft with the hoppers pumped dry.*

---

* For convenience, symbols and unusual abbreviations are listed and defined in the Notation (Appendix A).

The mass of solids present in the dredged material, m_s, is then

$$m_s = M \frac{\rho_w \rho_s}{\rho_s - \rho_w} \frac{d_1 - d_2}{d_2 - d_3} \quad (1)$$

where M is the mass of water that will fill the hoppers to overflow, ρ_s is the density of solids ($\sim$ 2.6 Mg/m^3), and ρ_w is the density of water (1 Mg/m^3).* In the derivation of Equation 1 it is assumed that there is no significant change in the cross-sectional area of the dredge hull at the water line at depths d_1, d_2, and d_3 and that there is no change in ship's trim as the hoppers are filled and emptied. Draft measurements on the Lyman were taken from the draft indicator on the ship's bridge. The pressure sensor for this indicator is located directly under the center of the hopper.

Mass and density of dredged material

27. The quantities reported in Table 2 are the total mass of sediment solids contained in the scow or hopper and the total mass of water. There was much less water in scows filled by bucket dredges than there was in hopper dredges. These data were used to calculate the ratio of the mass of solids to the mass of water and the mean density of the material in the scow or hopper. At Rochester, the quantities calculated from the draft measurements agreed well with the quantities estimated by sampling in the hoppers. The original ship's draft data were unavailable for Ashtabula but calculated hopper burdens based on draft measurements were supplied by the Buffalo District. Comparison with this study's measurements of the thickness of sediment in the hoppers shows that the reported mass of solids was much greater than that actually present.

28. The density gradient within the sediment in the scows at Seattle and the hopper at New York was calculated from measurements taken on samples from different depths, Table 3. The scows contained a surficial layer of high water content sediment which was less than 0.6 m thick; aside from this there was no significant variation of water content within the sediment in the scows.

---

* 1 Mg/m^3 = 1 g/cm^3; Mg = megagram.

Table 2

Amount of Dredged Material in Scow or Dredge or Hoppers

Site	Mass of Solids x 10^5 kg	Mass of Water x 10^5 kg	Mass Ratio Solids/Water	Mean Density, Mg/m^3
Ashtabula	(2.9)*	(5.9)*	(0.5)*	(1.3)*
New York				
Scow	(No data)			
Hopper				
Rochester	(2.4)**	(6.1)**	(0.4)**	(1.2)**
	2.1	6.1	0.3	1.2
Saybrook	5.6	9.4	0.6	1.3
Seattle				
535-m^3 scow	4.9	3.7	1.3	1.6
380-m^3 scow	3.5	2.6	1.3	1.6

Note: Values reported are calculated from the density of sediment samples and the volume of the hoppers.

*Data supplied by Buffalo District.

**Calculated from draft measurements.

Table 3

Density Gradient of Dredged Material Within Hoppers

Site	Depth below surface of dredged material, m	Density, Mg/m^3
Seattle (Manson scows, ∿ 3 m deep)	0.6	1.47
	1.8	1.47
	2.7	1.68
New York (Essayons, hopper, ∿ 9 m deep)	surface	1.19
	3.7	1.48
	7.0	1.50
	7.9	1.40

29. Numerous samples were needed to determine the distribution of dredged material in the hopper dredges. In instances where this sampling was not done, a useful approximation of the distribution of dredged material in the hoppers was made as follows. Sampling in the hoppers of the Lyman and Hoffman showed a layer of sediment with a density of about 1.7 Mg/m^3 to be overlain by a layer of water with a high concentration of suspended sediment (density $\sim$ 1.1 Mg/m^3). The transition between these two layers is a gradual one but, as a first approximation, all the material was assumed to be in two distinct layers. The thickness of these two layers was then calculated knowing the geometry of the hoppers and the mean density of the dredged material in the hoppers (Appendix B). As discussed earlier, the mean density may be calculated from the draft measurements. Appendix C discusses the density and distribution of dredged material in the hoppers.

Initial potential energy

30. The descent, impact, and bottom surge phases of the dredged material placement process are all driven by the potential energy of the dredged material at the moment of release. The initial potential energy of the dredged sediment relative to its energy when it is at rest on the bottom was calculated by subdividing the volume of material in the hoppers into several horizontal layers. For convenience the top surface of one of the layers was taken to be at lake level. The potential energy of each layer is then calculated as the work that would be done in raising the center of mass of the layer from the lake floor to its position in the hopper. The details of this calculation and an example are presented in Appendix D. The total potential energy of the dredged material at the moment of release, v_o, was found to be

$$v_o = \sum_{i=1}^{n} g \left[M_i Z_i - V_i \rho_w \min (Z_i, Z_o)\right] \qquad (2)$$

where n is the numer of layers, g is the acceleration due gravity, M_i is the mass of the $i^{\underline{th}}$ layer, Z_i is the height of the center of mass of the $i^{\underline{th}}$ layer above the lake floor, V_i is the volume of the $i^{\underline{th}}$ layer, ρ_w is the density of water, and Z_o is the water depth; min (Z_i, Z_o) is either Z_i or Z_o whichever is smaller, i.e. min (Z_i, Z_o) =

Z_i, if $Z_i < Z_o$, and min $(Z_i, Z_o) = Z_o$ if $Z_o < Z_i$. The calculation of v_o therefore required a knowledge of the draft of the loaded vessel, the dimensions of the hoppers, the density distribution of material in the hoppers, and the water depth at the discharge point. For the dredging operation at Rochester, v_o was typically 30 MJ.

Release of Dredged Material

31. How dredged material enters the receiving water depends on the mechanical properties of the material in the hoppers and on the configuration of the hopper, its doors, and the rate of door opening. Several important characteristics of the dredged material placement process are determined by the nature of the release: the insertion speed, the duration of the insertion period, and the form assumed by the dredged material in the receiving water. Release to the receiving water is the only aspect of dredged material placement over which direct control can be exercised in conventional disposal operations. This may be accomplished through the design of the scows or hopper or through control of their method of operation. Optimum design and operation can be attained when the relation between release characteristics and subsequent steps in the placement process is established. Controlled alterations in the condition of dredged material release were made when possible at the field study sites to better define these processes.

Methods

32. The size and mode of operation of scow or hopper doors was determined at each site. The average insertion speed was found from the size of the door opening, the quantity of dredged material, and the time required to complete discharge of the dredged material. The most detailed study was made at Rochester. The rate of door opening was measured by timing a telltale that was visible on the deck of the dredge. The open area as a function of time was then calculated from the door dimensions (Appendix B). The rate of emptying of the hoppers was

measured by taking a series of timed photographs of the hoppers during discharge. Water level was measured against a scale photographed in place in the hoppers. The measured water level was converted to volume of material with the aid of the hopper calibration curves available for the Lyman from builders drawings. The insertion speed of the dredged material was then found by dividing the emptying rate (m^3/sec) by the open door area (m^2).

Form of material released

33. During the release process soil and water are forced through the open area of the hopper door. Release of the dredged material in the form of cohesive blocks (clods) will be favored if the soil in the hoppers is cohesive, the door opening large, the water flow small, and the insertion speed small compared to the descent speed. Although study of clod formation was not an explicit part of this project, evidence of the presence or absence of clods was obtained from the acoustic and photographic measurements. Clods of dredged material in free fall through the water column were observed at Seattle with an echo sounder looking downwards alongside the scow. At Ashtabula and Rochester, upward- and sideward-looking echo sounders did not detect clods. No close-in acoustic data were obtained at other sites. Hence, it was concluded that clods were formed in the discharge at Seattle but were not formed during discharge from either of the hopper dredges.

34. Additional evidence on the formation of clods during the release of dredged material was obtained from bottom photographs taken at the New Haven disposal site where silt-clay sediment from maintenance dredging was released from scows. Clods of dredged material were found on the bottom when the disposal site was photographed 2 months after completion of disposal, as shown in Figure 6. The available evidence shows that formation of clods is favored when cohesive soil is bucket-dredged and subsequently released from scows with a low insertion speed. In the case of the hopper dredges, the extensive reworking of the soil during dredging and the large amount of free water released with the soil during discharge hinder the formation of clods;

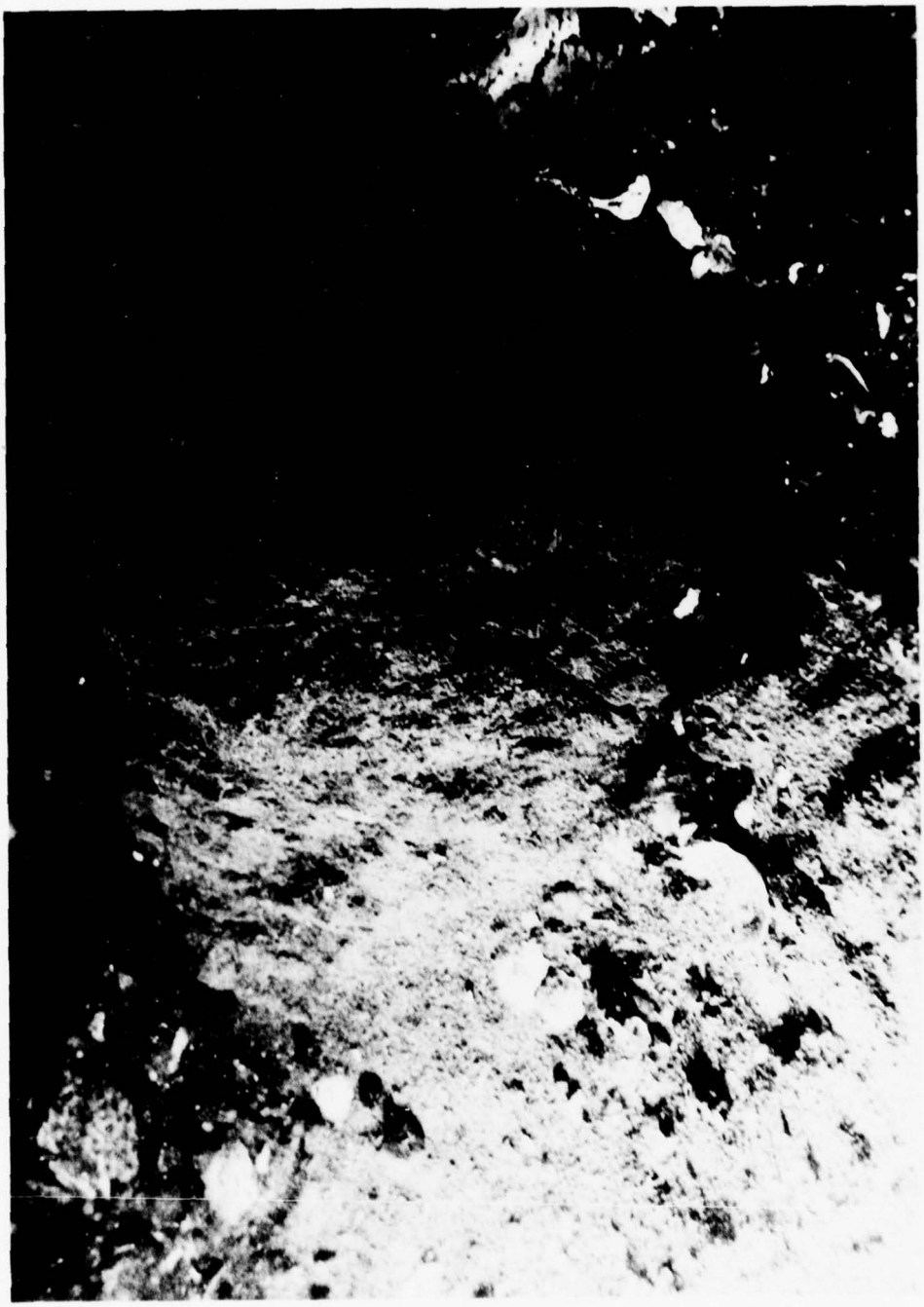

Figure 6. Clods of dredged material at New Haven disposal site.

the material released from hopper dredges behaves like a dense, viscous fluid.

Insertion speed

35. The mean insertion speed and the mean time required to release all the dredged material contained in the hoppers or scows are recorded in Table 4 for all of the sites studied. The mean insertion speeds differ by more than a factor of 10 between the different sites. This speed was determined by the ratio of door area to hopper area, the rate of door opening, the water content and plasticity (or viscosity) of the soil, and the pressure head over the door orifice. At Seattle the mechanical properties of the dredged material were similar to those at Saybrook but the rate of door opening was very slow. At Saybrook the door opening was almost instantaneous and the ratio of door to hopper area was smaller than at Seattle, resulting in a very high mean insertion speed. The mean insertion speeds attained by the hopper dredges are low because of slow door opening and low mean density of material in the hoppers.

36. The most detailed determination of the insertion speed was made at Rochester. The liquid surface level in the hoppers and the volume discharged as a function of time are shown in Figure 7. Zero time marks the start of opening of the first pair of hopper doors. Two other pairs of doors were opened within a few seconds for this experiment. The volume of material discharged per unit time is shown in Figure 8. The area of each door opening increases at a rate of about 0.2 m^2/sec until the maximum opening of 1.3 m^2 is reached (Appendix B). The insertion speed calculated from these data is shown in Figure 8.

37. The insertion speed drops as the hydraulic head in the hoppers decreases. This relation may be conveniently expressed in terms of an energy balance (Appendix E). The speed at which dredged material flows through the hopper doors, v_4, is found to be

$$v_4 = \left[2g\left(h - \frac{\rho_w}{\rho} d\right) - \frac{2\varepsilon}{\rho}\right]\left[1 - (A_4/A_o)^2\right]^{1/2} \quad (3)$$

where h is the height of material in the hopper, ρ is the bulk density of

Table 4

Mean Insertion Speed of Dredged Material and Mean Time Required to Complete Discharge

Site		Speed, m/sec	Time, sec
Ashtabula*		1.2	38
New Haven		3	20
New York**	(scow)	~2	~10
	(hopper)	≤1	~100
Rochester		1.2	45
Saybrook		6.5	4
Seattle		0.4	60

Note: Data are calculated from time required to discharge hopper or scow and the mean area of the discharge orifice except for Rochester where the mean speed over the time of discharge is reported.

*Assumed same as Rochester.

**Values for New York are estimates; no data taken.

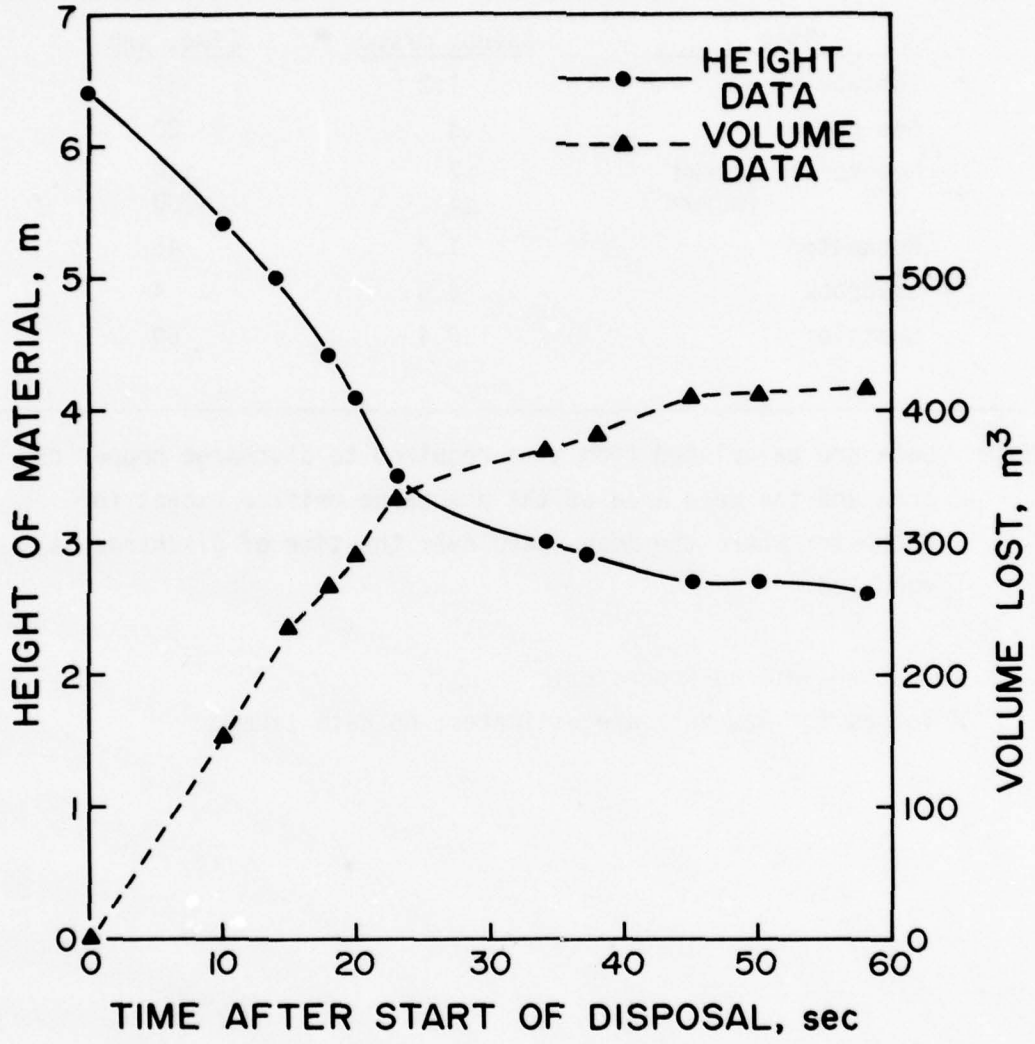

Figure 7. Height of material and volume lost vs. time, Rochester, 19 October 1976.

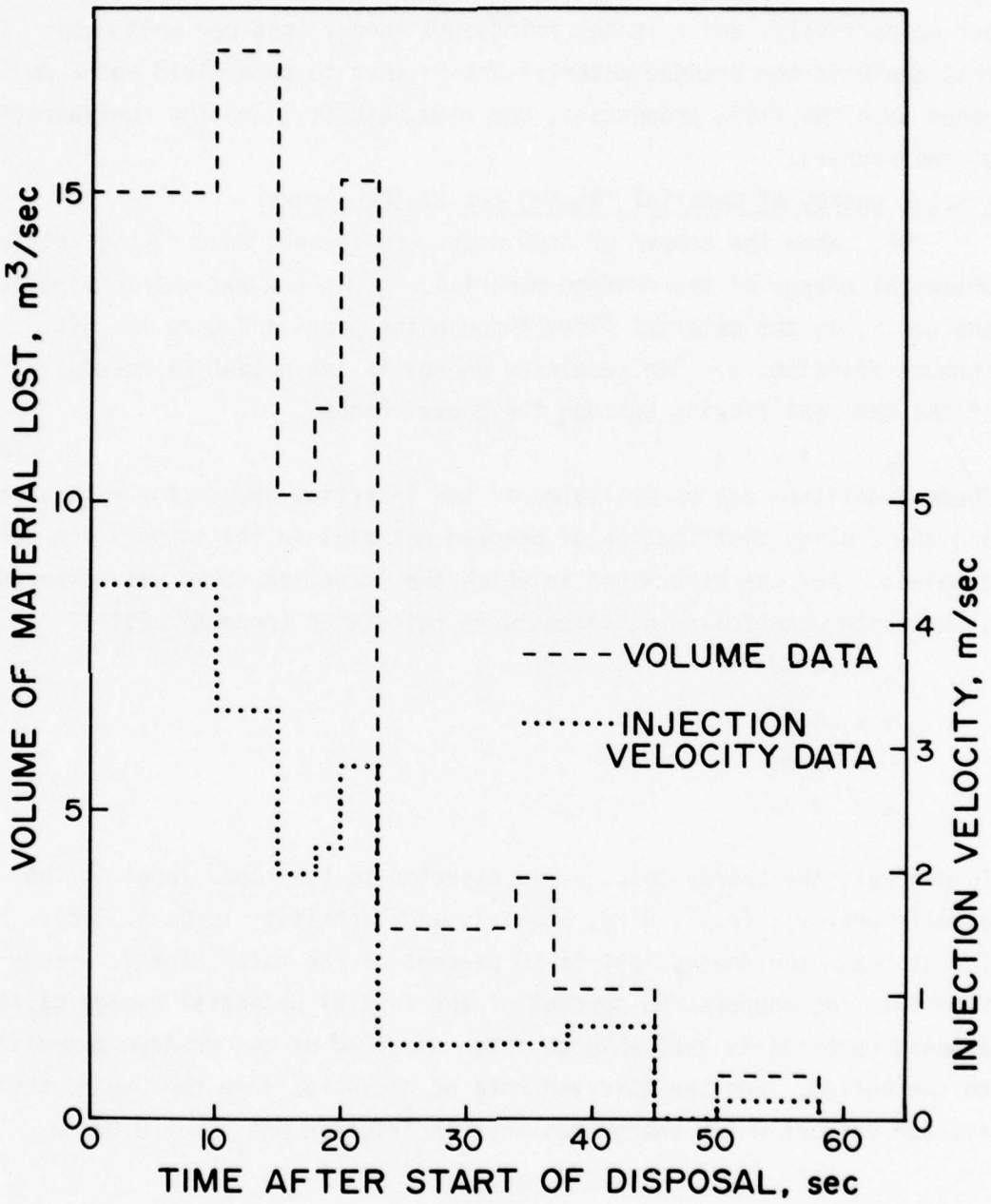

Figure 8. Volume discharged and injection velocity vs. time, Rochester, 19 October 1976, Disposal 8.

dredged material, d is the depth of the hopper doors below lake level, A_4 and A_o are the cross-sectional areas of the door opening and the hopper respectively, and ε is the frictional energy loss per unit mass. In this analysis the dredged material was assumed to be a fluid and ε depends upon the fluid properties, the flow velocity, and the configuration of the hoppers.

Kinetic energy of material flowing out of the hoppers

38. When the hopper or scow doors are opened, some of the initial potential energy of the dredged material, ν_o, is converted into kinetic energy, τ, as the material flows through the doors and some is lost through friction, ε. The remaining energy is the potential energy, ν, of the material flowing through the doors, hence

$$\nu_o = \tau + \nu + \varepsilon \tag{4}$$

These quantities may be evaluated if the insertion speed, the exit area, and the density distribution of dredged material in the hoppers are determined. For the experiment in which the insertion speed was measured at Rochester the following values were calculated (Appendix E):

ν_o = 20 MJ

τ = 6 MJ

ν = 11 MJ

ε = 3 MJ

In general, the energy lost, ε, is expected to be proportional to the kinetic energy τ (e.g., Bird, Stewart, and Lightfoot, 1960, p. 216). In this case the energy lost is 50 percent of the total kinetic energy flow from the hoppers; 85 percent of the initial potential energy of the dredged material is available to drive the flow of the dredged material to the bottom. For the observed rate of discharge from the Lyman, the average rate at which energy was lost in friction was about 0.07 Mw.

Descent

39. Processes that occur during descent of dredged material through the water column determine the impact velocity at the bottom, the location of the impact point, and the amount of material that

reaches the bottom. The dredged material may fall through the water column as independent, cohesive blocks of soil or as fine particles dispersed in fluid. The first case can be analyzed in terms of the free fall of a body through a fluid, the second, in terms of a jet of denser fluid passing through a less-dense fluid. The motion of the jet causes entrainment of the ambient fluid so that a volume of water much greater than the initial volume of dredged material is set in motion during descent. If the dredged material released in the water column contains both large and small particles, the fall of the larger particles may set the surrounding water in motion, generating a jet containing the small particles. Thus, the two cases described above are "end members" and all intermediate cases are possible. The field observations yield information on the free fall of clods and the velocity, size, and entrainment of the descending jet. Appendix F contains additional details on the descent phase.

Methods

40. Observations intended to elucidate the mechanics of the descent phase were made at Ashtabula and Rochester and were for hopper dredge discharges. Incidental data on descent were obtained at some of the other sites. Most data were obtained with an array of transducers positioned near the bottom under the dredge at the disposal site. At Ashtabula an echo sounder looking upwards was placed on the bottom. At Rochester an upward-looking echo sounder and a flow meter were suspended under the dredge. These instruments yielded information on fall speed, duration of fall, and the amount of fluid reaching the bottom. Lateral extent of the descending jet was measured with a side-looking echo sounder which could be swept in a horizontal plane. Some additional data were obtained from downward-looking echo sounders (to define impact area) and from travel time curves discussed in the next section.

Descent of clods

41. The descent of discrete clods of dredged material was observed directly only at Seattle, where the fall of individual clods was recorded by a downward-looking echo sounder adjacent to the scow at the time of discharge. Some clods were accelerating while in the field

of view; others had reached terminal velocity. The observed terminal fall velocities and the inferred clod size are listed in Table 5. These

Table 5

Observed Fall Velocities and Inferred Clod Size, Seattle

Fall velocity, m/sec	Clod size, m
0.35	0.02
0.47	0.03
0.79	0.05
0.91	0.06
1.26	0.11
1.53	0.13

range up to about 0.13 m; this is about the same as the size of the clods observed on the bottom at the New Haven disposal site.

42. The free fall velocity of clods of dredged material in water can be calculated but, because the drag depends on Reynolds number, this must be done by numerical methods. The calculation is shown in Appendix G. The terminal velocity and the time and distance over which a clod must fall to reach terminal velocity are calculated. The fall distance required to reach terminal velocity is much less than the water depth at all disposal sites if the clods are smaller than 1 m, so impact of clods with the bottom will always be at terminal velocity. This velocity is shown in Figure 9 as a function of clod size. The kinetic energy of the clod per unit mass is also shown in Figure 9. This quantity is useful in discussion of the impact of clods with the bottom.

43. The methods presented in Appendix G can also be used to evaluate the lateral deflection of falling blocks by current in the receiving water if so desired.

Jet descent velocity

44. Detailed information on jet descent of dredged material was obtained with a transducer and flow meter placed near the bottom under the hopper dredge Lyman at the time of discharge. The result of one of

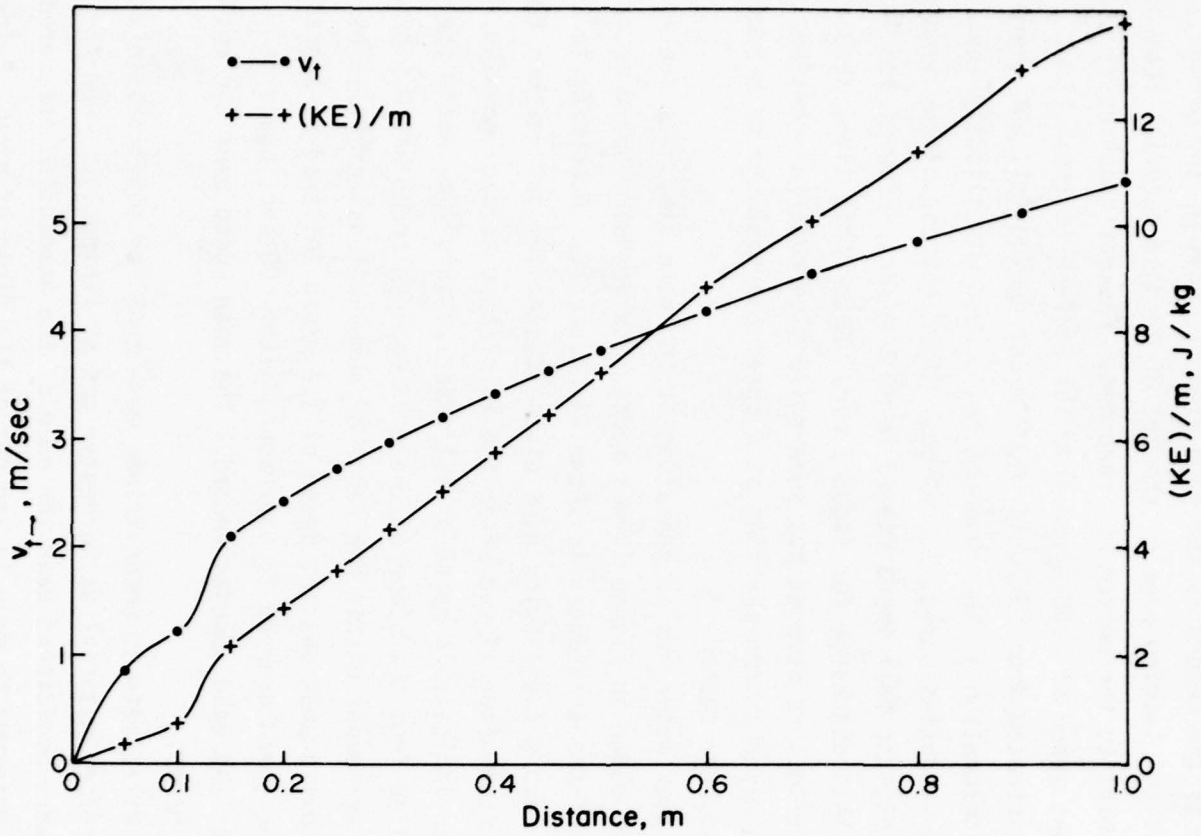

Figure 9. Terminal velocity, v_t, vs. grain diameter and kinetic energy KE/unit mass m. Density of spheres in water = 1.5 Mg/m^3.

these experiments is presented below as an example. The rest of the results are described in the supplementary site reports (Appendices).

45. A photograph of the inverted echo sounder record for a Lyman discharge (No. 7, 191076)* is shown in Figure 10. The heavy line at the bottom of the record is the echo from the hull of the dredge. The descent of the leading edge of the jet of dredged material from the release point to the bottom was recorded. Descent occurred at a nearly constant speed of 0.80 m/sec from the surface to the bottom. (The speed fluctuated from ∿0.70 to ∿0.90 m/sec during fall but there was no net acceleration.) The observed fall speed was slightly less than the mean insertion speed, 1.2 m/sec. After descent of the leading edge of the jet, the fall speed slowed to ∿0.5 m/sec. Flow of the jet continued in this discharge for about 1 min. After this time, descent of acoustic reflectors stopped but some reflective material remained adrift in the water column settling at a speed too small to be measured on the echo sounder record.

46. A flow meter was in operation at the same time that the echo sounder record shown in Figure 10 was made. The downward speed measured at the level of the transducer is shown in Figure 11. According to the echo sounder record the leading edge of the descending jet reaches the level of the flow meter 17 sec after the initiation of door opening. The flow meter indicated a speed of 1.1 m/sec at this time while the speed calculated from the slope of the echo sounder trace was 0.9 m/sec. These are in agreement within the range of observational error. The flow meter shows a peak descent speed of 1.2 m/sec followed by a gradual decrease. The speed dropped to background after ∿60 sec, again in agreement with the echo sounder record. The mean speed over the entire flow was 0.7 m/sec.

47. Similar sets of observations were made for additional discharges of dredged material at Rochester and at Ashtabula. When the transducers were positioned near the edge of the descending jet, dredged material was observed to move in and out of the field of view. Evidently, the descent of dredged material around the edge of the jet was irregular

---

* 191076 = 19 Oct 76.

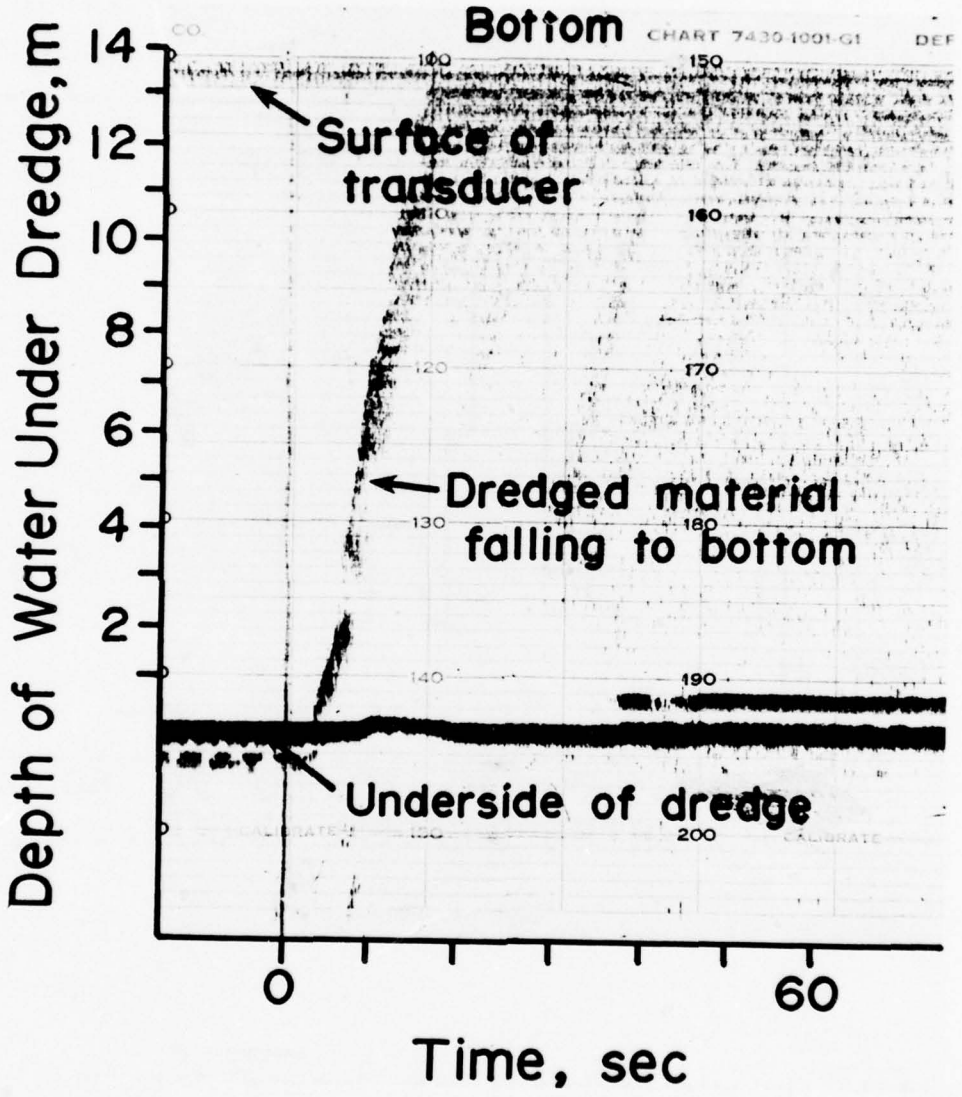

Figure 10. Upward-looking transducer record, Rochester, 19 October 1976.

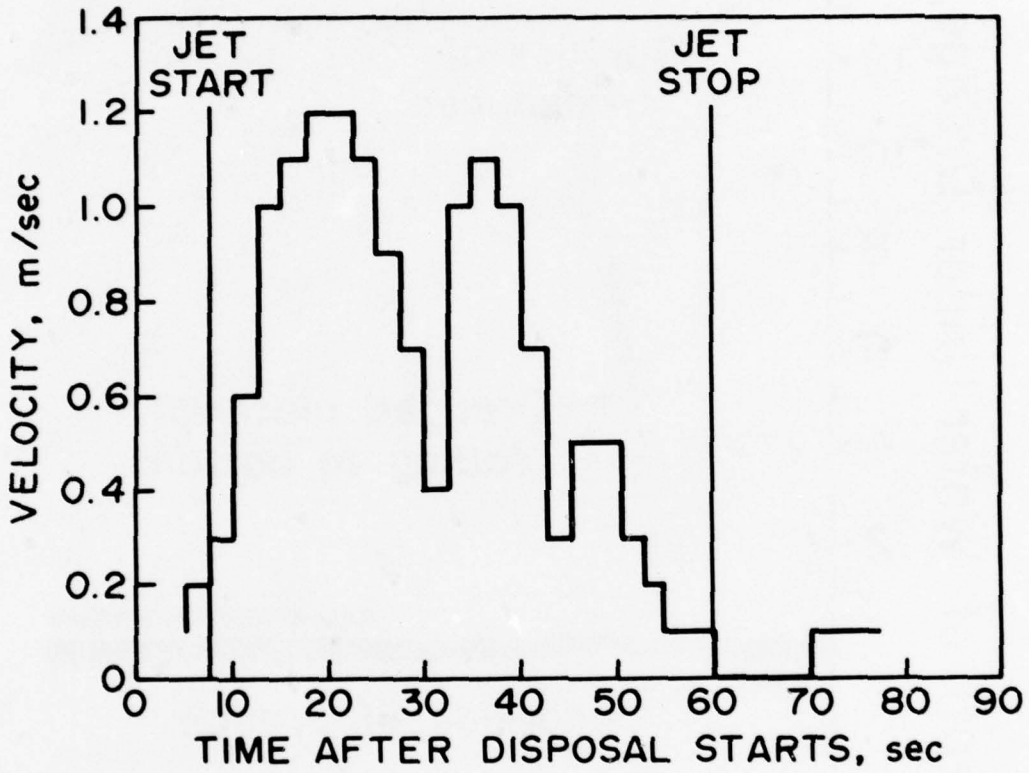

Figure 11. Flow meter velocity vs. time, Rochester, 19 Oct 1976.

in its development. Descent speeds ranging from 0.3 to 2 m/sec were observed with the inverted echo sounder over short time intervals. The corresponding flow meter records showed alternate high and low velocities. The duration of the descent phase indicated by the echo sounder and flow meter were in accord in all cases. When the initial level of dredged material in the hoppers of the Lyman was lowered 1.6 m (in discharge No. 4, 191076), thereby reducing the hydraulic head by half, the average descent speed measured by the flow meter was found to be reduced to 0.38 m/sec.

48. At the other study sites, observations were not made close enough to the discharge point to permit direct determination of the jet descent speed. However, the average speed of descent of the dredged material from surface to bottom was calculated from data taken at Seattle and Saybrook. The intercept of the bottom surge travel time curve (discussed in the next section) with the time axis gives the descent time. At Seattle the intercept was large enough to be measured with some confidence and shows that the mean fall speed is 0.5 m/sec. A lower bound on the fall time can be set at Saybrook from bottom surge meter records; this gives a minimum fall speed of 2.8 m/sec. The properties of the dredged material are not very different at Seattle and Saybrook. The difference in descent speed does correlate with the mean insertions speed, as shown in Table 6.

Table 6

Descent and Insertion Speeds

Site	Mean Insertion Speed, m/sec	Mean Descent Speed, m/sec
Seattle	0.4	0.5
Rochester	1.2	0.8
Saybrook	6.5	2.8

49. In theories of the flow in turbulent jets (Hayashi and Ito, 1975; Albertson et al., 1950), the velocity at any point along the jet

axis scales as the insertion velocity. Proportionality of the descent and insertion speeds is not proved by the results in Table 6, probably because of experimental uncertainties, but in the range of water depths studied, the increase of descent speed with increase of insertion speed is clear. Insertion speed of the dredged material can be controlled by design of the discharge vessel. This offers a practical means of controlling the placement of dredged material. For example, a large insertion speed could be used when it is desired to minimize transit time to the bottom, as when accurate placement in the presence of a strong ambient current is required. A small insertion speed will result in a smaller impact energy at the bottom and smaller dispersion of dredged material in impact and the bottom surge. The relation between insertion speed and descent time of dredged material deserves further study.

Jet descent, lateral spread, and integrated flow

50. The lateral spread of the descending jet was measured at Rochester. The most extensive data were obtained with the horizontally scanning echo sounder. An example of the results obtained is shown in Figure 12, which is for discharge No. 2, 191076. The figure shows the area occupied by the descending column of dredged material at a depth of 3.5 m below the hopper doors 12 sec after initiation of discharge and again at 20 sec after. The configuration of the hopper doors from which the dredged material was released and the location of the observing point are also shown. A separate jet formed from each door. The jets were displaced toward the bow of the dredge during their 3-m descent and the area of each increased by three times relative to the door area. A similar jet cross section was found for the other releases of dredged material at Rochester. All of the measurements indicative of the lateral size of the descending jet were used to construct the composite, generalized jet descent diagram shown in Figure 13. When water alone was released from the hoppers, the cross-sectional area of the jet was found to be larger at a depth of 3 m below the bottom of the dredge than when dredged material was released. This increase

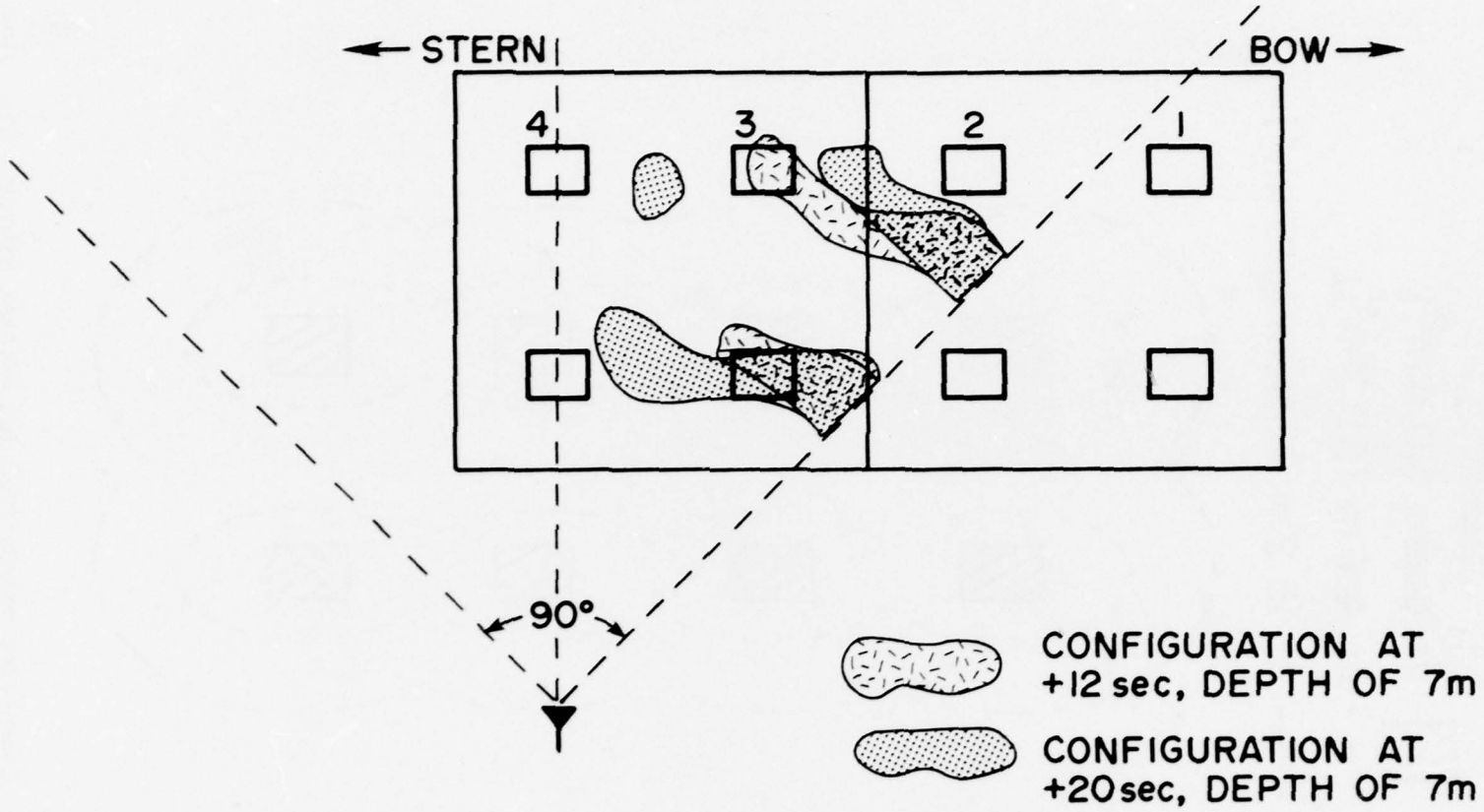

Figure 12. Plan view of hoppers and doors, dredge Lyman, and configuration of jets at depth of 7 m as determined by side-looking 200-kHz transducer.

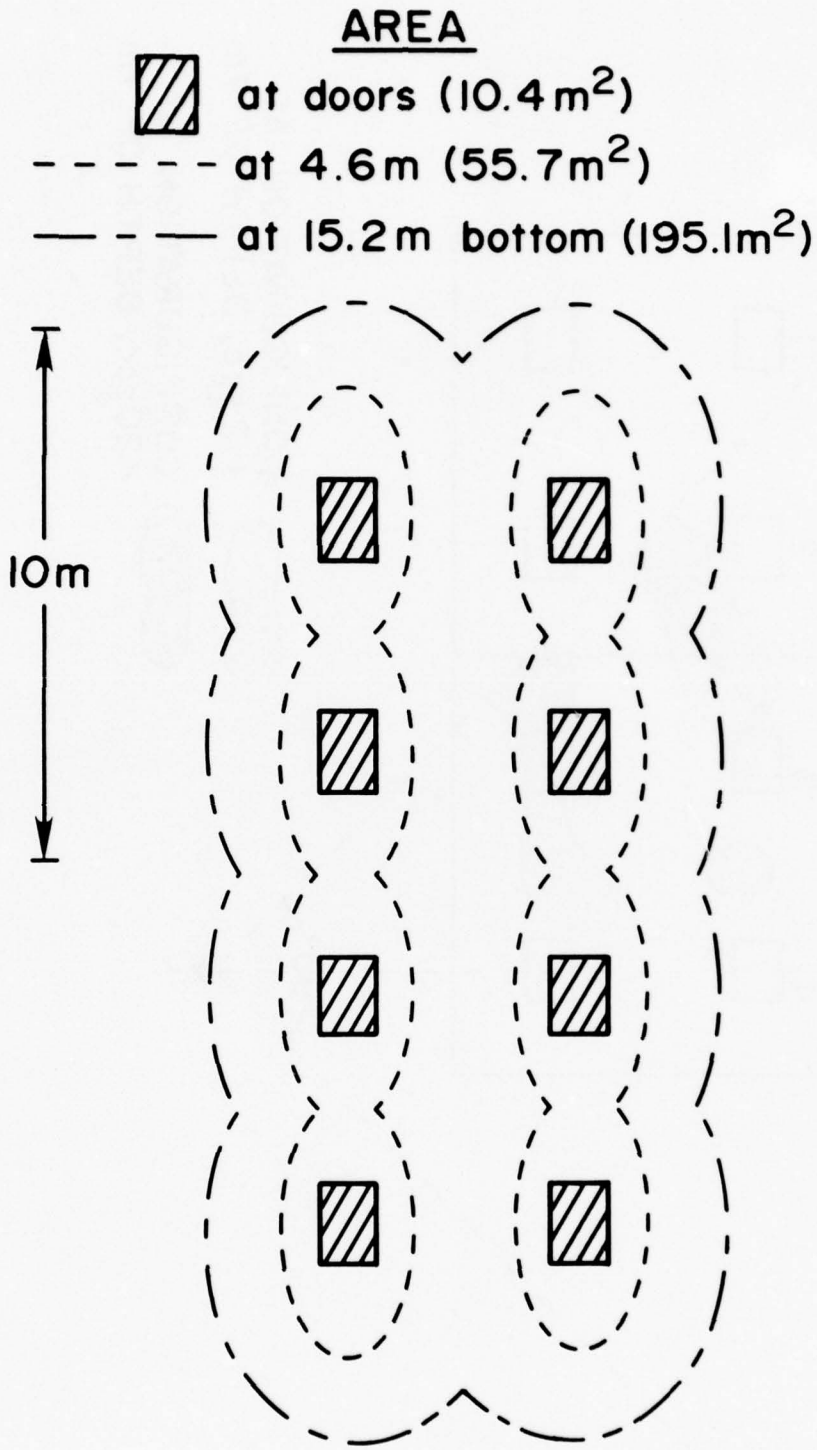

Figure 13. Composite, generalized jet descent diagram, plan view.

averaged 30 percent for the discharges measured.

51. The time required for the leading edge of the jet to descend through the water column was 12 to 15 sec; the flow in the jet then continued for 60 to 90 sec. A theoretical model that would be equivalent to this process would be the establishment and initial flow stages of an array of jets of dense fluid passing through less dense ambient fluid and impacting on a plate. Most theoretical analyses deal with steady-state jets or, as in the case of the Koh-Chang model, with a transient in which no steady flow is developed. Because of the time scales mentioned above, the steady state rather than the transient solutions are probably more nearly applicable to the descent of dredged material. In steady state the velocity distribution across a jet follows an error function (Albertson et al., 1950; Hayashi and Ito, 1975); the mean velocity over the jet section is then about half the velocity on the center line.

52. The quantities needed in a calculation of the downward transport by the jet are listed in Table 7 for each of the discharges at Rochester for which flow meter measurements were made. The amount of material released depended on what combination of hopper doors was open and the initial level of fluid in the hopper. The mean flow meter velocity for each discharge was calculated from diagrams like those in Figure 11. It was intended that the flow meter be located on the center line of the jet but its exact location within the jet could not be determined. In the following calculation, the measured flow velocity was assumed to be equal to the mean flow velocity over the cross section of the jet at the level of the flow meter. The mean velocity over the section was used with the duration of flow and the section area at the flow meter level to find the total quantity of fluid passing the section. The total area of the jet was found for the different combinations of door openings from Figure 13. Results of the calculation are presented as the ratio, Q/Q_o, of the quantity of fluid passing the flow meter section to the quantity injected. The value of Q/Q_o ranged from 10 to 195 with an average of 72. The

Table 7

Volume of Fluid Transported by Descending Jet at Rochester

Discharge No.	Hopper Contents*	Door Opened	Hydraulic Head Above Lake Level, m	Volume Released, Q_o m^3	Mean Velocity at Flow Meter m/sec	Flow Duration	Jet Area at Flow Meter m^2	Fluid Passing Section at Flow Meter, Q, m^3	$\frac{Q^{**}}{Q_o}$
2	S	3+4	2.7	107	0.57	114 sec	105	0.68×10^4	64
5	S	4	2.7	259	0.47	90 (inc)	61	0.29×10^4	>10
6	S	2+3	2.7	107	0.66	156 (inc)	105	1.08×10^4	101
3	W	4	2.7	359	0.55	120	117	0.77×10^4	22
4	W	4	1.2	29	0.38	100	149	0.57×10^4	195
7	W	4,3,2,1	2.7	443	0.68	54	462	1.70×10^4	38
Average				217	0.55	106	166	0.84×10^4	72

* S = dredged material, W = water.

** Q = Volume of fluid passing section at flow meter.

Q_o = Volume of fluid released.

quantity of fluid impacting the bottom was about 72 times greater than that released.

53. The rate at which ambient fluid is entrained by descending dredged material is described by an entrainment coefficient, α, where

$$\alpha = \frac{Q-Q_o}{TA_j\bar{u}} \tag{5}$$

where Q is the quantity of fluid passing the section at the flow meters, Q_o is the quantity released from the hoppers, T is the duration of downward flow, $\bar{u}$ is the mean flow speed and A_j is the surface area of the descending jet between the hull of the dredge and the cross section at the flow meter. The data in Table 7 give an α of about 0.6.

54. Because of the large amount of ambient water entrained, the descending jet will quickly acquire a lateral velocity equal to the current flowing in the receiving water. The impact point of the dredged material on the bottom will be displaced as a result of this lateral velocity. The amount of this displacement may be easily calculated from the current and descent time. Another practical consequence of entrainment is that ambient water will flow inward toward the hull of the dredge, as illustrated in Figure 14. This inflow effectively prevents escape of dredged material into the water surrounding the dredge. Observations made at Rochester showed that no dredged material appeared in the surface water around the dredge after discharge provided that the dredge was stationary in the water when the dredged material was released. If water was subsequently pumped into the hoppers and allowed to overflow, or if the hoppers were flushed out when the dredge was under way, a turbid cloud of dredged material was then visible in the surrounding water.

Energy balance of jet descent

55. Generalizations about this process useful in prediction can be made from available information on the energy changes that occur during descent. The potential and kinetic energy of the dredged material inserted in the water column was calculated earlier. Part of this

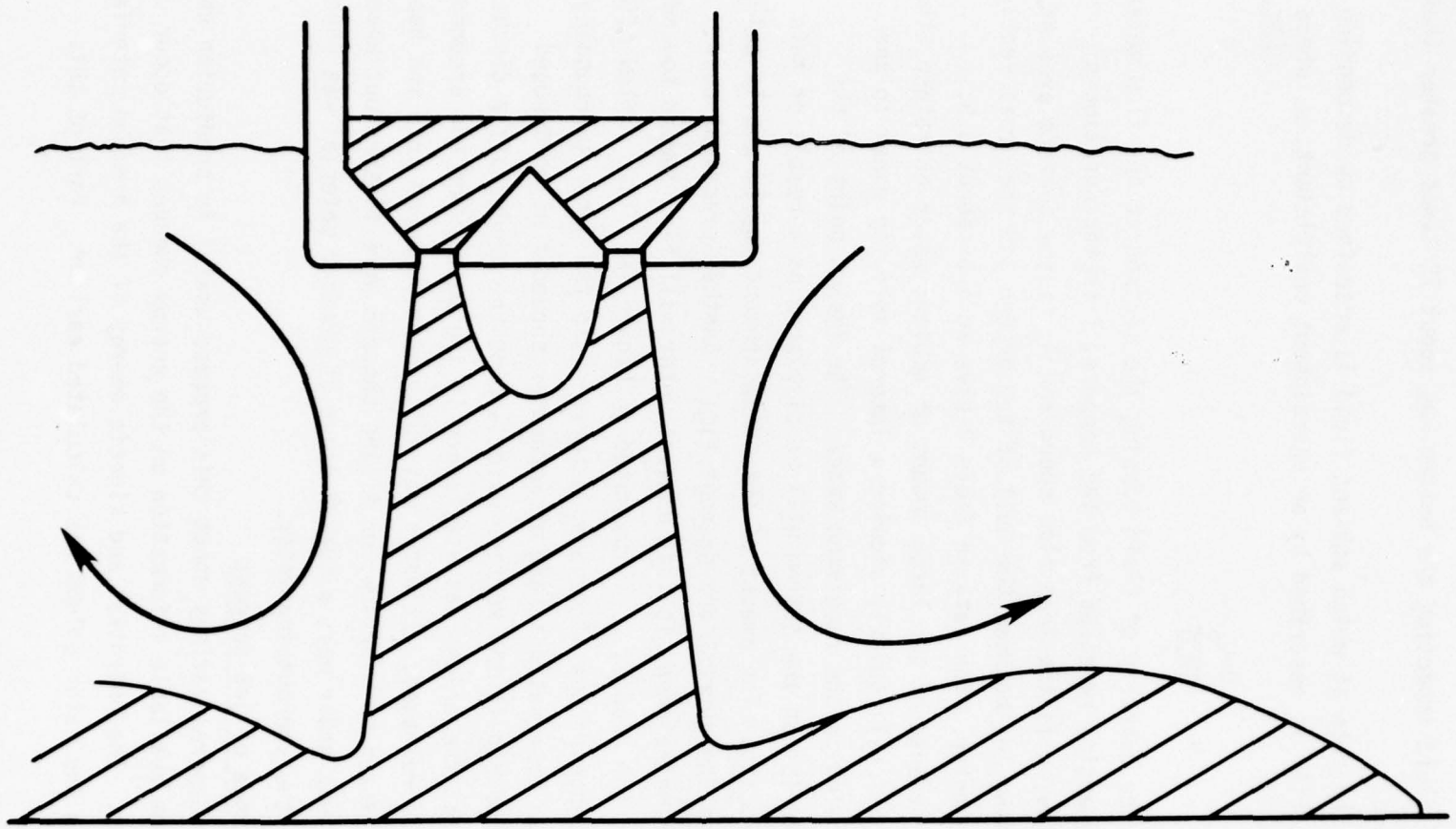

Figure 14. Inward flow of ambient water as a consequence of entrainment.

energy was used to accelerate entrained water, part was used to set the surrounding water in motion, and part was dissipated by friction and the work done against the dynamic pressure of the jet.

56. The observations made at Rochester (discharge numbers 5 and 6, 191076) showed an initial potential energy of 36 MJ. Of this energy, 32 MJ passed through the hopper doors during the discharge: 10 MJ leaving as kinetic energy and 22 MJ as potential energy. Through a horizontal plane 13.6 m below the hopper doors (1.4 m above the lake floor) v is 1.1 MJ and the total amount of kinetic energy was calculated from the flow meter records to be less than 3.2 MJ. Hence, a total of less than 4.3 MJ was observed at the bottom. A large fraction of the available energy was lost from the jet during descent. Some of this energy was used in setting the surrounding water into circulation. A current meter record, made 15 m from the impact point, suggested that this circulation proceeded at speeds of up to 0.8 m/sec, accounting for perhaps 1 MJ of the energy lost in descent. The rest must have been dissipated in friction and turbulent motion.

Impact and Formation of the Bottom Surge

57. At all the sites studied, the dredged material reached the bottom while traveling at speeds of about a meter per second. Clods of sediment impacting the bottom at this speed will be deformed and possibly broken up. A descending, dense, fluid jet is deflected by the bottom and runs radially away from the area of impact at a high speed. Although large clods of material are expected to remain in the impact area, a deflected jet of dredged material may travel hundreds of meters from the impact area before coming to rest. In the latter case, not only will the released dredged material not be deposited in the impact area but erosion of the bottom by the jet is likely to occur. Thus, the nature of the impact between the descending dredged material and the bottom is important in determining where the dredged material will eventually come to rest.

Methods

58. The impact event was examined in most detail at Rochester and Ashtabula. The observations made on the descending material serve to define the area, duration, and speed of the impact event. These observations included both acoustic and flow meter measurements as described in paragraphs 14 and 17. Additional measurements were made immediately outside of the impact area. Downward-looking 200-kHz acoustic transducers were used to define the thickness of the cloud of dredged material leaving the impact area. Bottom-mounted current meters recorded its speed.

59. The measurements made in the Great Lakes were on hopper dredge discharges. This dredged material impacted the bottom as a dense fluid. At Seattle, Saybrook, and New Haven, however, clods of material were detected. To investigate the behavior of clods of dredged material impacting on the bottom, mechanical tests were performed on dredged sediment from the Saybrook site. The stress-strain curves for this material were determined at strain rates likely to be achieved during impact. Both unconfined, submerged, axial compression and impact tests were done.

Jet impact

60. The impact of a jet of dredged material from a hopper dredge is also illustrated in Figure 13. The area of impact is

$$\pi(\bar{r} + Z \tan \beta)^2 \qquad (6)$$

where $\bar{r}$ is the effective radius of the orifice, Z is the height of the orifice above the bottom, and β is the angle of spread of the jet. Encountering the bottom, the jet begins to spread as a thin disk along the bottom. The initial spreading velocity is equal to the fall speed, i.e., about 1 m/sec. The initial thickness of the spreading disk is about 4 m and it carries a concentration of suspended sediment of about 8 kg/m^3. This corresponds to a density of 1.005 Mg/m^3. The Froude number for this flow is about 2.3; the flow is supercritical. Under

these conditions it is unlikely that any deposition of dredged material takes place in the impact area, except for large clods of sediment.

Impact energy

61. The total energy flowing into the impact area was about 4 MJ for a hopper dredge discharge (Rochester, Discharges 5 and 6, 191076, Appendix F). Information on the spread of material away from the impact point was not available for this particular discharge operation. However, it was estimated from the current meter information taken on another discharge operation that the flow of turbid water out of the impact area had an energy of about 2 MJ. This value is comparable to but smaller than the energy flow into the impact area, suggesting that some energy was lost in the deflection of the jet as it encountered the lake floor. Several loss mechanisms are possible; lake floor sediments may be deformed or eroded. Clods descending with the dredged material may be deformed or disaggregated. Energy may be radiated away from the impact area in the form of elastic waves in the bottom sediments and the lake water. It should be possible to detect this radiated energy with a geophone placed on the lake bottom or a hydrophone in the ambient water.

Impact of clods

62. If a clod of dredged material impacts the bottom at high speed, it will disintegrate and the contained material will be dispersed. If the impact speed is low, the clod will be deposited intact. The condition necessary to avoid disintegration is that the kinetic energy of the clod at arrival be dissipated in plastic deformation of the clod or the bottom before material failure occurs. Since, as shown in Figure 9, the kinetic energy per unit mass of a falling clod increases as the clod size increases, it is expected that there is an upper bound to the size of clod that can be deposited on the bottom intact. A series of experiments was done with dredged material from the Saybrook site to determine the maximum size of clod that can be deposited intact.

63. Blocks of dredged material were allowed to free fall at speeds in the range of v_t given in Figure 9 and to impact with an earth pressure

cell. The output from the cell was displayed on an oscilloscope as a record of force vs. time. This determined the duration of impact. The total amount of deformation produced by the impact was measured and used to determine the mean deformation rate. This was found to be between $\frac{1}{2}v_t$ and $\frac{1}{4}v_t$. Unconfined compression tests were done on samples of the same dredged material over a wide range of strain rates. The force-displacement curve was found to pass through a maximum corresponding to failure by liquifaction of the soil. The work done in deforming each sample to failure was calculated by integration of the force-displacement curve; the results are presented in Figure 15. The capacity to absorb energy in plastic deformation increases as the deformation rate increases. For each size clod the kinetic energy per unit mass and the terminal fall speed can be read from Figure 9. The deformation rate on impact can be calculated from v_t. This determines the amount of energy that the clod can absorb without failure, as shown in Figure 15. Also shown in Figure 15 is the energy density as a function of clod size. The two curves cross for a clod size of about 0.8 m; larger clods are expected to disintegrate, smaller to remain intact after impact with the bottom.

64. The analysis presented here shows that there is an upper limit to the clod size that can be placed on the bottom without breakup and how this size is related to measurable properties of the dredged material. The predicted upper limit to size is somewhat larger than the observed size of the clods on the bottom at the New Haven disposal site, but it is expected that more refined and extensive measurements of the properties of the dredged material would yield a better quantitative result. Additonal information on impact properties of dredged material can be found in Appendix H.

Spread of the Bottom Surge and Deposition

65. Impact of the descending jet with the bottom deflects the flow of dredged material and entrained water to form a surge or density current, which spreads away from the impact point across the bottom.

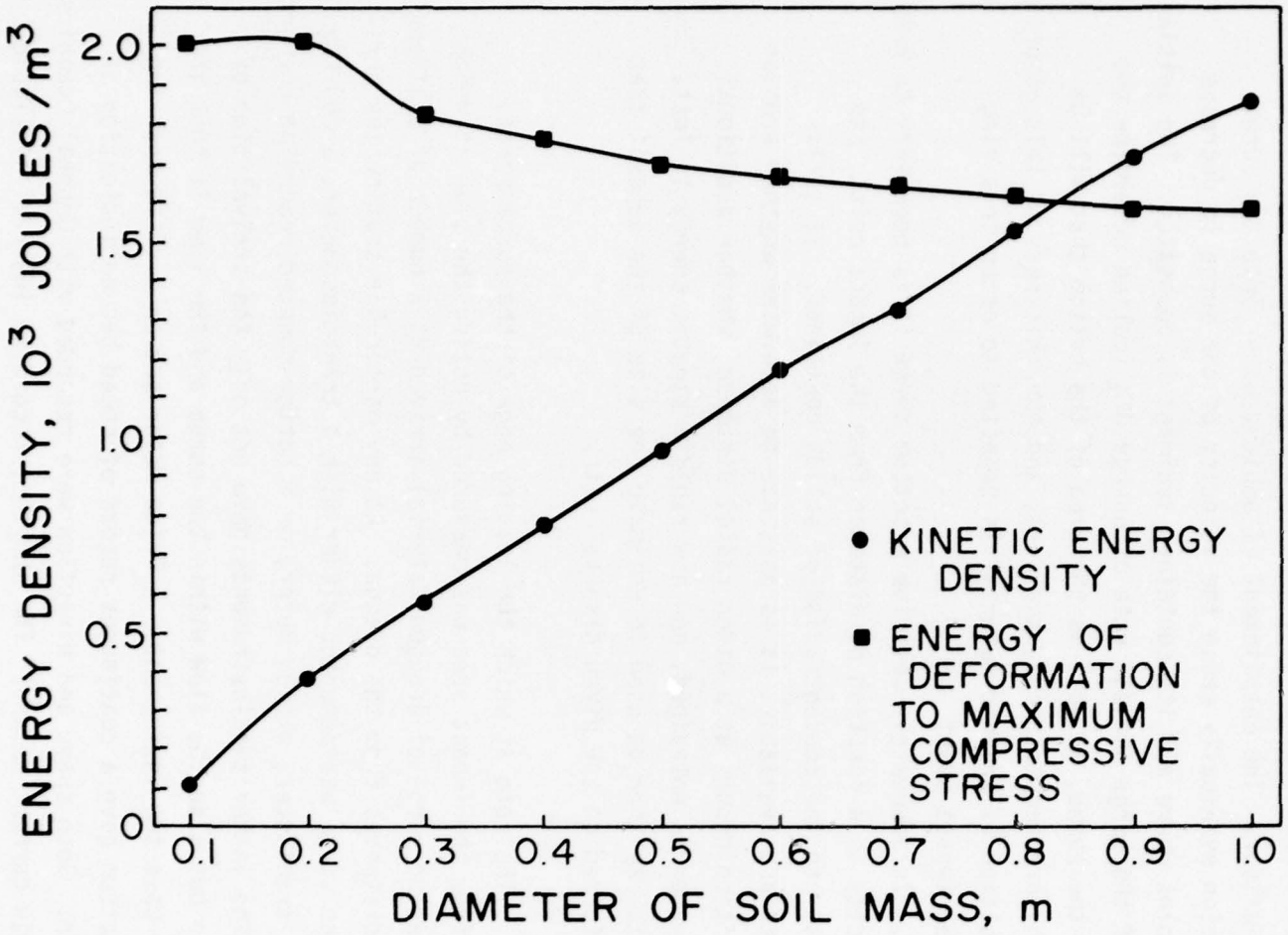

Figure 15. Energy of deformation to maximum compressive stress and kinetic energy density vs. diameter, North Cove dredged material.

This surge spreads radially outward in the shape of a thin, expanding toroid of turbid water. Both its thickness and speed decrease as its radius increases. As the surge proceeds outward it sheds behind it a thin, slowly moving cloud of suspended dredged material which settles to the seafloor. The entrainment of ambient water into the surge and friction eventually cause the velocity of the surge to decrease to the point where all its contained sediment is deposited. The initial energy of the surge and the rate of energy dissipation determine the range of the surge, as well as the area of the bottom that will be covered by dredged material, the form, and the thickness of this deposit. The deposition of dredged material is expected to occur in a ring around the impact point.

66. To adequately describe a bottom surge it is necessary to know its velocity as a function of distance from the impact point, its thickness, and the concentration of solids contained. If sufficient data are available, it is possible to determine whether erosion or deposition occurs at a given radial distance, whether additional ambient water is entrained, and how rapidly kinetic energy is lost. These data may then be used to estimate the size of the deposit that will be formed on any given disposal site.

Methods

67. The rate at which the leading edge of the surge spread outward from the impact area was measured by noting the time at which the spreading surge of dredged material arrived at a number of stations various distances from the dredge. At any particular station the arrival of the surge was detected either with a transmissometer, a 200-kHz acoustic transducer, a flow meter, or a bottom-mounted recording current meter. The latter two instruments gave not only the arrival time of the surge but also the flow within the surge and the time it took the surge to pass the instrument. A Price meter set on a rigid mounting on the bottom gave a continuous record of speed but no indication of direction. Both speed and direction were recorded with General Oceanics model 2010 current meters. The shortest recording interval available,

14 sec, did not provide full resolution of the internal velocity structure of the surge but gave a satisfactory record of its larger scale flow characteristics.

68. The vertical thickness of the cloud of turbid water was measured at a number of locations by one of three methods. In the first method, a transmissometer was held stationary about 1 m above the bottom. When this instrument detected the arrival of the surge, vertical profiles were made until the water cleared. An alternate method used a vertical array of four transmissometers at the stations. The instruments were spaced 1 m apart and held stationary while the surge passed them. The third method was to observe the layer of turbid water with a stationary, downward-looking 200-kHz acoustic transducer. The fluid in the bottom surge, because of the contained solids, returned a good echo of the 200-kHz acoustic pulses. The passage of the bottom surge and its vertical development was followed with the echo sounder. It was found in some cases, however, that the later parts of the surge were obscured by gas bubbles released during its passage. By these methods the thickness of the surge and the change in thickness in time as well as the lifetime of the turbid cloud were measured at a number of locations at various distances from the discharge point.

69. To monitor the concentration of suspended sediment in the surge, the transmissometers were used and water samples were taken with submerged pumps. The pumps were suspended about 1 m above the bottom and continuously pumped water to the boat above. When the first turbid water arrived at the surface, samples were taken either continuously or at specified intervals until the water ran clear. Water samples taken simultaneously with transmittance readings provided a check on the transmissometer calibration and were particularly useful when the concentration of sediment was too great to be measured by optical methods. For studying the surge, however, water samples must be used cautiously because the rapid changes in concentration that occur make it difficult to establish that the sampling has been adequate.

70. Table 8 presents a summary of the methods employed at each study site. A typical configuration of instruments is shown by Figure 16.

Speed of the bottom surge

71. The speed at which the leading edge of the bottom surge advances is presented in a travel-time diagram. The time of arrival of the surge, as detected by any of the observing methods, is plotted against the distance of the observing point from the center of the dredge. Figure 17 is an example of a travel-time diagram constructed from data taken at Ashtabula. The time is figured from the time of hopper door opening, which was signaled from the dredge. This time signal may be subject to significant error at this locality; it is thought to be as much as 15 sec late in some cases.

72. If the travel-time curve is to represent only the run of the surge over the bottom, both time and distance should be figured from the impact of dredged material on the bottom. A time correction can be calculated from the water depth and the descent speed, and a distance correction from the descent speed and the ambient current. An additional correction may be required for the displacement of the surge itself by the current in the overlying water. If there were no friction between the surge and the water above, application of this correction would be inappropriate, but if this friction is larger than that of the surge over the bottom, it should be applied. All three corrections have been tried on the travel-time data in Figure 17. The descent corrections make only a small change in the travel time curve, but the corrections for background current produce a wide dispersion of the data points. Thus, it appears that the advance of the bottom surge is independent of the flow of the ambient water.

73. The travel time data shown in Figure 17 were obtained on a wide range of azimuths about the dredge. There is no evidence of variation of travel time with direction. It is concluded that the spread of the bottom surge is radially symmetric about the impact point, although there may be lobes and clefts in the advancing front of turbid water.

Table 8

Methods of Observing the Bottom Surge

Method	Seattle	Ashtabula	New York	Rochester	Saybrook
Optical transmittance					
Fixed elevation	✓	✓	✓	✓	✓
Vertical profiles	✓	✓	✓	✓	✓
Acoustic		✓		✓	✓
Current meters					
Price		✓		✓	
General Oceanics		✓	✓	✓	✓
Pumped samples		✓		✓	

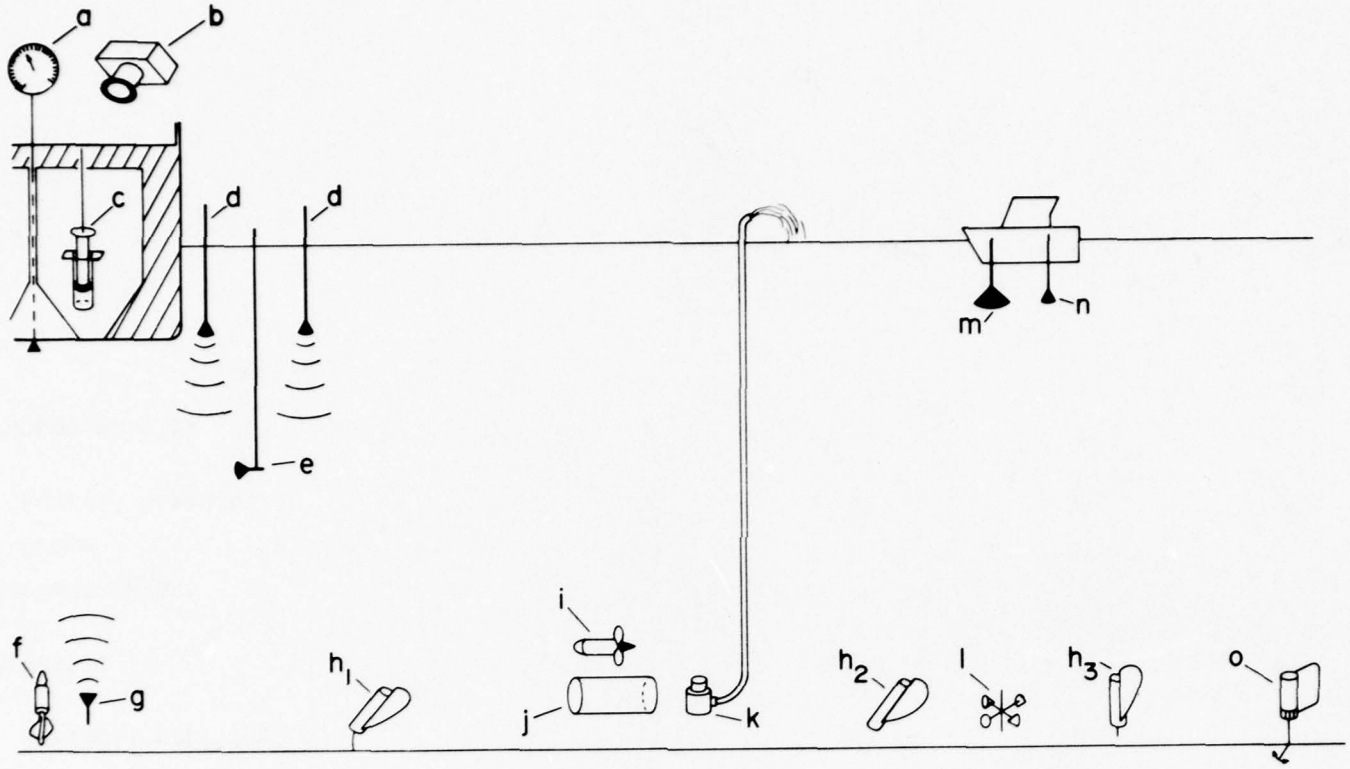

a- DRAFT INDICATOR
b- TIMED PHOTOGRAPHS
c- SYRINGE SEDIMENT SAMPLES
d- DOWN-LOOKING 200kHz
e- SIDE-LOOKING 200kHz
f- FLOWMETER UNDER HULL
g- UPWARD-LOOKING TRANSDUCER 200kHz
h- GO SURGEMETERS
i- FLOWMETER
j- TRANSMISSOMETER
k- WATER PUMP
l- PRICE CURRENT METER
m- 7kHz TRANSDUCER
n- 200kHz TRANSDUCER
o- BRAINCON CURRENT METER (BACKGROUND)

Figure 16. Typical configuration of instruments used at a study site.

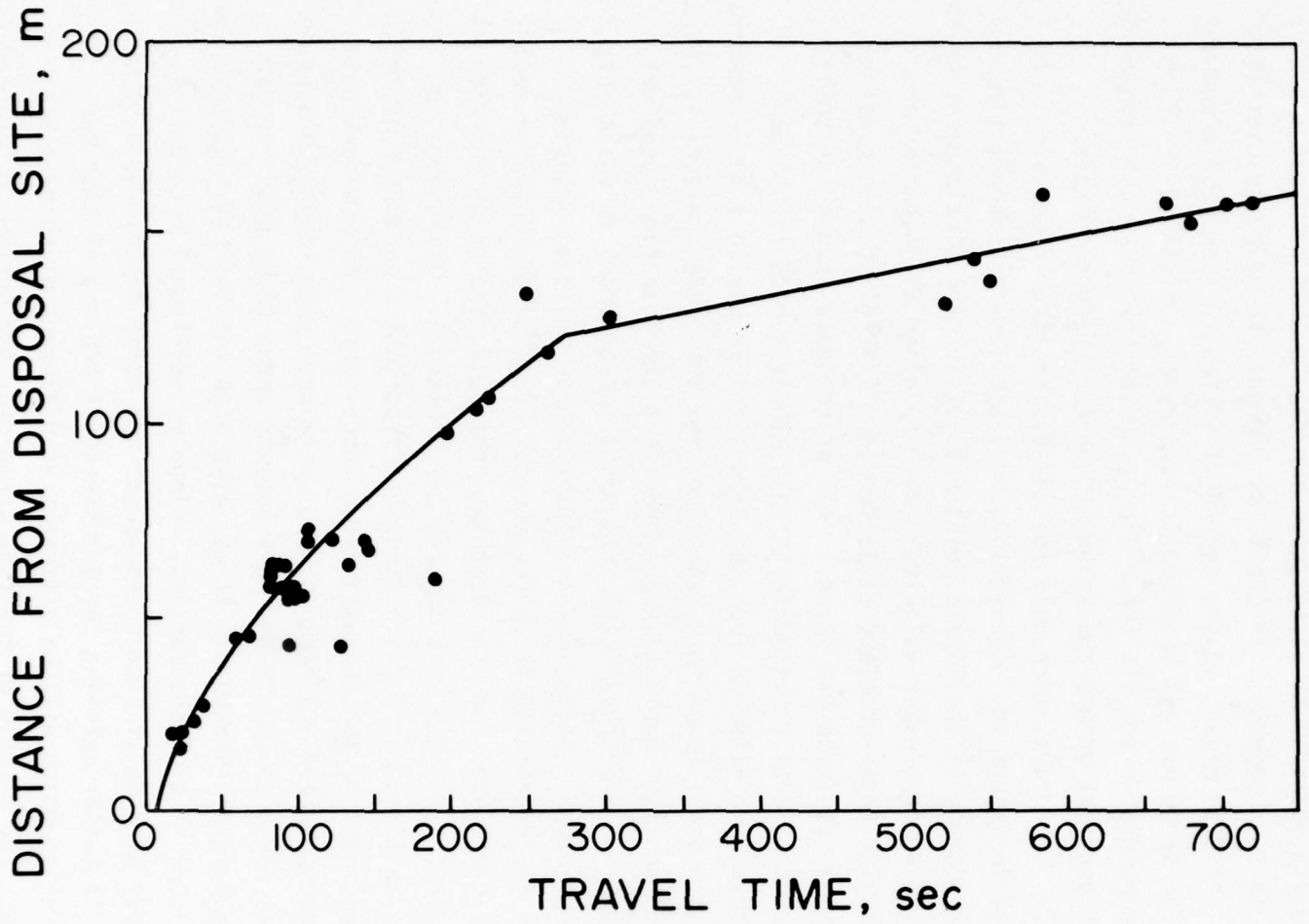

Figure 17. Travel-time diagram from Ashtabula data.

74. The slope of the travel-time curve at any point is the speed of advance of the front of turbid water. The initial portion of the travel-time curve in Figure 17 is drawn to the measured initial spreading velocity measured at Rochester. The data points are best fit by a curve with two segments. In the first segment the velocity decreases from 1.1 to 0.16 m/sec; in the second it decreases from 0.05 m/sec to zero. The surge was not observed to run beyond a distance of 170 m. The data points do not fit the $t^{\frac{1}{2}}$ law expected for an axially symmetric surge of constant volume spreading at constant Froude numbers.

75. The travel-time data for all of the other study sites are assembled in Figure 18. Corrections were applied for descent time and for displacement of the impact point but not for the displacement of the surge with ambient water velocity. Data obtained at Rochester are comparable to those obtained at Ashtabula. (The disposal operations were similar at these two sites.) All of the data points for Seattle show that the surge traveled relatively slowly across the bottom. The Seattle site differed from the lake sites in having a much greater water depth and a lower insertion speed for the dredged material. At Saybrook the water depth was also great but the insertion speed was very high; the one travel-time data point for Saybrook showed a very high surge speed, indicating that insertion speed is an important variable in determining the surge speed. Even though the water depth at Seattle was 4.5 times the depth at Ashtabula, the surge velocity at Seattle was lower than that observed at Ashtabula. This seems to indicate that the water depth is not as important a parameter as the insertion velocity in controlling the surge speed. At New York both the surge speed and the range of the surge were very large. Insertion speed was not measured at New York but was known to be high for the scow discharges. Presumably it was also high for the Essayons because of the large size of the hoppers. Clearly, additional observations made under a range of insertions speeds and water depths would be most helpful in better defining the dependence of the travel-time curve on the variables which will be different at different disposal sites.

76. The details of the flow speed near the bottom in the head of

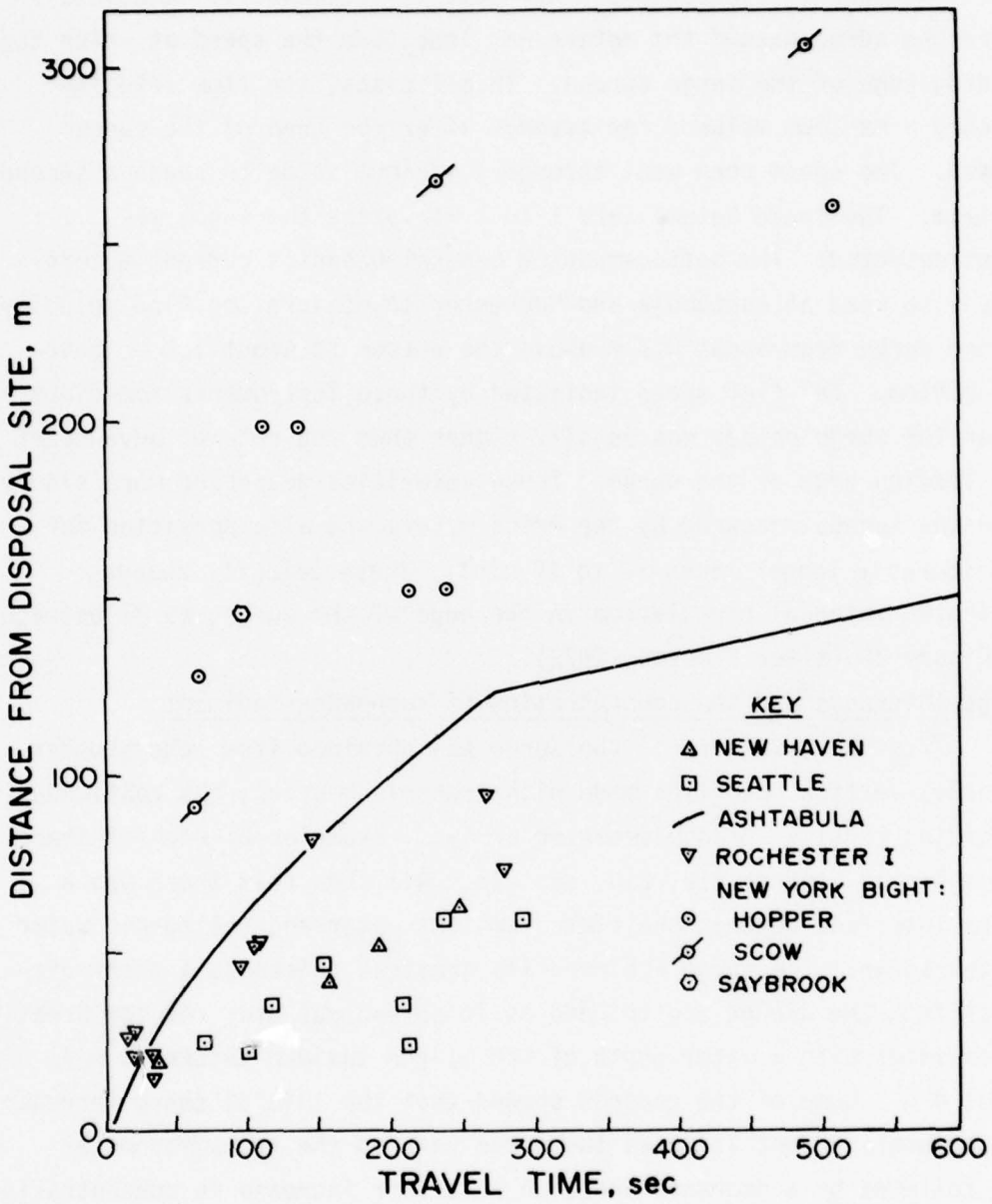

Figure 18. Travel-time diagram from data from all other sites.

the surge are shown by the current meter records in Figure 19. The Price current meter records were made about 0.30 m above the bottom for discharges at Ashtabula and Rochester. The velocity immediately after the surge passed the meters was less than the speed at which the leading edge of the surge spread. In all cases, the flow velocity reached a maximum value a few seconds after the head of the surge passed. The speed then went through a minimum value to reach a second maximum. The speed became zero 1 to 2 min after the surge was first detected. The bottom-mounted General Oceanics current meters were also used at Ashtabula and Rochester to measure the flow velocity in the surge from about 0.2 m above the bottom to about 1.0 m above the bottom. The flow speed indicated by these instruments immediately after the surge passed was usually higher than the rate of advance of the leading edge of the surge. These velocities decreased more slowly than the speeds measured by the Price meters and also persisted for considerably longer times (2 to 15 min). These velocity changes indicated internal circulation in the head of the surge, as illustrated in Figure 20 (after Simpson, 1972).

Surge thickness and the concentration of suspended sediment

77. The thickness of the surge was obtained from echo sounder records, vertical profiles made with transmissometers, and continuous recording vertical transmissometer arrays. Examples of each of these are shown in Figures 21a, 21b, and 21c. All show that there was a sharp interface between the clear, ambient water and the turbid water of the surge. The surge achieved its greatest thickness a short distance from the dredge and thinned as it spread outward. At the Great Lakes sites with a water depth of ~20 m, the maximum thickness was about 4 m. Some of the records showed that the initial sharp increase in sediment concentration as the surge reached the transmissometer was followed by a decrease and then a further increase in concentration. The leading surge of turbid water was followed by a small zone of clearer water (Figure 21). This is a relatively minor feature of the surge, probably due to the internal circulation immediately behind the head.

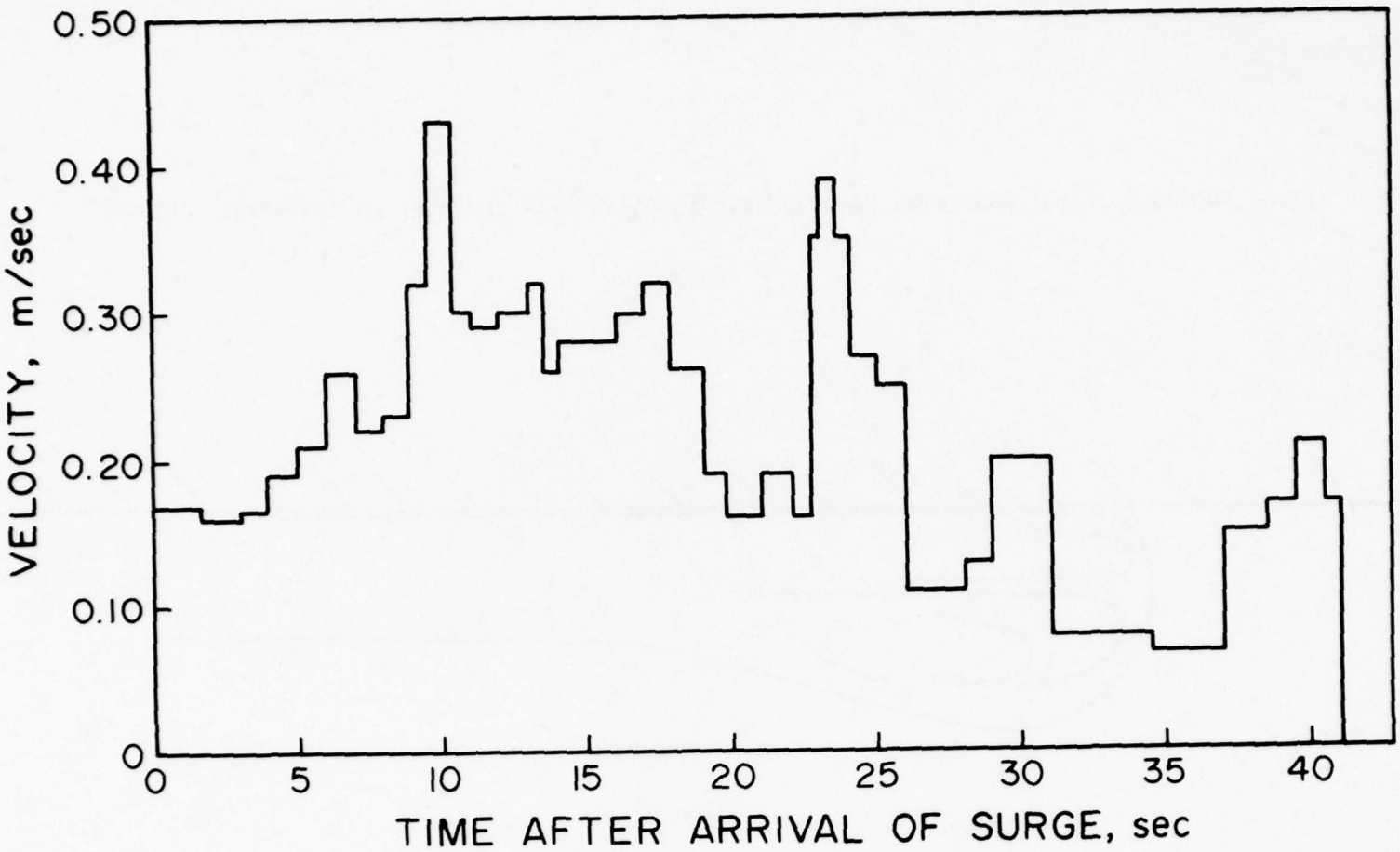

Figure 19. Price current meter record, Ashtabula, 26 May 1976.

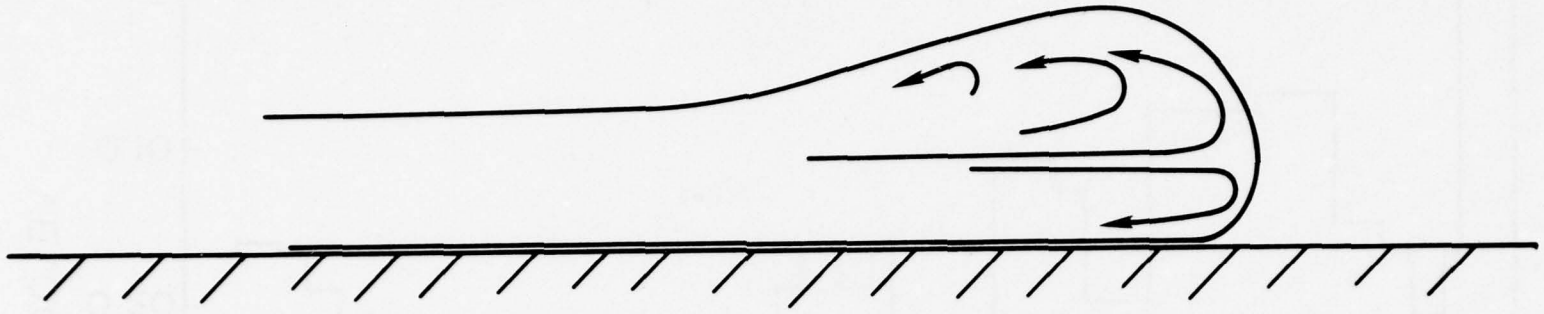

Figure 20. Schematic of internal circulation in the head of the surge (after Simpson, 1972).

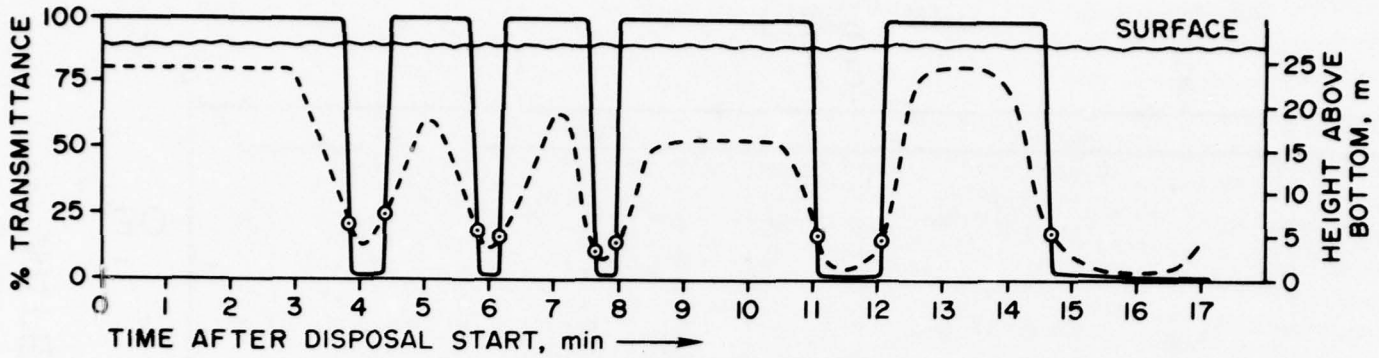

Figure 21a. Height of surge determined by vertical transmissometer profiles, New York Bight, 31 August 1976, Disposal 1.

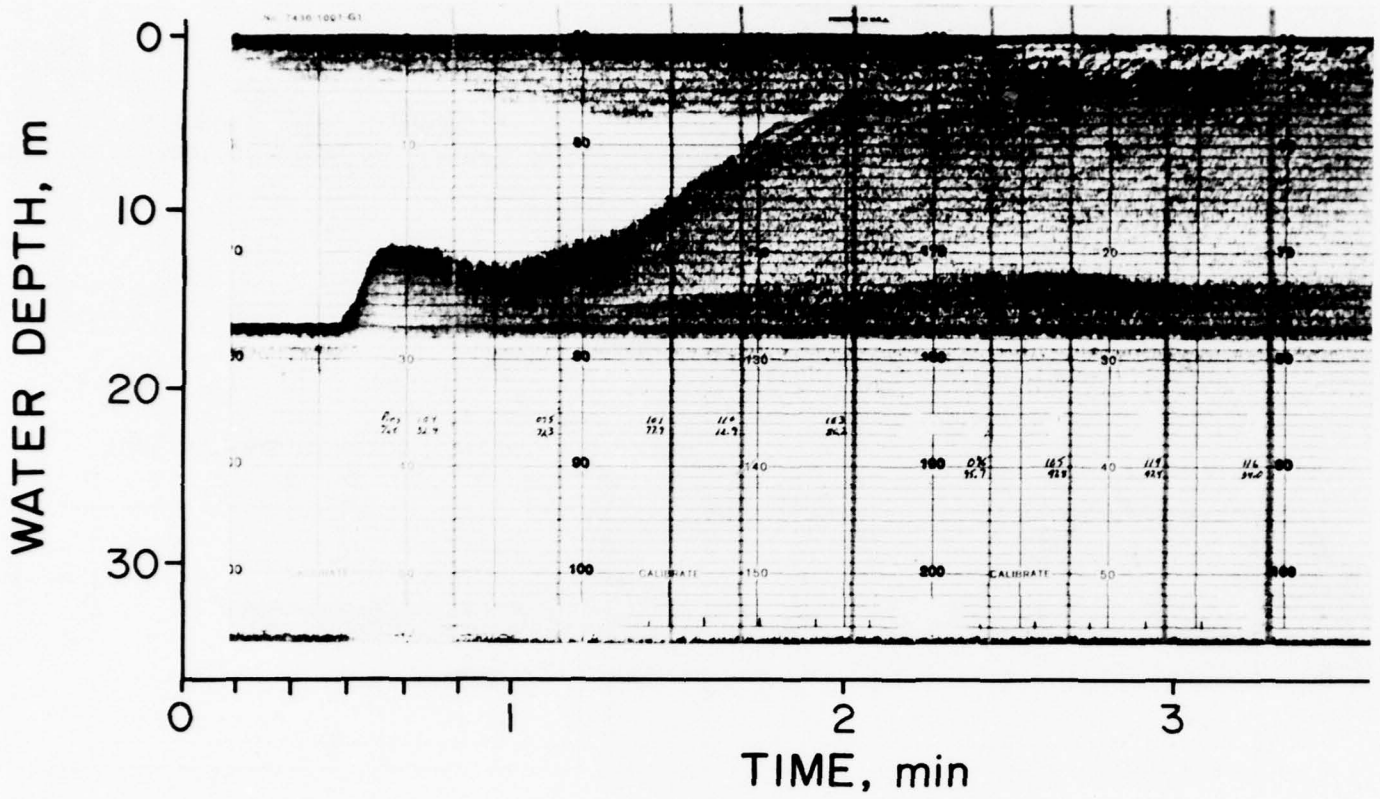

Figure 21b. Height of surge determined from 200-kHz record, 18 May 1977.

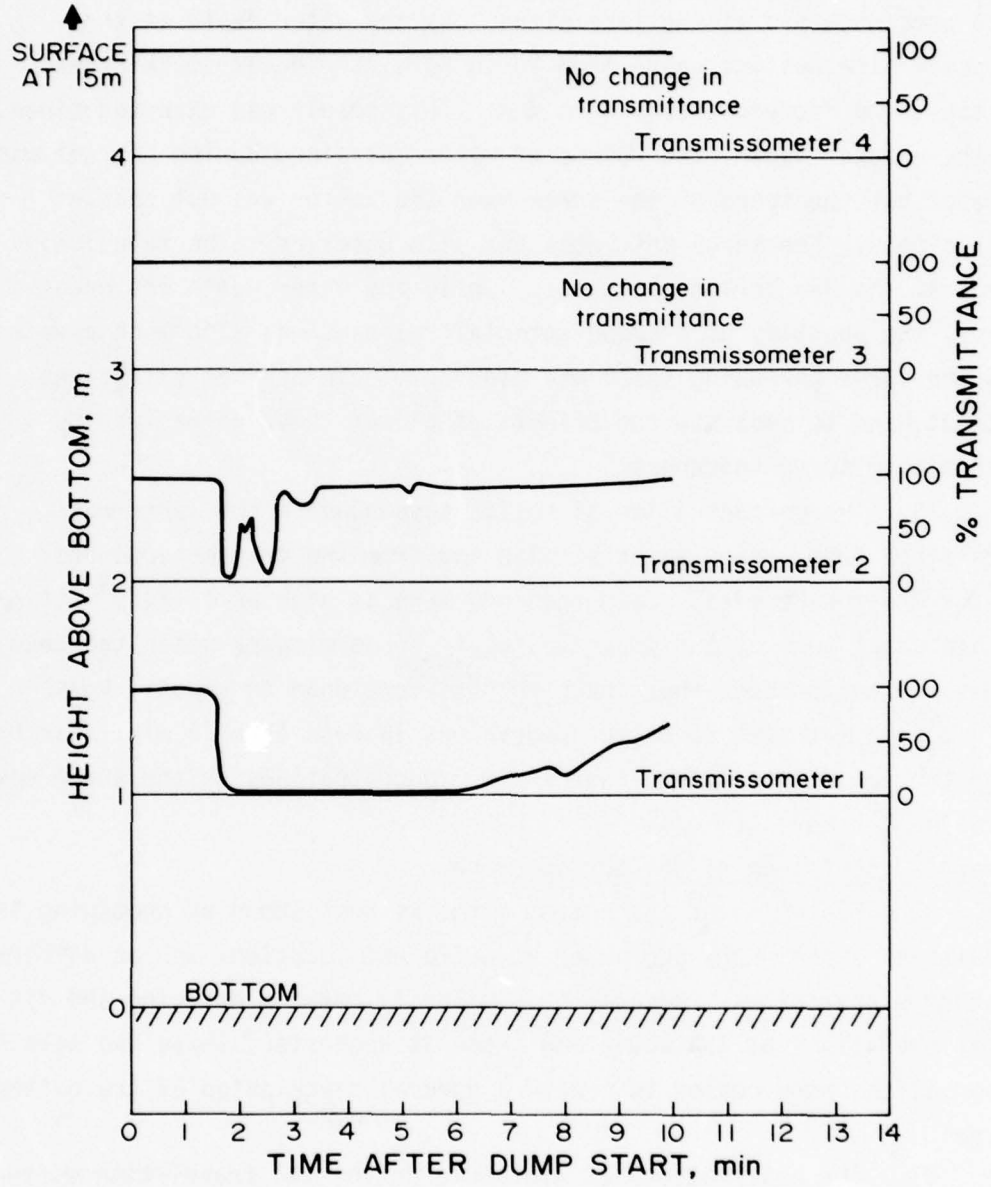

Figure 21c. Height of surge determined from four transmissometers in a vertical array, 26 May 1976.

78. The thickness of the bottom surge was found to depend on water depth; the greater the depth, the thicker the surge. The best data were obtained at the lake sites. As the water depth at the disposal site was increased from 20 to 50 m, the greatest thickness of the surge increased from 4 to 7 m. This result was expected since, at the greater depth, the volume of water entrained during descent was greater but the speed of the surge over the bottom was not changed appreciably. The surge thickness was also observed to be relatively large at the New York Bight sites. While the water depth was greater there, the quantity of dredged material released was also much greater and the surge spreading speed was higher. There are not sufficient data at hand to separate the effects of all of these variables in determining surge thickness.

79. The concentration of solids suspended in the surge was determined from pumped water samples and from the transmissometers. At the Great Lake sites concentrations were as high as 11 kg/m^3 (11 g/ℓ) within about 50 m of the impact point.* Three minutes after the head of the surge had passed, the concentrations were down to about 1 kg/m^3 (1 g/ℓ) and returned to background values in less than 15 min. Farther from the impact point, at about 150 m, concentrations in the surge never exceeded 3.0 kg/m^3 (3 g/ℓ).

General description of the bottom surge

80. Evolution of the bottom surge is best shown by combining the results of experiments performed at different locations and on different discharge operations. Because of similarity between dredging and disposal operations at Ashtabula and those at Rochester, these two sets of observations were pooled to create a general description of the bottom surge.

81. The observations at Ashtabula define the travel-time curve used in this description. Using this curve to define the time of arrival at any particular location, the subsequent variation in the surge height, the concentration of suspended material, and the velocity after the passage of the surge head were all plotted as a function of time and distance from the discharge point. These data were smoothed

* $1 kg/m^3$ = 1 g/ℓ.

to produce the contoured diagrams shown in Figures 22, 23, and 24.

82. A general description of the bottom surge is developed in the series of cross sections shown in Figure 25. The volume, sediment mass, and energy of the surge as it spreads over the bottom are shown in Figure 26 which has been constructed from the data in Figures 14, 22, 23, and 24. The first dredged material to leave the impact area moves outward in a thin layer about 3 m thick. The outward flow of water behind the advancing front of the surge is faster than the speed of advance of the front and, consequently, the surge height increases a short distance from the impact point. One-and-a-half minutes after the discharge the impact phase has come to an end and all the dredged material in motion is contained in the surge. (A small amount of material is in suspension throughout the water column over the impact area but this material accounts for only a few percent of the amount released.) At this time, 2.6×10^4 m^3 of water and dredged material are in motion (Figure 26). The total amount of sediment in motion is equal to the amount discharged; there has been no net loss and little net gain of sediment during impact. The energy loss during impact is probably also small since, when the impact is complete, the surge has an energy, H, of about 3.9 MJ. About half of this initial energy of the surge is stored as potential energy, ν, of the turbid cloud and the other half is the kinetic energy, τ, of the surge motion. This energy is dissipated as the dredged material moves away from the impact point. The surge thins and slows as it spreads, but a well-defined head and upper surface are maintained.

83. During descent the volume of dredged material and entrained water increases to $\sim$70 times the amount discharged. Entrainment continues as the surge spreads. The volume of the surge reaches a maximum value about 4 min after discharge when the surge is between 39 and 111 m from the center of the impact area. From the end of the descent phase until this time entrainment proceeds at a rate of 150 m^3/sec and the surge attains a volume of 4.9×10^4 m^3 or about 140 times the volume released. The volume of the surge then begins to decrease at about the same rate.

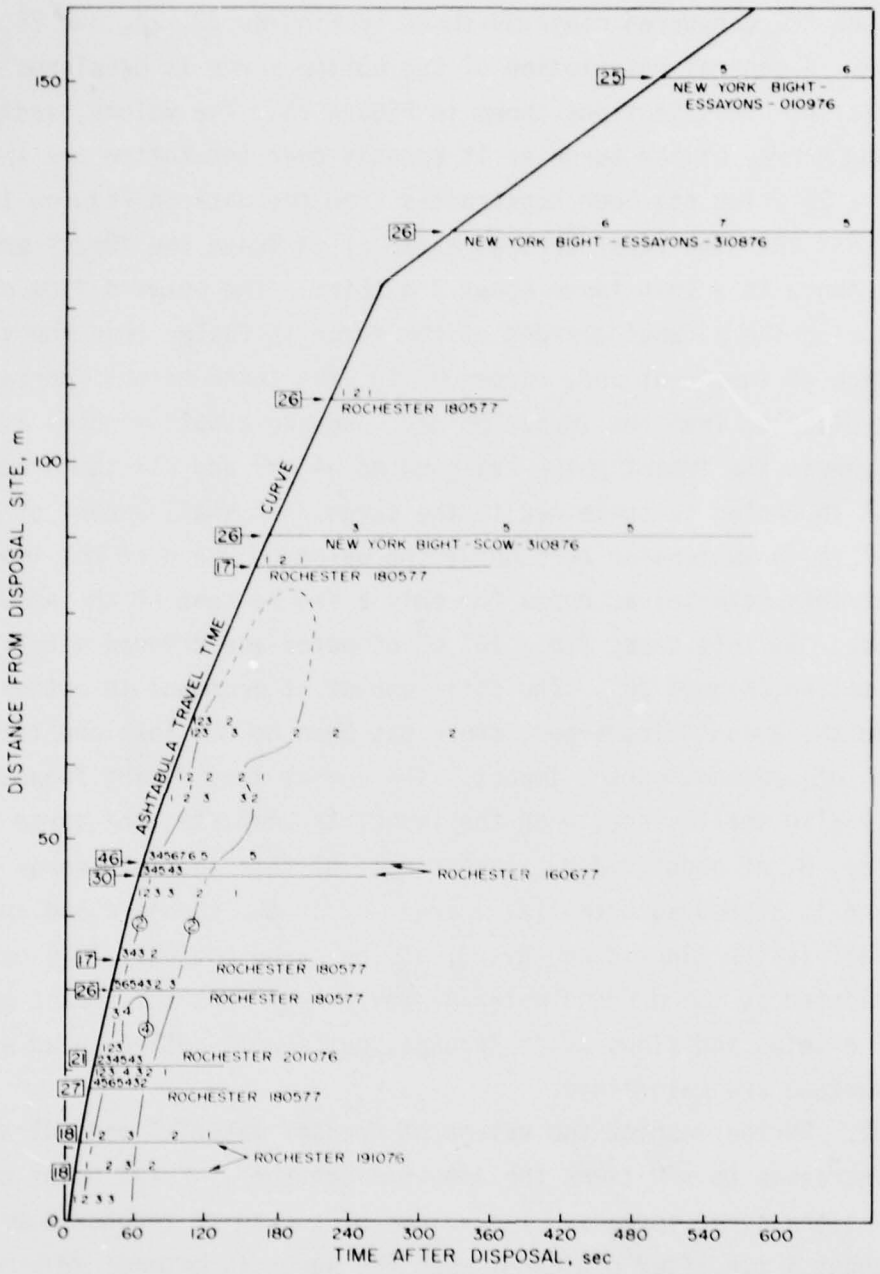

Figure 22. Contour diagram defining the height of the bottom surge. Contours drawn from vertical transmissometer profiles, Ashtabula and Rochester. Data on horizontal lines from 200-kHz records (except New York Bight: vertical transmissometer profiles). Figures in boxes are depth, in meters. Data adjusted to Ashtabula travel-time curve. Contour interval = 2 m.

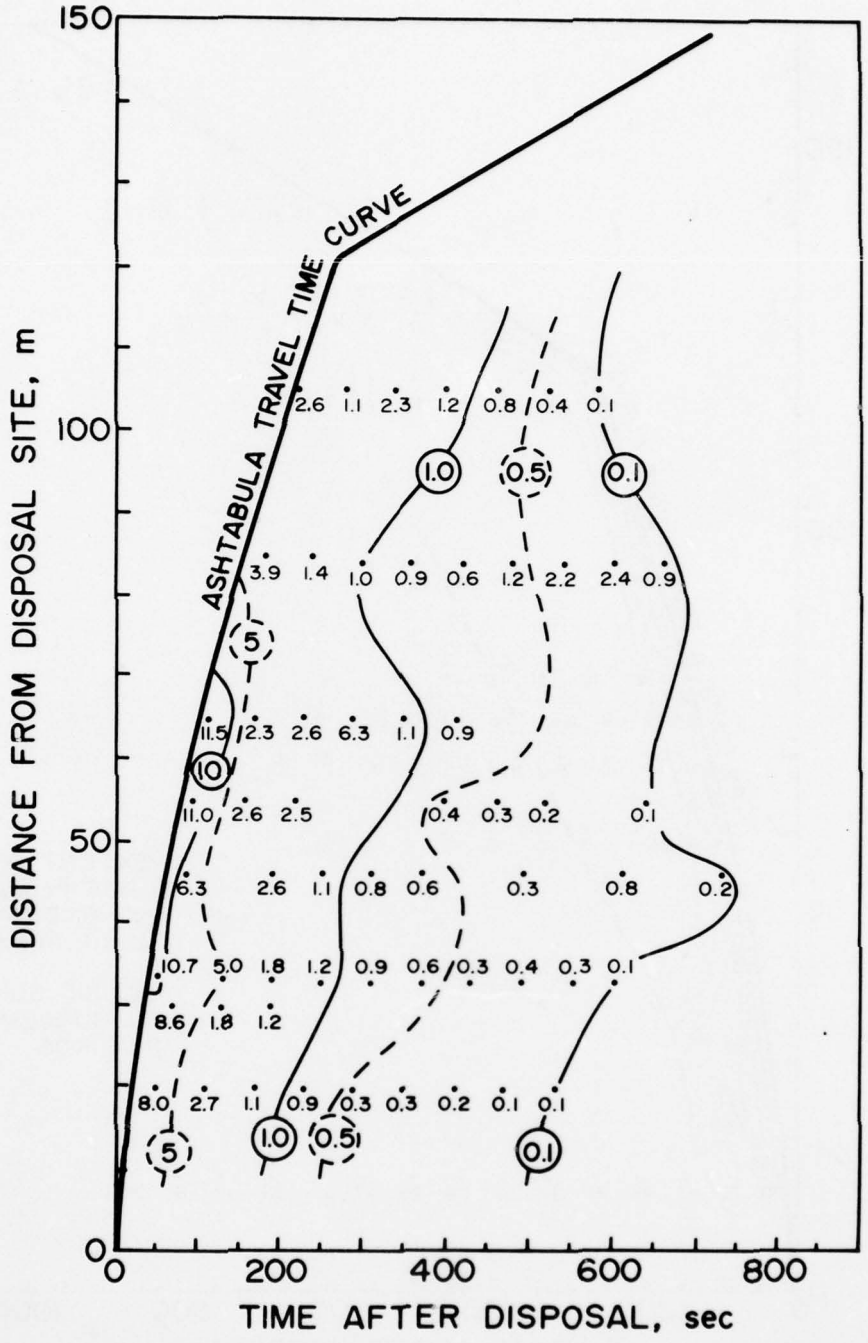

Figure 23. Contour diagram defining the concentration of suspended material in the bottom surge. Data from pumped samples concentration in kilograms per meter^3, adjusted to Ashtabula travel-time curve. Contour interval as noted.

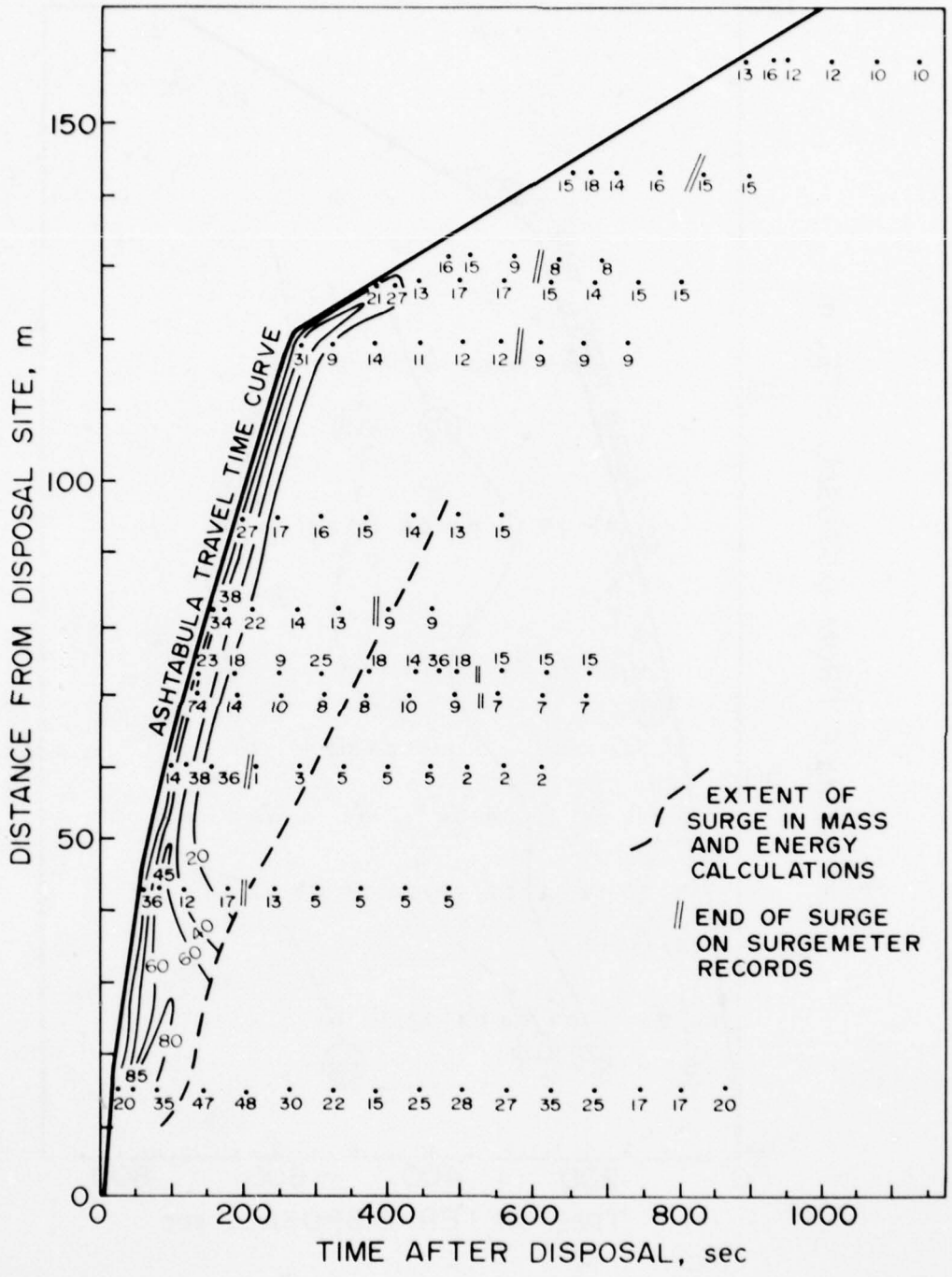

Figure 24. Contour diagram defining velocity of bottom surge after passing of head of surge. Data adjusted to Ashtabula travel-time curve. Contour interval 20 cm/sec.

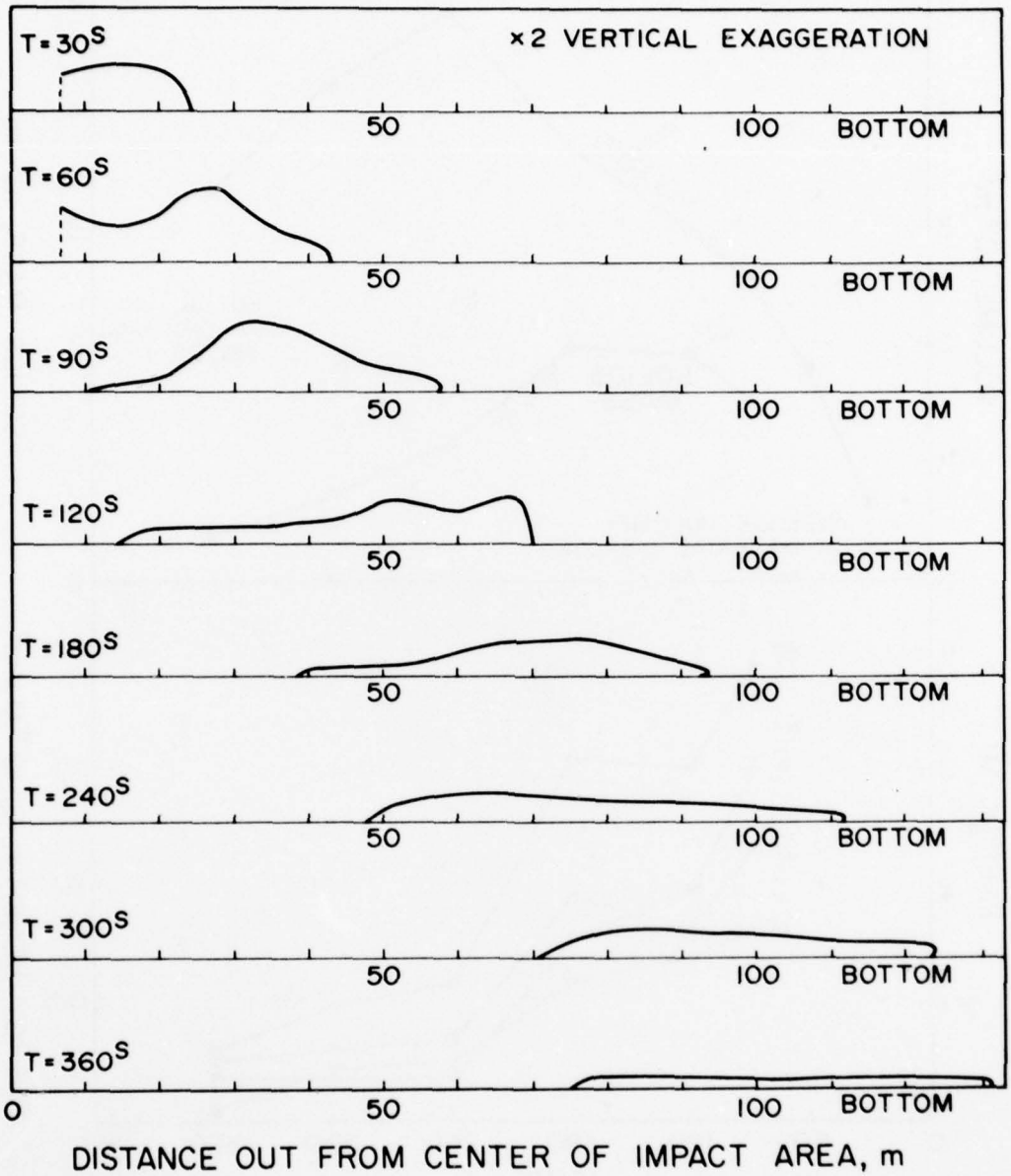

Figure 25. Cross sections showing development of surge at intervals after start of disposal.

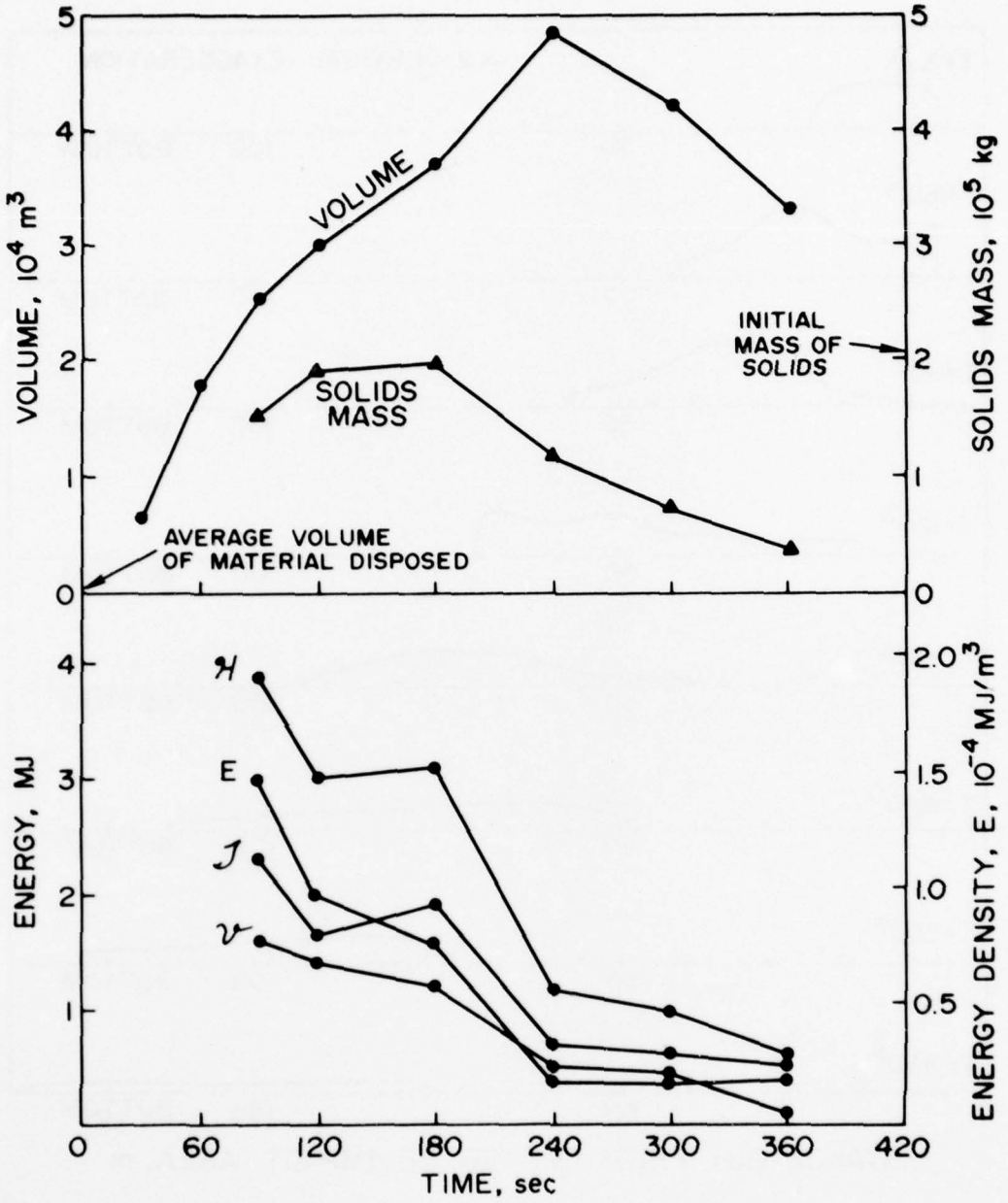

Figure 26. Volume, sediment content, and energy of bottom surge as it spreads over the bottom.

84. The water velocities within the surge are apparently sufficient to maintain the dredged sediment in suspension and adequate to cause a small amount of erosion of the lake floor during the initial stages of the surge. The total amount of sediment in motion in the surge increases slightly from the end of the impact phase 90 sec after the discharge to a time 120 sec after the discharge while the surge is between 15 and 69 m from the impact point (Figure 26). The mass of sediment in motion does not begin to decrease until the surge is between 39 and 93 m from the impact point. At this time, 180 sec after discharge, suspended sediment is lost from the surge at a rate of 10^3 kg/sec and settles to the lake floor at a rate of 1 cm/sec. At these rates almost all ($\sim$ 95%) of the suspended sediment should settle from the moving surge in about 4 min. If there is no lateral drift of this sediment during its settling, it will be deposited in a ring between $\sim$50 and 160 m from the impact point.

85. The range of the surge outwards from the impact area depends on its initial energy and the rate at which this energy is dissipated. During the spread of the surge, its kinetic energy may be increased either by the transfer of energy from moving water above the surge or by the conversion of potential energy to kinetic energy as the center of gravity of the suspended sediment sinks. The kinetic energy is lost primarily by friction along the top and bottom of the surge, by work done in entrainment of ambient water and against the pressure at the head of the surge. The surge energy is shown in Figure 26. After the impact phase is complete, the surge has a total energy of 3.9 MJ. Potential energy is converted to kinetic energy at a rate of about 0.006 Mw, as shown by the average slope of the v curve in Figure 26. As the ambient water is set in motion during the descent of the dredged material, the surge gains energy at an estimated rate of only about 0.0001 Mw. Energy is dissipated at a greater rate than it is gained. As the surge does work to entrain water, it loses energy at a rate of 0.015 Mw, the average slope of the H curve in Figure 26 from 90 to 240 sec. After entrainment is completed and the volume of the surge

begins to decrease, the rate of energy loss is reduced to 0.005 Mw, the slope of the H curve from 240 to 360 sec. Also, shown in Figure 26 is the curve of total energy density, E , of the surge. At these rates, all the surge energy will be lost in about 6.5 min. Since the surge is observed to persist for about 15 min, the net rate of energy loss must be further decreased towards the termination of the surge phase.

PART IV: CONCLUSIONS

Summary of the Placement Process

86. The successive steps in the process by which dredged material reaches its resting place on the bottom are summarized here. They apply for any disposal site, but the numerical values given in the examples are for disposal operations at the Great Lakes sites studied in this project.

87. The placement process starts with the dredged material at rest in the hoppers of the containing vessel at the disposal site. Its initial potential energy, which supplies the energy to drive all subsequent processes, depends on the mass of the dredged material and the water depth. For a typical 690-m^3 hopper dredge and a water depth of 18 m, the initial potential energy is 30 MJ.

88. Insertion of the dredged material into the receiving water starts as soon as the hopper doors are opened. The insertion speed is determined by the design of the doors, the hydraulic head of the dredged material in the hopper, and the properties of the material, particularly the water content. The form in which the dredged material is released depends on these same properties; it may enter the receiving water as a fluid, or as solid blocks (clods), or as any combination of these. Both the insertion speed and the form of the material released have important effects on the subsequent events in the placement process. Some of the initial potential energy of the dredged material is used in work done against friction in its passage out of the hopper doors. In the example used in this study, about 85 percent of the initial energy remains after insertion is completed.

89. Clods of dredged material reach their terminal velocity after fall through a small fraction of the water depth at the disposal site. The clods then descend at constant speed and are displaced by whatever current is flowing in the ambient water. The fluid component

of the material released falls to the bottom in a jet. Over the range of water depths studied, the descent speed is constant (unless there is a strong density gradient in the water column). A large amount of ambient water is entrained by the descending jet and much of the initial potential energy of the dredged material is lost. In the example, the volume of fluid reaching the bottom is 70 times greater than the volume of dredged material released at the surface and only 13 percent of the initial potential energy remains to enter the impact zone. Large-scale circulation is set up in the surrounding water by descent of the jet.

90. Clods of dredged material impacting the bottom may either disintegrate or deposit intact. The larger the block, the greater the probability of disintegration. If the blocks do not disintegrate, there is no further dispersion of the dredged material. With point dumping, a conical mound of dredged material will be formed on the bottom by the accumulating clods.

91. The impact of the fluid jet of dredged material with the bottom and the disintegration of clods generates a surge which spreads radially outwards. After impact is completed, the surge spreads as an expanding toroid; the expansion continues until the kinetic and potential energy of the surge are dissipated. The surge has a well-defined thickness which first increases and then decreases as the surge entrains ambient water and spreads outwards. Dredged material is deposited from the surge when its spreading velocity has sufficiently slowed. In the example, the surge entrains ambient water until its head reaches a radius of $\sim$110 m from the impact point; deposition of dredged material begins when the head is at a radius of $\sim$95 m and continues to $\sim$160 m. If point dumping is practiced, there will be erosion of the natural bottom at the impact point and the dredged material will form a deposit in the form of a circular ring surrounding the impact area. The radius of the ring depends on the water depth and the rate at which the surge loses energy as it spreads over the bottom.

92. The amount of dredged material lost to the ambient water in the placement process is very small, less than 1 percent in most cases.

Variables Controlling the Placement of Dredged Material

93. A large number of variables influence the quantitative aspects of the placement of dredged material at any given site. The variables that have been identified as most important are listed here. They are divided into two groups, those determined by the dredging and disposal methods chosen and those characteristic of the disposal site.

a. Dredging/disposal method.

i. Quantity of material released. In this study the quantities released ranged from 29 to 6120 m^3. The same qualitative behavior was observed at all of the sites. The data are not sufficient to separate the effects of the other variables but it appears that, for larger quantities, the thickness of the bottom surge and its range are increased. (The uncertainty arises because the observations with large quantities were made at sites where the water depth is also relatively great.)

ii. Insertion speed. A wide range of insertion speeds is possible depending on the design of the hoppers and the hopper doors and on the mechanical properties of the dredged material. Increased insertion speed favors injection of the dredged material into the receiving water as a fluid rather than as clods and decreases the travel time to the bottom. It also increases the spreading speed of the bottom surge. Its effect on entrainment during descent has not been determined.

iii. Properties of the dredged material. The cohesion and water content of the material to be released influence the insertion speed and the form assumed by the material when it reaches the receiving water. Insufficient data

are available to establish these relations on a quantitative basis.

iv. Speed of the discharging vessel. No data are available since all observations were taken with the discharging vessel stationary. It is expected that motion of the vessel at moderate speeds would be equivalent to the effect of current in the receiving water, discussed in the next section.

b. Disposal site characteristics

i. Depth. The same placement processes were observed to operate in water depths ranging from 15 to 67 m. There is no direct effect of depth on the descent of clods, since these quickly attain their terminal speed. For clods larger than 0.15 m, the terminal speed is greater than the maximum observed speed of the jet ($\sim$1.5 m/sec). Additional ablation is expected in the fall of clods in deeper water, but the magnitude of this has not been determined. In deeper water more entrainment occurs in the jet descent phase and there is more dilution of the dredged material before it reaches the bottom. There is no increase in the jet impact speed. The spreading speed of the bottom surge is not much increased so, because of the larger quantity of fluid entering the surge, its thickness is increased.

ii. Current in the receiving water. Because of the large entrainment, the descending jet will acquire the lateral velocity of the receiving water and the impact point will be displaced. The amount of this displacement is easily calculated. The lateral drift of descending clods can be calculated by the same methods used to find their fall speed. At the Saybrook disposal site the placement of the dredged material took

place under strong tidal currents. Since the same processes were observed under these conditions, it appears that a strong current in the receiving water need not be a serious impediment to the accurate placement of the dredged material nor will it result in undue dispersion during placement. The spread of the bottom surge is not influenced by the current but the wake water left behind the moving surge will drift with the current. However, the wake water carries only a relatively small amount of the dredged material.

iii. Density gradient in the water column. A sufficiently great density gradient in sufficiently deep water can result in arrest of the descent phase. The depth at which this will occur can be calculated. Although highly stratified conditions may be encountered it is most unlikely that deep enough water would be encountered in any dredged material disposal operation in coastal waters or lakes.

iv. Bottom hardness. If the bottom is soft, part of the kinetic energy of clods falling on the impact area will be expended in plastic deformation of the bottom. The greater the energy so used, the less will be available to cause disintegration of the clods. A soft bottom is expected, therefore, to reduce the dispersion of dredged material falling in the form of clods.

v. Critical erosion velocity of the bottom. The more susceptible the natural bottom at the disposal site is to erosion, the greater will be the amount of sediment mixed with the dredged material in the impact area. Erosion in the impact area will result in dilution of the dredged material by sediment from the disposal site before its final deposition. Repeated discharges

at one point may result in the formation of a crater in the impact area.

vi. Bottom slope. If the bottom in the disposal area is not horizontal, there will be an additional term due to gravity in the energy balance equation for the bottom surge. If the bottom slopes upwards from the impact point, the rate of loss of energy from the surge will be increased and the range of the surge reduced. No observations of this effect have been made. However, the slope of the sides of a pit designed to retain dredged material within a defined area on the bottom could be calculated from the surge energy data given in this report. The design of such retention pits is a subject worthy of further investigation.

vii. Bottom roughness. The greater the roughness of the bottom in the disposal area, the greater will be the rate of loss of surge energy. The surge is expected to have a shorter range over a rough bottom than a smooth one. The friction law for the flow of the surge over the bottom would have to be worked out to put this relation in quantitative form. It may be useful to introduce artificial roughness elements on the bottom to limit the range of the surge at some disposal sites.

94. A total of 11 important variables controlling the disposal process have been listed above. It is clear that the separate effects of each of these can not be found from field measurements at a small number of disposal sites. However, good data on several of these -- such as the water depth--have been acquired. Further field work will permit evaluation of the others. Specific field programs to determine them separately could be designed to optimize the use of research resources.

Further Research

95. An important objective for future research is to find the dependence of the placement process on the site and material variables identified in this study. Field studies are needed to find:

a. The friction law for spread of the bottom surge and its dependence on roughness and turbulence in the ambient water.

b. The dependence of the surge speed and range on the quantity of dredged material released.

c. The relation between the mechanical properties of the dredged material and the insertion speed, the formation of clods, and the impact properties of the solid material that reaches the bottom.

d. How hopper design and operation influence the processes listed under c above.

e. The maximum speed of the discharging vessel at which the disposal processes described in this report will still continue to operate.

96. A compact deposit of dredged material--such as is required to minimize dispersion by a tidal stream or other currents--is formed only when most of the material released makes its way to the bottom in the form of clods that do not disintegrate upon impact. The preliminary experiments described in Appendix H should be developed to find the relation between dispersion and mechanical properties of the dredged material. For example, the impact tests that have been done in air should be done under water. The relation between impact strength and properties of the dredged material that can be measured in the field should be found by laboratory testing and confirmed in field studies.

97. The studies reported here provide the basis for the design of a pit containment disposal site. Such a site could be of great value in disposing of dredged material that is too contaminated to make dispersion acceptable. A field trial of a containment pit would be a valuable test of the practicality of many of the results reported here.

AD-A055 647 YALE UNIV NEW HAVEN CONN DEPT OF GEOLOGY AND GEOPHYSICS F/G 8/8
FIELD STUDY OF THE MECHANICS OF THE PLACEMENT OF DREDGED MATERI--ETC(U)
APR 78 H J BOKUNIEWICZ, J GEBERT, R B GORDON DACW39-76-C-0105
UNCLASSIFIED WES-TR-D-78-7-VOL-1 NL

2 OF 2
AD A055 647

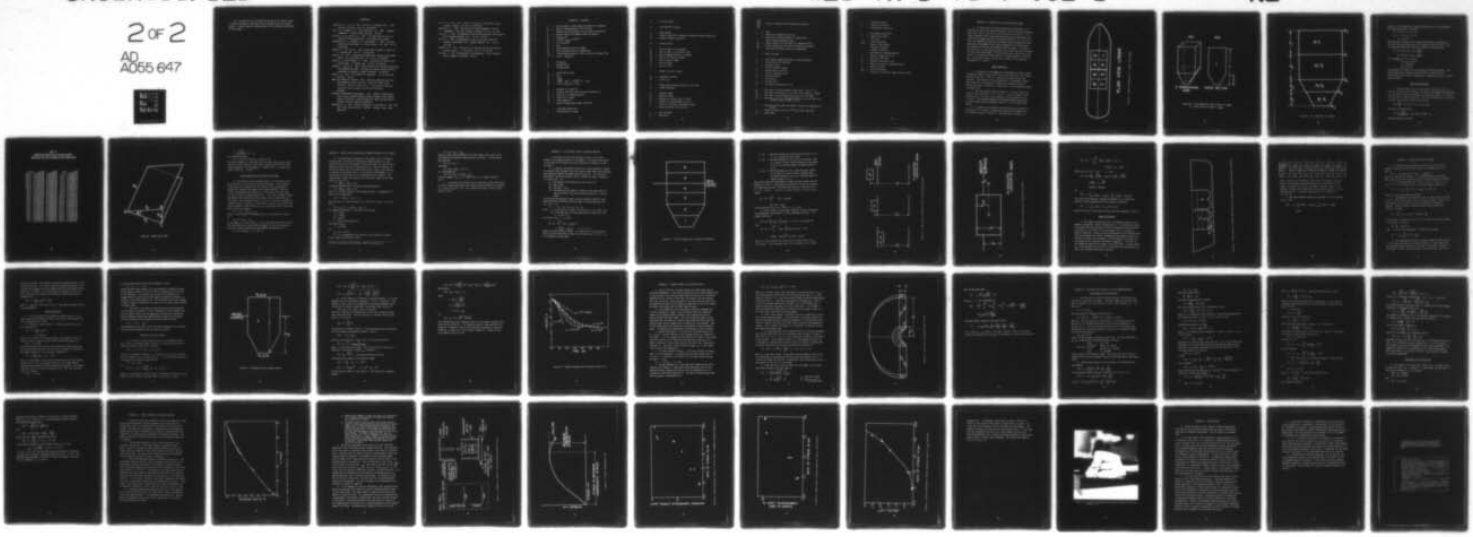

END
DATE FILMED
8-78
DDC

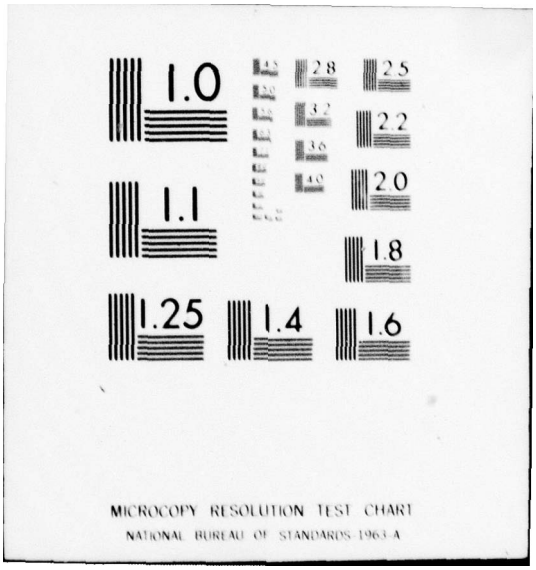
1.0
1.1
1.25
1.4
1.6
2.8
2.5
3.2
2.2
3.6
2.0
4.0
1.8
MICROCOPY RESOLUTION TEST CHART
NATIONAL BUREAU OF STANDARDS-1963-A

98. The hydraulics of the bottom surge and of jet descent should be studied, perhaps by laboratory tests on appropriately scaled model systems. A better physical understanding of the entrainment coefficient is also needed.

REFERENCES

Albertson, M. L. et al. 1950. Diffusion of submerged jets. Trans. Am. Soc. Civil Eng. Vol 115: pp 639-697.

Bird, R. B., Stewart, W. E., and Lightfoot, E. N. 1960. Transport phenomena. J. Wiley & Sons, New York. 780 pp.

Bishop, A. W. and Henkel, D. J. 1957. The measurement of soil properties in the triaxial test. Edw. Arnold, Ltd, London.

Bokuniewicz, H. J., Gordon, R. B., and Kastens, K. 1976. Form and migration of sand waves in a large estuary. Mar. Geol. Vol 24: pp 185-199.

Gedney, R. T. and Lick, W. 1972. Wind-driven currents in Lake Erie. J. Geophys. Res. Vol 77: pp 2714-2723.

Gordon, R. B. 1974. Dispersion of dredge spoil dumped in near-shore waters. Est. and Coast. Mar. Sci. Vol 2: pp 349-358.

Gordon, R. B. and Pilbeam, C. C. 1975. Circulation in Central Long Island Sound. J. Geophys. Res. Vol 80: pp 414-422.

Hayashi, T. and Ito, M. 1975. Initial dilution of effluent discharging into stagnant sea water. Discharge of sewage from sea outfalls, supplement to Progress in Water Technology. pp 253-263.

Lambe, T. W. 1951. Soil testing for engineers. J. Wiley and Sons, New York. 165 pp.

NALCO Environmental Sciences. 1976. Hydraulic regime of Lake Erie near Ashtabula, Ohio, June 1975 - June 1976, NALCO ES No. 550107040. Quarterly Report to U. S. Army Engineer Waterways Experiment Section prepared by NALCO Environmental Sciences.

Northwest Environmental Consultants. 1976. Sediment investigation: pilot survey, Duwamish Waterway aquatic disposal field investigation, Elliott Bay, Contract report for NOAA, National Marine Fisheries Service, Seattle, Washington.

Paskausky, D. F. 1971. Winter circulation in Lake Ontario. Proc. 14th Conf. Great Lakes Res 1971: 593-606. Internat. Assoc. Great Lakes Res.

Proni, J. R. et al. 1976. Acoustic tracking of ocean-dumped sewage sludge. Science. Vol 193: pp 1005-1007.

Redfield, A. C. 1950. The analysis of tidal phenomena in narrow embayments. Pap. Phys. Oceanogr. Meteorol. Vol 11: pp 1-35.

Riley, G. A. 1952. Hydrography of Long Island and Block Island Sounds. Bull. Bingham Oceanogr. Coll. Vol 13: pp 5-39.

Riley G. A. 1956. Oceanography of Long Island Sound, 1952-1954. Physical oceanograph. Bull. Bingham Oceanogr. Coll. Vol 15: pp 15-46.

Simpson, J. E. 1972. Effects of the lower boundary on the head of a gravity current. J. Fluid Mech. Vol 53: pp 759-768.

Williams, J. 1973. Oceanographic instrumentation. Naval Institute Press, Annapolis, Maryland. 189 pp.

APPENDIX A: NOTATION

A = area of section across which jet velocity is measured

A_i = area of bottom surface of $i^{\underline{th}}$ subvolume

$\bar{A}$ = effective cross-sectional area of vessel at waterline

A_j = surface area of jet between vessel and bottom

$A_s = 18 \nu \rho_w / \rho_a \, D^2$

$A_t = (111/8) \, (\rho_w/\rho_a) \, v^{3/5}/D^{1.6}$

$A_u = 0.33 \, (\rho_w/\rho_a)/D$

$A_v = A_u/2$

A_o = cross-sectional area of a hopper

A_4 = cross-sectional area of a hopper door

A_{16} = cross-sectional area of a jet 16 m below the hopper door

$a = \rho/2 \, [1 - (A_4/A_o)^2]$

$B = g(1-\rho_w/\rho_a)$

B_f = buoyant force

$b = 4\mu(A_4/A_o)h/R_h^2$

C_D = coefficient of drag

$C_1 = B/A_s$

$C_2 = -B/A_s^2$

$C_3 = \sqrt{A_u/B} \, \tanh^{-1} \, (\sqrt{A_u/B} \, \dot{z}_2) - A_u t_2$

$C_4 = -1/2 \, \ln \, (B/A_u - \dot{z}_2^2) - A_u z_2$.

D = diameter of a particle

d_i = distance from lake level to bottom surface of V_i

d_1 = draft full of dredged material

d_2 = draft full of water

d_3 = draft pumped dry

d = depth of hopper doors below lake level

ε = frictional energy loss

E = energy density of surge

f = friction factor

g = gravitational constant

H = total energy

h = height of material in hoppers or height of hopper subdivision

h_i = height of hopper subvolume i

KE = kinetic energy

M = mass of water to fill hoppers

M_c = mass of water in cylindrical flow

M_d = mass of dredged material in hoppers

M_i = mass of $i^{\underline{th}}$ layer of hoppers

M_o = mass of vessel, empty

m = mass of sphere

m_s = mass of solids

n = number of layers in model

p_o = atmospheric pressure

p_4 = p_o plus $\rho_w d$

Q = volume passing through section at flow meter

Q_o = volume discharged

R_e = Reynolds number

R_h = hydraulic radius

R_o = distance to trailing edge of toroid

R_1 = distance to leading edge of toroid

r = radius in cylindrical coordinate system

$\bar{r}$ = effective radius of the orifice

s = shear strength

S_t = sensitivity

S_1, S_2, S_3 = sides of triangle for door opening calculation

t = time

T = duration of downward flow in jet

τ = total kinetic energy through all hopper doors

τ' = kinetic energy through one door

τ'_{16} = kinetic energy past flow meter 16 m below bow doors

τ''_{16} = kinetic energy pass flow meter 16 m below stern doors

Δt = time interval between successive measurements

$\bar{u}$ = mean flow speed

V = total hopper volume available or volume discharged

V_i = volume of the $i^{\underline{th}}$ subvolume

ν = potential energy

ν_o = initial potential energy

$\bar{v}$ = average velocity across A

v_i = velocity measured in jet

v_t = terminal velocity

v = jet velocity

v_o = velocity at A_o

v_4 = jet velocity through doors, A_4

W_i = work done in raising center of mass from Z = 0 to $Z = Z_i$

W_i' = work done to bring top of V_i to lake level, where Z_o = depth

W_i'' = work done to bring bottom surface of V_i to lake level

W_i''' = work done to lift V_i from where bottom of V_i is at lake level to where center of mass is at Z_i

Z = height of orifice above the bottom, cylindrical coordinate for height

Z_i = height of center of mass of $i^{\underline{th}}$ layer above lake floor

Z_o = water depth

z = distance traveled

$\dot{z}$ = velocity of particle

$\ddot{z}$ = acceleration of particle

α = entrainment coefficient

β = angle of jet spread

γ = $-g(\rho h - \rho_w d)$

ε_{max} = strain at maximum

θ = angle of door opening

μ = effective viscosity

ν = kinematic viscosity

ρ = bulk density of dredged material

ρ_a = density of particle in air

ρ_i = density of $i^{\underline{th}}$ layer

ρ_m = density of material in jet

ρ_s = density of solids in dredged material

ρ_w = density of water

σ_{max} = stress at maximum

ϕ = cylindrical coordinate, angle around cylinder

APPENDIX B: DIMENSIONS OF THE HOPPER DREDGE LYMAN

1. In describing the disposal operations at Rochester, it is necessary to define the hopper dimensions, the rate at which the hopper doors open, and the mass and cross-sectional area of the ship. The hopper dimensions were either measured directly or obtained from blueprints of the Lyman supplied by the Buffalo District, CE. The rate at which the hopper doors open was calculated from the dimensions of the doors and a measurement of the rate of movement of a telltale which was attached to the door and extended above the hopper. The mass of the ship and its cross-sectional area at the water line were calculated from the draft measurements. These dimensions were used in the calculation of the density and total amount of dredged material in the hopper, its potential energy, and the rate at which it was discharged (Appendices C, D, and E).

Hopper Dimensions

2. The hoppers of the Lyman may be represented by eight volumes arranged as shown in Figure B1, in two sets of four with a low bulkhead between the two sets. There is a door at the bottom of each subdivision. Each volume is in turn comprised of a rectangular volume which tapers at its bottom as a frustum of a pyramid to the door opening, as shown in Figure B2a. Figure B2b is a cross section through one subdivision.

3. The total hopper volume available, V, is 703 m^3; hence the volume of each subdivision is V = 87.9 m^3. The total height of each subdivision, h, is 6.40 m, and the height of the pyramidal section is 1.83 m. The bulkhead separating the forward hopper section from the stern hopper section extends to within 1.5 m of the top of the hoppers.

4. In general, for estimating the distribution of sediment in the hoppers, it is useful to divide each section of the hopper into four layers as shown in Figure B3. Each layer has a volume V_i, a

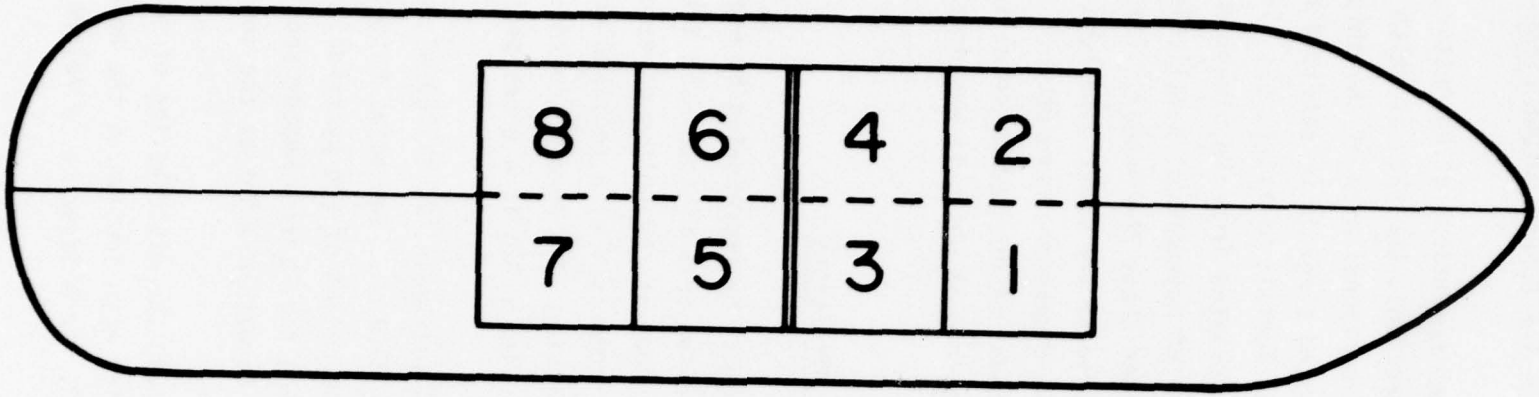

PLAN VIEW, LYMAN

Figure B1. Hopper configuration, U.S. Hopper Dredge Lyman.

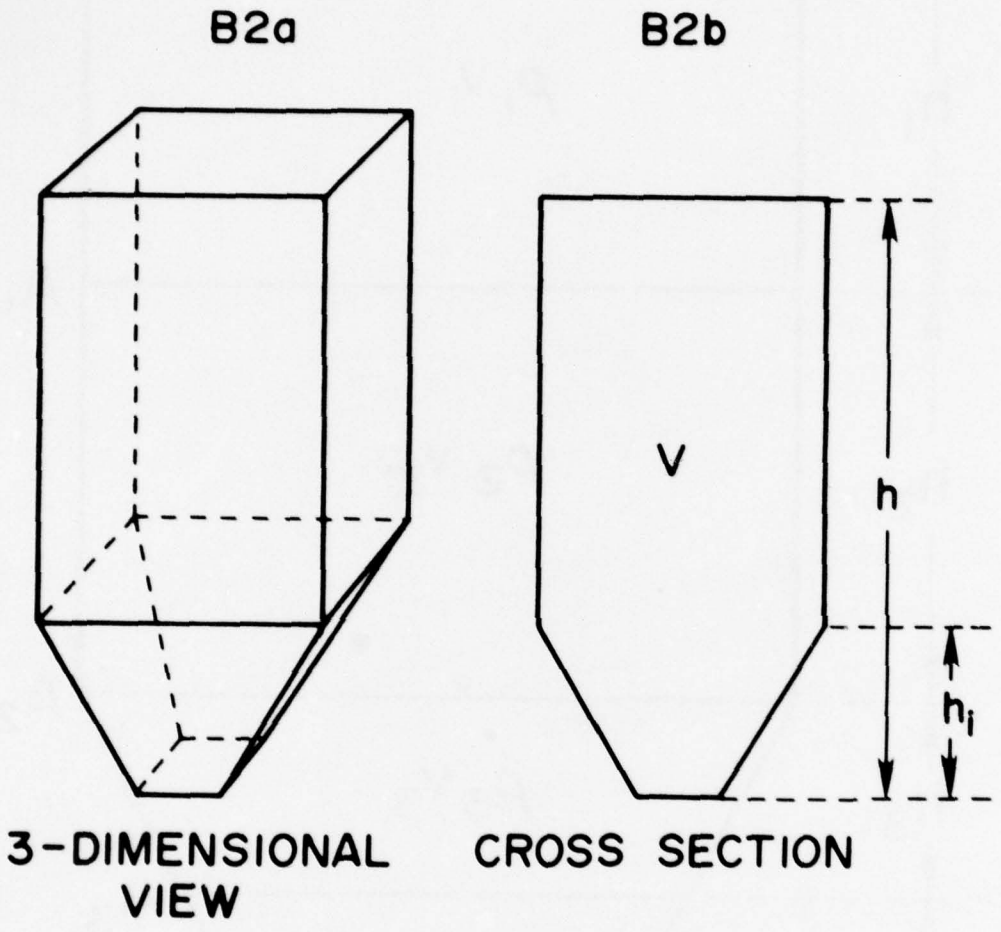

Figure B2a. Three-dimensional view of hopper on Lyman.
b. Cross section of hopper on Lyman.

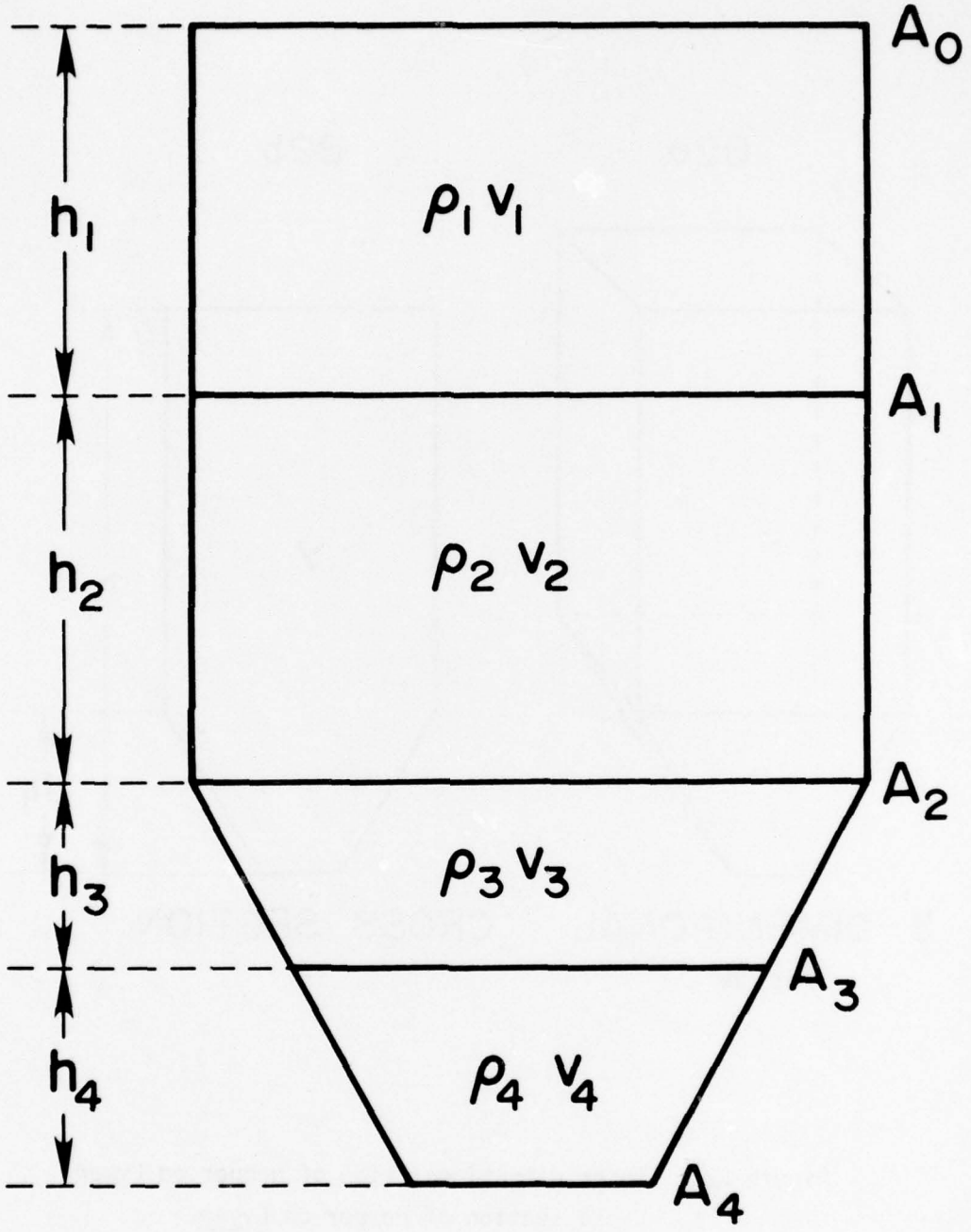

Figure B3. Four subvolumes of a hopper.

height h_i and is bounded by a cross-sectional area A_i on the bottom of the layer (Figure B3). Of course,

$$(1)\quad V = V_1 + V_2 + V_3 + V_4$$

$$(2)\quad h = h_1 + h_2 + h_3 + h_4$$

$$A_4 = 1.30\ m^2$$

Note that A_4 is the area of the hopper door opening, and that $8A_o$ is the total cross-sectional area of the hoppers, equal to $50.8\ m^2$. For the truncated pyramid the following geometrical relations hold:

$$(3)\quad V_3 = \frac{1}{3} h_3 (A_2 + A_3 + \sqrt{A_2 A_3})$$

$$V_4 = \frac{1}{3} h_4 (A_3 + A_4 + \sqrt{A_3 A_4})$$

For the Lyman, $h_3 + h_4 = 1.829\ m$

$V_3 + V_4 = 15.32\ m^3$

$A_2 = 18.86\ m^2$

$A_4 = 1.03\ m^2$

The quantities in Table B1 are calculated from these dimensions. The total volume of all eight pyramidal frustra is $123\ m^3$; for each pyramid the center of mass is located at a distance of $0.77\ h_i = 1.402$ m above the door.

Rate of Door Opening

5. The doors take 18 sec to fully open, and the exit area as a function of time may be calculated. One door on the hoppers has dimensions S_1, S_2 as shown in Figure B4 and open at a rate $d\theta/dt$ where t is time and θ is the angle of the door opening. Since the triangle ABC is an isosceles triangle, the following relation may be given:

$$(4)\quad \frac{S_3/2}{S_1} = \sin(\theta/2),\ S_3 = 2S_1 \sin(\theta/2)$$

The area of triangle ABC is:

$$(5)\quad \frac{1}{2} \frac{S_3/2}{\tan(\theta/2)} \cdot S_3 \text{ or } \frac{1}{2} S_1 \sin\left(\frac{\theta}{2}\right) \cdot S_3$$

Hence the total exit area is

TABLE B1

Quantities Determined by Truncated Pyramid

Dimensions for Area of Hopper on the Dredge Lyman

H3, cm	V3, cm^3	A3, cm^2	H4, cm	V4, cm^3
177.8	0.1525E+08	0.1531E+05	5.3	0.6736E+05
167.1	0.1508E+08	0.2031E+05	15.8	0.2376E+06
157.8	0.1489E+08	0.2531E+05	25.1	0.4328E+06
149.4	0.1467E+08	0.3031E+05	33.5	0.6503E+06
141.7	0.1443E+08	0.3531E+05	41.2	0.8880E+06
134.5	0.1418E+08	0.4031E+05	48.4	0.1145E+07
127.8	0.1390E+08	0.4531E+05	55.1	0.1419E+07
121.4	0.1361E+08	0.5031E+05	61.5	0.1709E+07
115.3	0.1330E+08	0.5531E+05	67.6	0.2015E+07
109.6	0.1298E+08	0.6031E+05	73.3	0.2336E+07
104.0	0.1265E+08	0.6531E+05	78.9	0.2671E+07
98.6	0.1230E+08	0.7031E+05	84.3	0.3020E+07
93.5	0.1194E+08	0.7531E+05	89.4	0.3382E+07
88.5	0.1156E+08	0.8031E+05	94.4	0.3757E+07
83.7	0.1118E+08	0.8531E+05	99.2	0.4144E+07
79.0	0.1078E+08	0.9031E+05	103.9	0.4542E+07
74.4	0.1037E+08	0.9531E+05	108.5	0.4953E+07
70.0	0.9946E+07	0.1003E+06	112.9	0.5374E+07
65.6	0.9513E+07	0.1053E+06	117.3	0.5807E+07
61.4	0.9069E+07	0.1103E+06	121.5	0.6251E+07
57.3	0.8616E+07	0.1153E+06	125.6	0.6704E+07
53.2	0.8152E+07	0.1203E+06	129.7	0.7168E+07
49.3	0.7678E+07	0.1253E+06	133.6	0.7642E+07
45.4	0.7194E+07	0.1303E+06	137.5	0.8126E+07
41.6	0.6700E+07	0.1353E+06	141.3	0.8620E+07
37.8	0.6197E+07	0.1403E+06	145.1	0.9123E+07
34.1	0.5685E+07	0.1453E+06	148.8	0.9635E+07
30.5	0.5164E+07	0.1503E+06	152.4	0.1016E+08
27.0	0.4634E+07	0.1553E+06	155.9	0.1069E+08
23.5	0.4095E+07	0.1603E+06	159.4	0.1123E+08
20.1	0.3547E+07	0.1653E+06	162.8	0.1177E+08
16.7	0.2991E+07	0.1703E+06	166.2	0.1233E+08
13.3	0.2426E+07	0.1753E+06	169.6	0.1289E+08
10.1	0.1854E+07	0.1803E+06	172.8	0.1347E+08
6.8	0.1273E+07	0.1853E+06	176.1	0.1405E+08
3.6	0.6837E+06	0.1903E+06	179.3	0.1464E+08

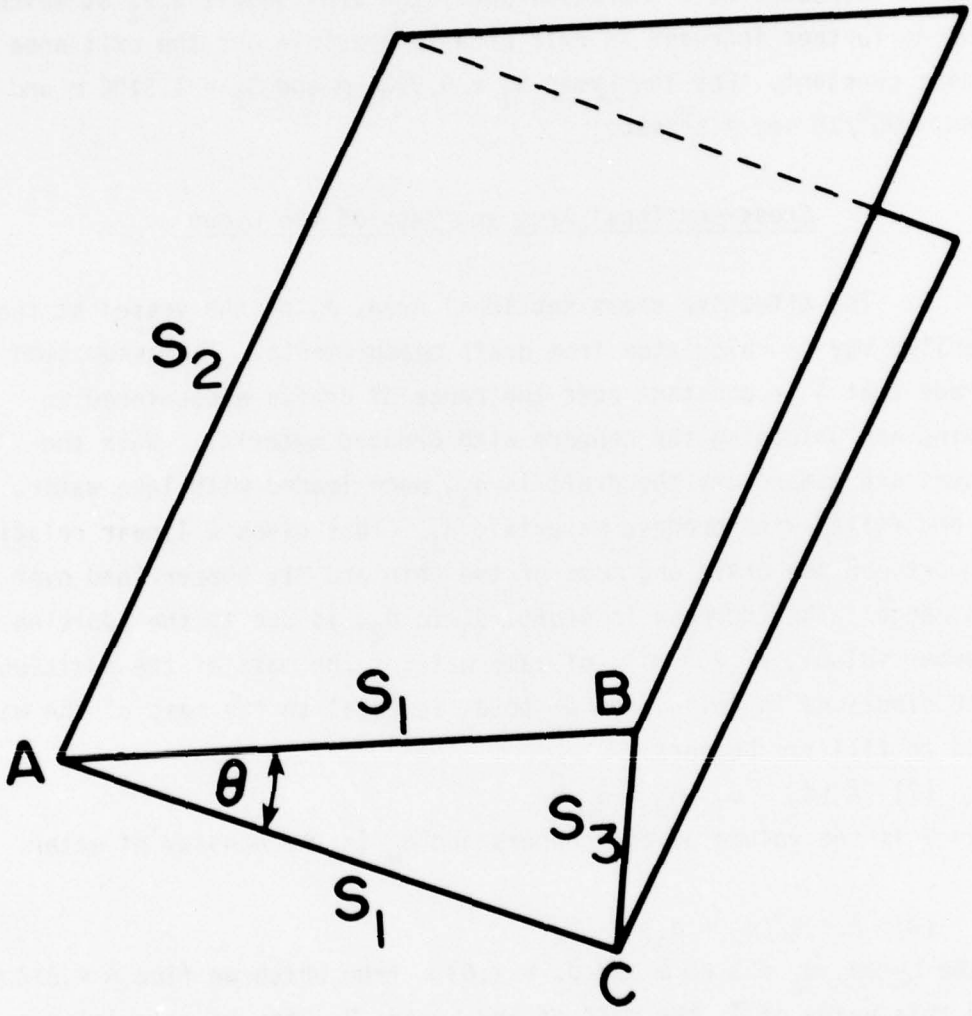

Figure B4. Hopper door sketch.

$$A = \frac{S_3^2/2}{\tan(\theta/2)} + S_3 \times S_2$$

So, rearranging terms,

(6) $A = 2S_1 \sin(\theta/2)[S_1 \cos(\theta/2) + S_2]$

The area increases as θ increases until the area equals S_2S_1 at which point no further increase in exit area is possible and the exit area remains constant. For the Lyman S_1 = 0.9906 m and S_2 = 1.3106 m and $d\theta/dt \sim 90^o/18$ sec = 5^o/sec.

Cross-sectional Area and Mass of the Lyman

6. The effective cross-sectional area, $\bar{A}$, of the vessel at the waterline may be calculated from draft measurements. The assumption is made that $\bar{A}$ is constant over the range of drafts encountered in loading and unloading the hoppers with dredged material. When the hoppers are pumped dry the draft is d_3, when loaded with lake water, d_2, and filled with dredged material, d_1. This gives a linear relationship between the draft and mass of the ship and its hopper load over this range. The increase in draft, d_3 to d_2, is due to the addition of a hopper volume, V (703 m^3), of lake water. The mass of the additional water displaced in going from d_3 to d_2 is equal to the mass of the water added to fill the hoppers.

(7) $\bar{A}(d_2 - d_3)\rho_w = \rho_w V$

where V is the volume of the hoppers and ρ_w is the density of water. So,

(8) $\bar{A} = V/(d_2 - d_3)$

On the Lyman, d_2 = 3.68 m and d_3 = 2.63 m from which we find $\bar{A}$ = 670 m^2. With this value of $\bar{A}$, the mass of the Lyman, M_o, may be calculated as the mass of water displaced when the hoppers are pumped dry, or

(9) $M_o = \bar{A}\rho_w(d_3) = 1.7 \times 10^6$ kg.

APPENDIX C: DENSITY AND DISTRIBUTION OF DREDGED MATERIAL IN THE HOPPER*

1. The total mass of material in the hoppers may be calculated from the draft of the vessel loaded with dredged material, d_1, the draft of the ship with the hoppers filled with water, d_2, and the cross-sectional area of the ship at the waterline, $\bar{A}$. When the hoppers are filled with water the total weight of the ship is $g(M_o + V\rho_w)$ where M_o is the mass of the empty ship, V is the volume of the hoppers, ρ_w is the density of water and g is the acceleration due to gravity. The total weight of water displaced by the ship must be equal to the total weight of the ship or

(1) $g\bar{A}d_2\rho_w = g(M_o + V\rho_w)$

Likewise, when the ship is filled with dredged material,

(2) $g\bar{A}d_1\rho_w = g(M_o + V\rho)$

where ρ is the bulk density of the dredged material. Subtracting (1) from (2) and rearranging,

(3) $\rho = [\frac{\bar{A}}{V}(d_1 - d_2) + 1]\rho_w$

The total mass of dredged material, m_d, (solids plus water) in the hopper is

(4) $M_d = \rho V = \rho_w [\bar{A}(d_1 - d_2) + V]$

For disposal operation No. 8 on 191076 at Rochester:

$d_1 = 3.865$ m

$d_2 = 3.680$ m

$\bar{A} = 670$ m^2

$V = 703$ m^3 (See Appendix B).

With these values,

$\rho = 1.18$ Mg/m^3

and

$M_d = 8.3 \times 10^5$ kg

2. If, as suggested by the sampling, this sediment is present in the hoppers in two layers, then

---

*A sample calculation from Rochester, 191076, Discharge No. 8.

(5) $M_d = V_1\rho_1 + V_2\rho_2$

where V_1 and V_2 are the volumes of the two layers, and ρ_1 and ρ_2 are the densities of material comprising the two layers. It also must be the case that

(6) $V_1 + V_2 = V$

Therefore,

(7) $V\rho_1 + V_2(\rho_2 - \rho_1) = M_d$

or, rearranging (7)

(8) $V_2 = (M_d - V\rho_1)/(\rho_2 - \rho_1)$

For this example, let ρ_1 = 1.1 Mg/m^3 and ρ_2 = 1.7 Mg/m^3, hence V_2 = 89 m^3.

3. In Appendix B the hoppers were divided into eight subdivisions. In each of these subdivisions the volume occupied by material of density of ρ_2 must be $V_2/8$ or 11 m^3. This requires the layer to have a thickness of 1.58 m.

APPENDIX D: THE POTENTIAL ENERGY OF DREDGED MATERIAL

1. The energy to drive the placement process is the stored energy of the dredged material in the hoppers. This may be calculated if the shape of the hoppers and the distribution of material in them are known.

2. In general, the hoppers consist of a large rectangular volume of constant cross-sectional area and a small volume whose cross-sectional area decreases towards the hopper doors (Figure D1). For the energy calculation, divide the hoppers into six volumes as shown in Figure D1. For subdivision i let

ρ_i = the density of the material in the subdivision

V_i = the volume

M_i = the mass = $\rho_i V_i$

Z_i = the height of the center of gravity of the mass above the level selected as the zero potential energy (e.g., the sea floor)

To calculate the potential energy, sum the potential energy of each mass obtained by calculating the work done in raising the mass from $Z = 0$ to $Z = Z_i$.

(1) $$v_o = W_1 + W_2 + W_3 + W_4 + W_5 + W_6$$

where: v_o is the potential energy of the material in the hopper, and

W_i is the work done in raising the center of mass of M_i from $Z = 0$ to $Z = Z_i$.

For subdivisions 1, 2, 3, and 4

(2) $$W_i = \int_0^{Z_i} (M_i g - V_i \rho_w g)\, dZ$$

$$= g(M_i Z_i - V_i \rho_w Z_i) \qquad i = 1, 2, 3, 4$$

where ρ_w is the density of water. For subdivisions 5 and 6 the work done in raising the center of mass of each layer from $Z = 0$ to $Z = Z_i$ is calculated in three steps:

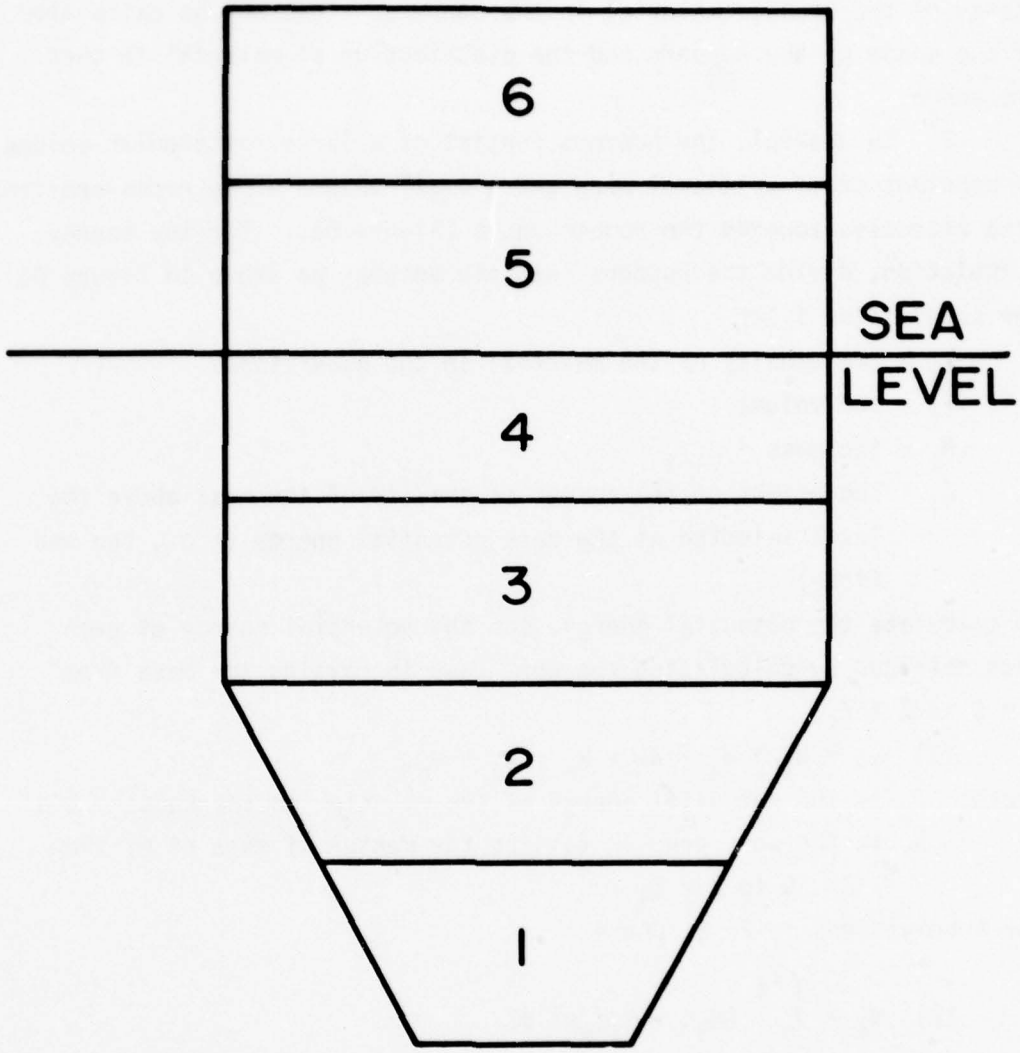

Figure D1. The six volumes used in energy calculations.

1) W_i' = the work required to bring the top surface of V_i to $Z = Z_o$, Z_o being the water depth.

2) W_i'' = the work required to lift V_i out of the water, that is, to move V_i from a position where its top surface is at Z_o to a position where its bottom surface is at Z_o.

3) W_i''' = the work needed to lift V_i from the water surface to Z_i, that is to move V_i from a position where its bottom surface is at Z_o to a position where its center of mass is at Z_i.

These three steps are illustrated in Figure D2 which defines two new heights Z_i' and Z_i'', indicating the position of the center of mass of the volume at each step. The total work done W_i is then the sum of W_i', W_i'', and W_i'''. The first of these quantities is easily calculated,

$$(3)\quad W_i' = \int_0^{Z_i'} (M_i g - V_i \rho_w g)dZ$$

$$= gZ_i' (M_i - V_i\rho_w)$$

If the thickness of V_i is h_i, then $Z_i' = Z_o - h_i/2$.

3. As the volume V_i rises above the water surface, the buoyant force decreases as the amount of volume submerged decreases. The buoyant force B_f is

$$(4)\quad B_f = \frac{V_i}{h_i} \rho_w g d_i = \frac{V_i}{h_i} \rho_w g(Z_o - Z + h_i/2) \quad \text{See Figure D3}$$

Then

$$(5)\quad W_i'' = \int_{Zi}^{Z_i''} [M_i g - \frac{V_i}{h_i} \rho_w g(Z_o + h_i/2 - Z)]dZ$$

$$= M_i g h_i - V_i \rho_w g \frac{h_i}{2} = h_i g \{M_i - V_i\rho_w/2\}$$

where d_i is the distance from lake level to bottom surface of d_i. The term W_i''' has no buoyancy force in the integral and is simply

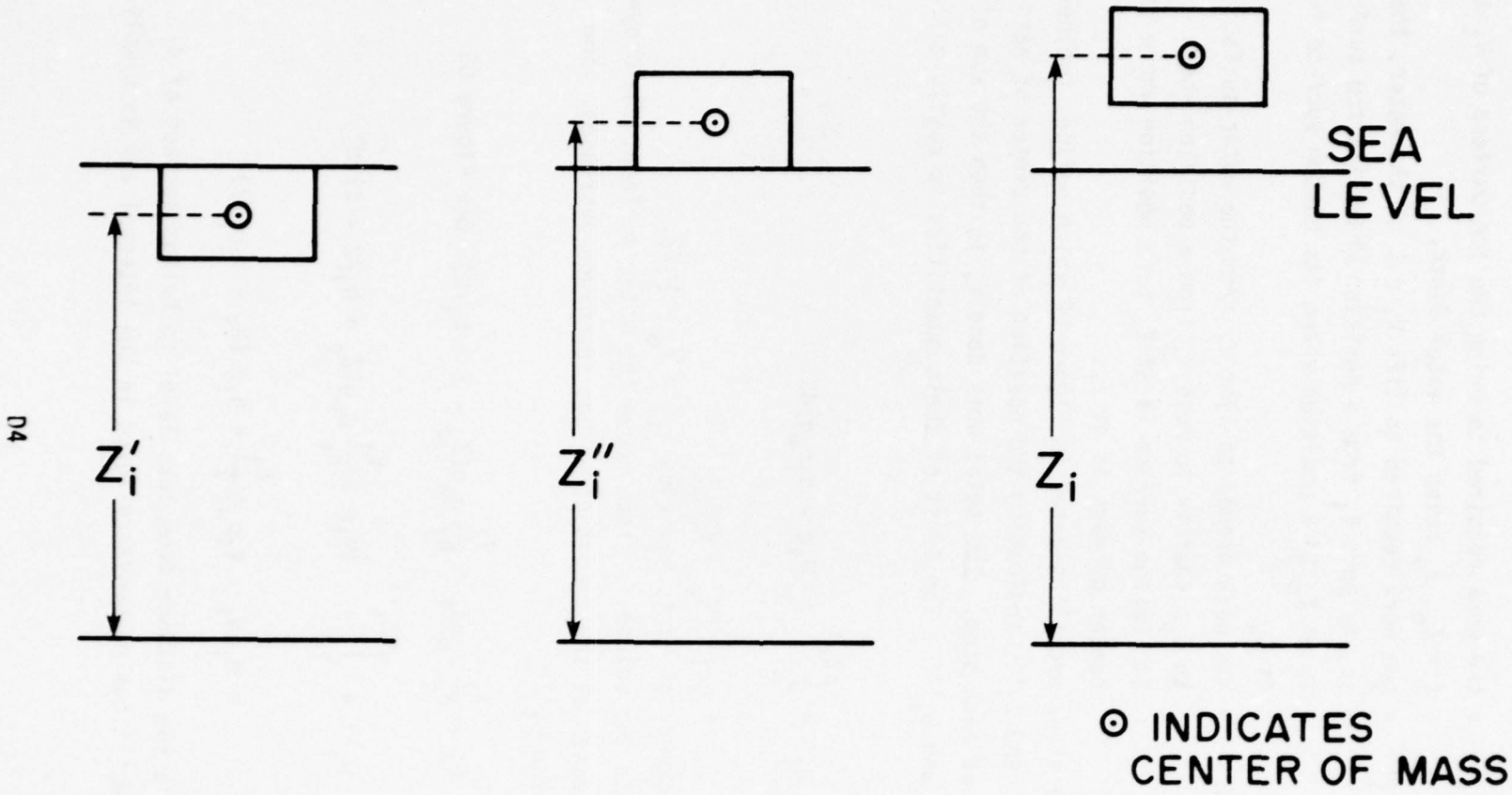

Figure D2. Three steps in raising the center of mass above sea level.

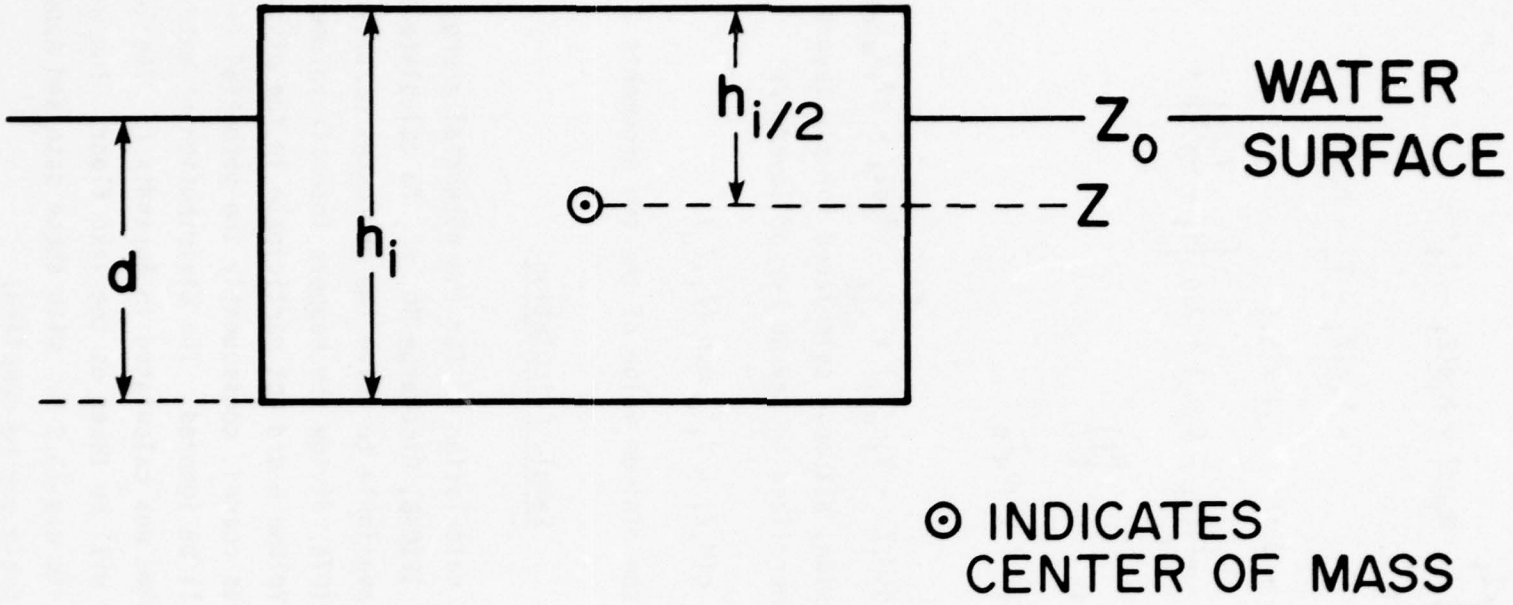

Figure D3. Sketch of dimensions used in buoyancy calculation.

$$(6)\quad W_i''' = \int_{Z_i''}^{Z_i} M_i g\,dZ = M_i g(Z_i - Z_i'')$$

$$= M_i g(Z_i - Z_o - h_i/2)$$

Thus, $W_i = W_i' + W_i'' + W_i'''$ $\quad i = 5,6$

$$(7)\quad W_i = g\left(Z_o - \frac{h_i}{2}\right)(M_i - V_i\rho_w) + h_i g\left\{M_i - \frac{V_i\rho_w}{2}\right\} +$$

$$M_i g\left(Z_i - Z_o - \frac{h_i}{2}\right)$$

$$= M_i g(Z_i) - gV_i\rho_w Z_o$$

So,

$$(8)\quad {}^{\nu}o = \sum_{i=1}^{4} g(M_i Z_i - V_i\rho_w Z_i) + \sum_{i=5}^{6} (M_i g Z_i - gV_i\rho_w Z_o)$$

Note that this expression, although calculated for six layers for clarity, is easily generalized to any number of layers as

$$(9)\quad {}^{\nu}o = \sum_{i=1}^{n} g[M_i Z_i - V_{i\ w} \min\,(Z_i, Z_o)]$$

where min (Z_i, Z_o) is the minimum value of the two arguments Z_i and Z_o.

Sample Calculation

4. This sample calculation is for the potential energy in the hoppers at Rochester, 191076, Discharge No. 8. To calculate the potential energy that was available to drive the processes occurring during Discharge No. 8 on 191076, divide the hoppers into six volumes as shown in Figure D4. Volume 6 did not participate in the discharge since only the bow hopper was opened; consequently the potential energy contained in volume 6 will be ignored. The distribution of material in the hoppers at this time was calculated in Appendix C. The level of zero potential energy will be taken as the lake floor. The water depth, Z_o, at the disposal site was 18.3 m. With these data and Appendices B and C, the following table may be compiled.

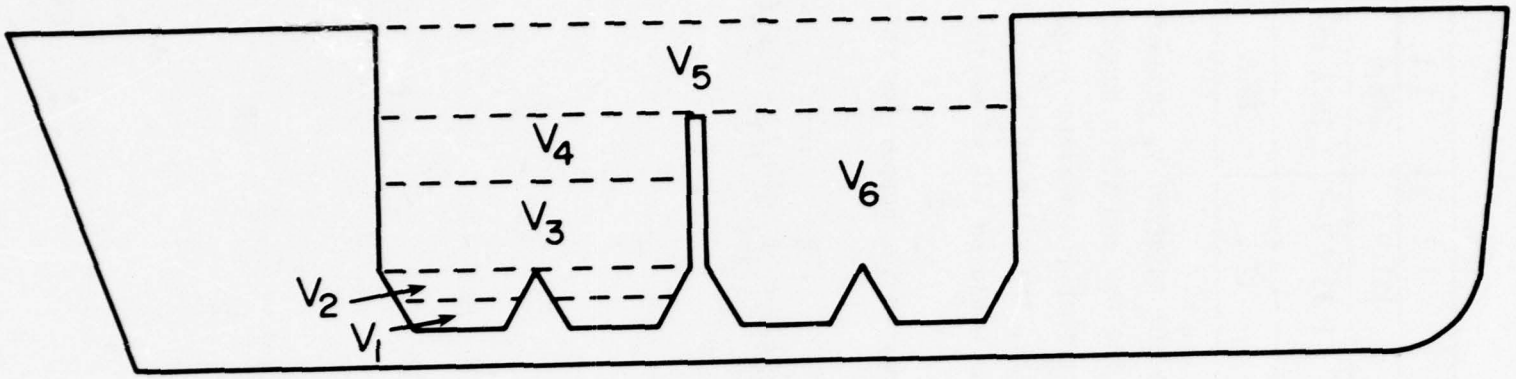

Figure D4. Cross section of a hopper dredge showing six volumes used in potential energy calculations.

i =	1	2	3	4	5
ρ_i (Mg/m^3)	1.7	1.1	1.1	1.1	1.1
V_i (m^3)	45.8	17.4	121.0	108.0	230.0
M_i (kg)	7.79×10^4	1.91×10^4	1.33×10^5	1.19×10^5	$2.53 \times 10^{5*}$
Z_i (m)	16.1	16.6	17.5	19.0	20.5

*Note: There is an uncertainty in the value of V_5 because the exact height of the bulkhead separating the bow and stern hoppers is not known. The value of V_5 listed is probably a maximum value; if the bulkhead is higher than assumed here, the value of V_5 would be correspondingly smaller. A minimum value would be 115 m^3 making M_i = 1.3×10^5 kg.

5. The total potential energy in the hopper for this operation is (ρ_w = 1.0)

$$(10) \quad v_o = \sum_{i=1}^{3} g(M_i Z_i - V_i \rho_w Z_i) + \sum_{i=4}^{5} g(M_i Z_i - V_i \rho_w Z_o)$$

$$= 20 \text{ MJ}$$

APPENDIX E: ENERGY FLOW FROM THE HOPPERS

1. The energy passing through an area dxdy, due to a flow of material of density ρ_m moving with velocity v, perpendicular to the area is

(1) $dH = \frac{1}{2} \rho_m v^2 dxdy\ vdt + Zg(\rho_m - \rho_w)dxdy\ vdt$

where ρ_w is the density of water, Z is the elevation of the surface above the level of zero potential, and g is the acceleration of gravity.

2. If the flow persists for a time, T (i.e. $v = v(Z)$, $0 < t < T$ and $v = 0$, $t > T$) through an area A, the energy passed through A is

(2) $$H(Z) \sim \frac{1}{2} \rho_m \int_0^T A\, \bar{v}^3\, dt + Zg(\rho_m - \rho_w) \int_0^T A\, \bar{v} dt$$

where $\bar{v}$ is the average velocity across A.

3. As dredged material descends, water is entrained and the area, velocity, and duration of the jet must change with depth. However, the total amount of solid material passing a section at any depth is constant. Hence the total, effective weight passing through any section is constant.

(3) $$g \int_0^T A(\rho_m - \rho_w)\, \bar{v} dt = \text{constant} \equiv \frac{dv}{dZ}$$

This constant is defined to be dv/dZ, or the change in potential energy, v, with depth. Obviously

(4) $$\frac{d}{dZ} = g(\rho_m - \rho_w)\, V$$

where is the volume discharged. The energy then becomes

(5) $$V = \frac{1}{2} \rho_m \int_0^T A\, \bar{v}^3\, dt + \frac{dv}{dZ} Z$$

4. When integrating the flow of energy through the hopper doors, Z is not constant because the distance between Z = 0 (the lake floor) and the hopper doors increases as the load is discharged. However, if the change in draft is small compared to the water depth, this varia-

tion can be ignored. The density of material through the doors is also a function of time. This effect cannot be ignored because the stratification that takes place in the hoppers may allow the density to vary from 1.0 to 1.7 Mg/m^3. Thus, when doing the integration from a set of discrete data, the energy flow through the hopper doors may be computed from:

$$(6) \quad H = \frac{1}{2}\sum_i \rho_i A_i \bar{v}_i^3 \Delta t + \frac{d\nu}{dZ} Z$$

where ρ_i = density of $i^{\underline{th}}$ layer, and Δt = time interval between successive measurements.

Sample Calculation

5. The total energy flow through the hopper doors for a discharge operation at Rochester (191076, #8) may be calculated with the aid of Appendices B, C, and D.

6. The total kinetic energy, τ', flowing through one door on this operation is

$$(7) \quad \tau' = \frac{1}{2}\sum_i \rho_i A_i \bar{v}_i^3 \Delta t$$

$$\tau' = 1.44 \text{ MJ/door}$$

Since all four doors of the forward hopper were opened for this discharge, the total kinetic energy passing through the hoppers was

$$(8) \quad \tau = 5.76 \text{ MJ}$$

The total potential energy which flows through the hopper doors may be calculated with the aid of the table for the sample calculation of the hopper contents for this operation (Appendix D).

$$(9) \quad \nu = \sum_i V_i Z g(\rho_i - \rho_w) = 12 \text{ MJ}$$

where Z is the depth of water below the hopper doors at the discharge point (15.0 m). This is an upper limit to ν since some material remained in the hoppers after the discharge was complete. We estimate that this value of ν may be too large by 1 MJ. Thus, the corrected value of ν becomes

$$(10) \quad \nu = 11 \text{ MJ}$$

The total energy which flows from the hoppers is then

(11) $H = \tau + \nu = 17$ MJ

Before the doors were opened, 20 MJ was available as potential energy in the hoppers; there is a loss of 3 MJ or 15 percent due to friction in the discharge. The friction loss is due to the motion of the dredged material passing out of the hoppers and should, therefore, be related to the kinetic energy flux. The frictional loss in this example is equal to about 50 percent of the total flux of kinetic energy through the hopper doors.

7. The rate of discharge was available from direct measurement in this sample calculation. If this information is not available, the flow of kinetic energy from the Lyman may be estimated as two-thirds of the difference between the stored potential energy in the hoppers and the integrated flux of potential energy through the doors,

(12) $\tau = \frac{2}{3}\left(\nu_o - \frac{d\nu}{dZ} Z\right)$

The quantities on the right side of the above equation may be evaluated from the draft measurements and the shape of the ship.

Theoretical Insertion Speed

8. To develop a simple energy balance for the dredged material as it exits in the hopper shown in Figure E1, assume that the material behaves according to Bernoulli's equation:

(13) $p_o + \rho gh + \frac{1}{2}\rho v_o^2 = p_4 + \frac{1}{2}\rho v_4^2 + \varepsilon$

where p_o is atmospheric pressure, v_o is velocity at A_o (cross-sectional area of a hopper), p_4 is p_o plus $\rho_w d$, and ε is the frictional energy loss. The equation of continuity requires that

(14) $A_o v_o = A_4 v_4$

So,

(15) $p_o + \rho gh + \frac{1}{2}\rho\left(\frac{A_4}{A_o}\right)^2 v_4^2 = p_4 + \frac{1}{2}\rho v_4^2 + \varepsilon$

where p_o is atmospheric pressure and p_4 is atmospheric pressure plus $\rho_w d$, where d is the distance from hopper doors to lake level. Hence

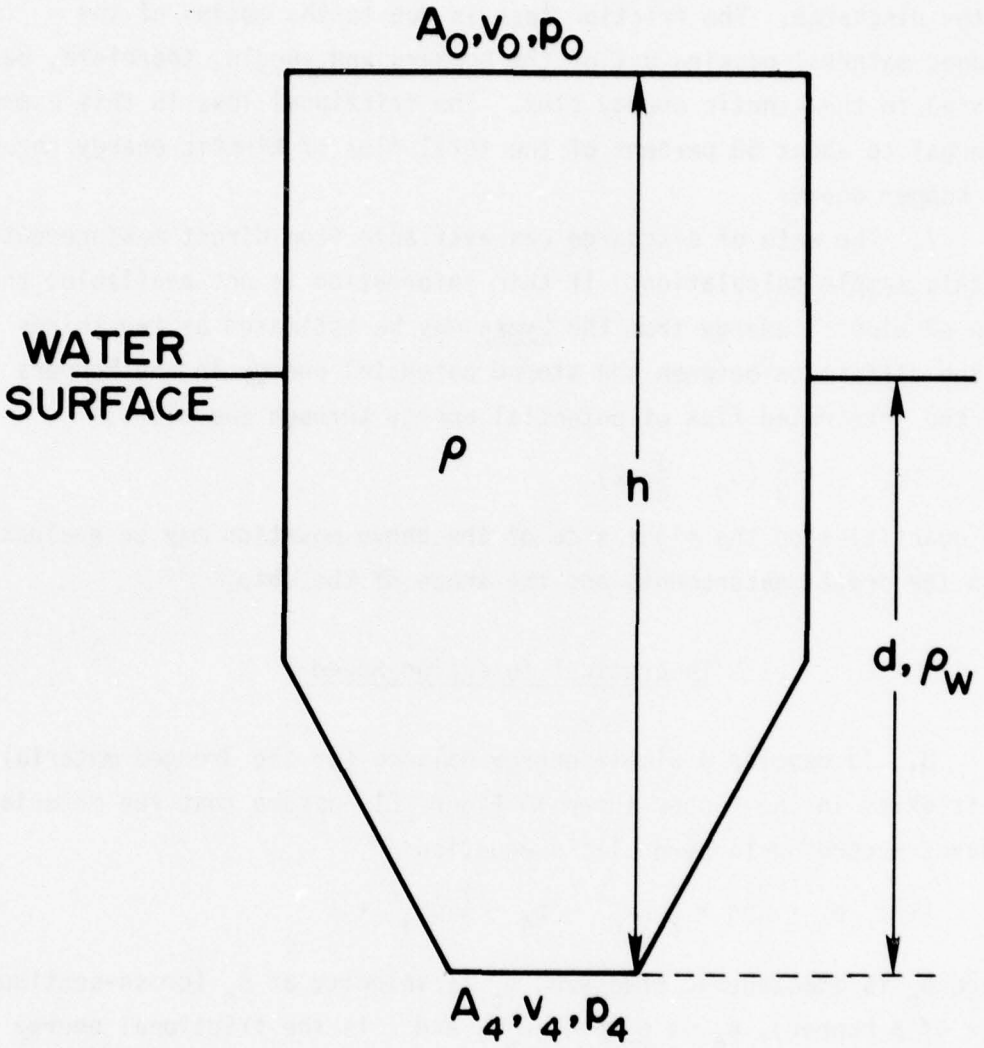

Figure E1. Parameters used in energy balance.

$$(16)\quad \rho g h + \frac{1}{2}\rho\left(\frac{A_4}{A_o}\right)^2 v_4^{\,2} = \rho_w g d + \frac{1}{2}\rho v_4^{\,2} + \varepsilon$$

$$(17)\quad v_4 = \sqrt{\left[\frac{2g}{\rho}(\rho h - \rho_w d) - \frac{2\varepsilon}{\rho}\right] \Big/ \left[1 - \left(\frac{A_4}{A_o}\right)^2\right]}$$

9. In this model A_4 if the area of the door opening. It is time dependent and is calculated in Appendix B. If A is a constant (independent of time), there is an additional relationship between h and d. If the ship is always in hydrostatic equilibrium, that relation is

$$(18)\quad hA_o\rho + M_o = d\bar{A}\rho_w \quad \text{(for A = constant)}$$

where M_o is the mass of the ship and $\bar{A}$ is the ship's cross-sectional area at the waterline. From this relation, it follows that an increment in h is given by

$$(19)\quad \delta h = \frac{\bar{A}\rho_w}{A_o\rho}\,\delta d$$

The energy loss through friction, ε, may be estimated after the fashion of Bird, Stewart, and Lightfoot (1960, p. 216) as

$$(20)\quad \varepsilon = \frac{1}{2} v_1^{\,2} \frac{h}{R_h} f\rho$$

where R_h is the hydraulic radius, and f is the friction factor.

$$(21)\quad R_h = \frac{A_o}{z} = \frac{A_o}{\text{wetted perimeter}}$$

where z is the distance traveled. The friction factor is given as a function of the Reynold's number, R_e, defined as

$$(22)\quad R_e = \frac{2R_h v_1 \rho}{\mu}, \quad \mu \text{ being the effective viscosity.}$$

As given by Bird, Stewart, and Lightfoot (1960),

$$(23)\quad f = \frac{16}{R_e} \qquad R_e < 2.1 \times 10^3$$

$$(24)\quad f = 0.08/R_e^{\,1/4} \qquad 2.1 \times 10^3 < R_e < 10^5$$

If the Reynold's number is less than 2.1×10^3, Bernoulli's equation becomes

$$(25)\quad \rho gh + \frac{1}{2}\rho\left(\frac{A_4}{A_o}\right)^2 v_4^2 = \rho_w gd + \frac{1}{2}\rho v_4^2 + 4\mu\left(\frac{A_4}{A_o}\right)v_4 h/R_h^2$$

Rearranging,

$$(26)\quad av_4^2 + bv_4 + \gamma = 0$$

where

$$a = \frac{\rho}{2}\left[1 - \left(\frac{A_4}{A_o}\right)^2\right]$$

$$b = 4\mu\left(\frac{A_4}{A_o}\right) h/R_h^2$$

$$\gamma = -g\,(\rho h - \rho_w d)$$

So,

$$(27)\quad v_2 = [-b + \sqrt{b^2 - 4a\gamma}]/2a$$

This equation was used to generate curves for the hopper discharge rate using various values of μ. The observed height of the material in the hopper as a function of time is best reproduced assuming an effective viscosity, μ, euqal to 4×10^4 N sec/m^2 (Figure E2). Energy is lost at an average rate of 0.1 Mw.

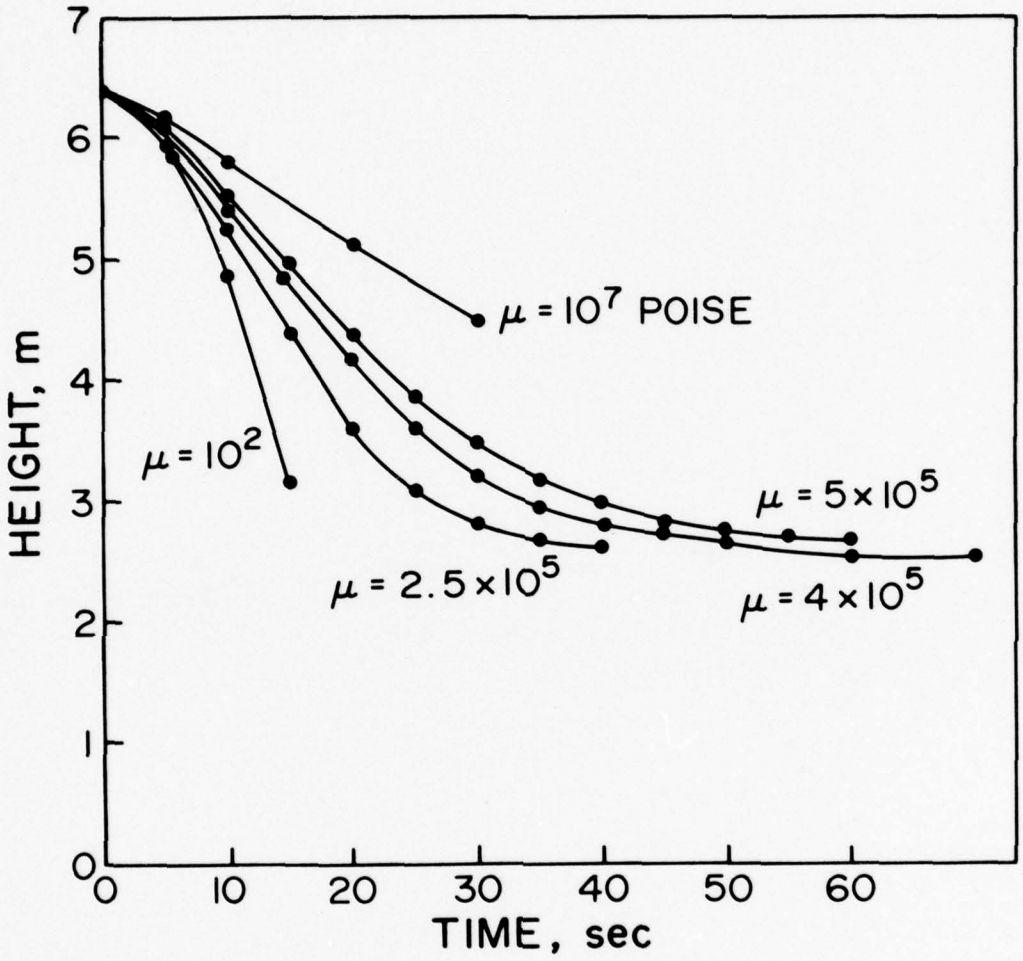

Figure E2. Hopper discharge rate for several values of μ.

APPENDIX F: ENERGY BALANCE IN THE DESCENT PHASE

1. Just as the flow of energy through the hopper doors may be calculated (Appendix E), the flow of energy across any plane perpendicular to the velocity of the falling dredged material may also be calculated. Required are the velocity of the flow, its density, the area through which the flow occurs, and the height of the plane above the lake floor. By comparing the total flux of energy at some level to the flux through the doors, the energy lost in transit may be found.

2. As an example of this calculation, consider discharges Nos. 5 and 6 at Rochester, 191076. First calculate the total potential energy in the hoppers before discharge, then estimate the flow of energy through the hopper doors. The flow of energy through a plane just above the lake floor will then be calculated from flow meter and acoustic data, and the energy lost in descent will be estimated. Some of this energy goes into setting up a circulation in the surrounding water. An expression to approximate this energy will also be derived.

3. Before discharge No. 5, the draft of the loaded vessel was d_1 = 3.92 m. The bulk density of this dredged material is (Appendix C) 1.23 Mg/m^3. If it is assumed that the material is present in two layers, one with a density of 1.7 Mg/m^3 and the other with a density of 1.1 Mg/m^3, thickness of these layers must be 2.02 and 4.38 m, respectively (Appendix C). The total initial potential energy, ν_o, in this hopper load is then 36 MJ (Appendix D).

4. The total potential energy, ν, that flows through the hopper doors is 23 MJ (Appendix E). Assuming that the total energy lost in friction, ε, is one-half of the total flux of kinetic energy through the doors, τ, then,

(1) $\tau = 2/3\ (\nu_o - \nu) = 9$ MJ

5. During discharge No. 5, two doors were opened and 260 m^3 of material was released. A flow meter at the arbitrary level of zero potential energy recorded the velocity of the descending jet as it reached the lake bottom (Appendix F). The flow of kinetic energy past the flow meter is calculated to be

$$(2)\quad \tau'_{16} = \frac{1}{2}\rho_s A_{16}\,\Delta t \sum_i v_i^3 = 0.11\ \text{MJ}$$

where τ'_{16} is kinetic energy past flow meter 16 m below bow doors, A_{16} is the cross-sectional area of the jet 16 m below the two doors, ρ_s is the density of the jet, Δt is the time interval between successive measurements of the velocity, v_i. Four doors were opened on discharge No. 6 and 1.1 x 10^2 m^3 of dredged sediment was released; τ''_{16} = 0.26 MJ where τ''_{16} is kinetic energy past flow meter 16 m below stern doors. So, through a plane 16 m below the hopper doors, the total flow of energy is only 0.37 MJ. More than 31 MJ were lost during descent.

6. Some of this energy is available to drive a large-scale circulation of the surrounding water. A current meter at Rochester placed 15 m from the discharge location (201076, Discharge No. 2) recorded high velocities for about 10 min after the turbid cloud of material had passed the station. This is taken as evidence of a large-scale circulation of clear water above the bottom surge.

7. To investigate the flow of ambient water set up by the descending jet, consider the water flow in a flattened toroid as shown in Figure F1. Point A is at Z = 0, r = R_o (Z, r, and ϕ being the cylindrical coordinates of the system). If the velocity there is v_o, then between R_o and R_1 (R_o is distance to trailing edge of toroid and R_1 is distance to leading edge of toroid) the velocity is given by the continuity equation as,

$$(3)\quad v(Z,r) = v_o \frac{R_o}{r}\left(1 - \frac{2Z}{Z_o}\right),\ 0 \le Z \le Z_o,\quad R_o \le r \le R_1$$

where Z_o is the water depth. At the inner and outer edges of the toroid, it is convenient to approximate the flow around the edge by flow in a cylinder of length $2\pi R_o$ and $2\pi R_1$, respectively, and to define the velocity with respect to the axis of the cylinder.

8. Since only half of the cylinder forms the edges of the volume, the kinetic energy at the inner edge is

$$(4)\quad \tau_o = \frac{1}{4}\left(\frac{1}{2} M_c\left(\frac{Z_o}{2}\right)^2\right) \frac{v_o^2}{(Z_o/2)^2}$$

$$\tau_o = \frac{\pi^2}{4}\rho_w R_o\left(\frac{Z_o}{2}\right)^2 v_o^2$$

ρ_w = density of water

M_c = mass of water in cylindrical flow

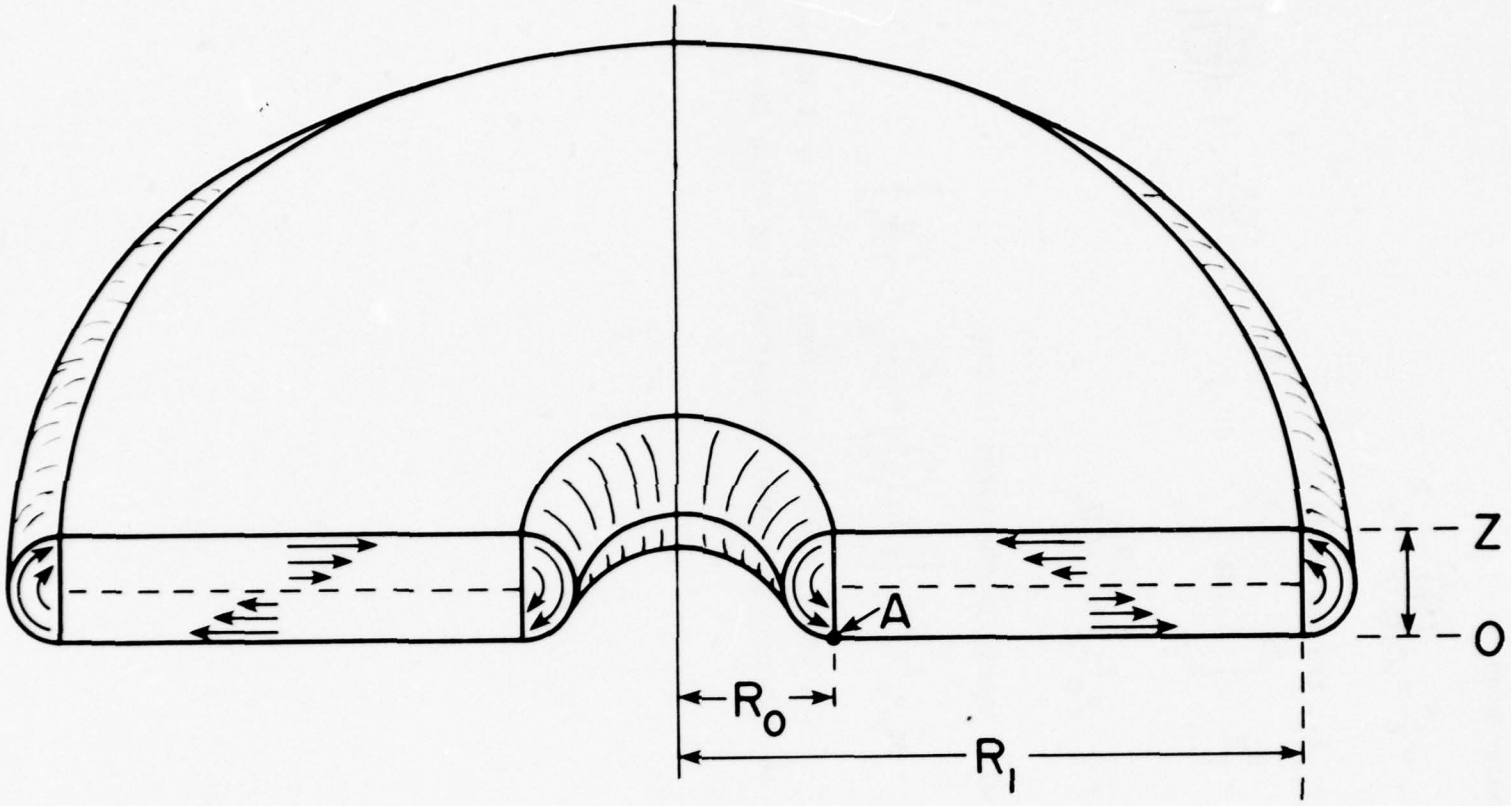

Figure F1. Toroid used to represent spread of surge.

and, at the outer edge,

$$(5) \quad \tau_1 = \frac{\pi^2}{4} \rho_w R_1 \left(\frac{Z_o}{2}\right)^2 v_o^2$$

For $R_o \leq r \leq R_1$, the energy is

$$(6) \quad \tau = \frac{\rho_w}{2} \int_0^{2\pi} r d\phi \int_{R_o}^{R_1} dr \int_0^{Z_o} dZ \left[\frac{v_o R_o}{r} \quad 1 - \left(\frac{2Z}{Z_o}\right)\right]$$

$$= \frac{\pi}{3} \rho_w v_o^2 R_o^2 \ln\left(\frac{R_1}{R_o}\right) Z_o$$

The total kinetic energy in the surge is then

$$(7) \quad \tau = \pi \rho_w v_o^2 R_o^2 Z_o \left[\frac{1}{3} \ln\left(\frac{R_1}{R_o}\right) + \frac{\pi Z_o}{16 R_o} + \frac{\pi Z_o}{16 R_1}\right]$$

If $Z = 20$ m, $R_o = Z_o$, and $v_o = 0.3$ m/sec, then $R_1 < 150$ m if 10 percent (2 MJ) of the energy lost in descent is available to drive the circulation.

APPENDIX G: CALCULATED FALL VELOCITY OF SOLID DREDGED MATERIAL

Calculation of Fall Velocities

1. The velocity of a particle falling through a fluid may be calculated for simple particle shapes. Consider a spherical particle (diameter, D; density in air ρ_a) falling in a still fluid (density, ρ_w). Its mass, m, is

$$(1) \quad m = \frac{\pi}{6} D^3 \rho_a,$$

and the equation of motion of the particle is

$$(2) \quad \frac{\pi}{6} D^3 \rho_a \ddot{z} = - \frac{\pi D^2}{4} \frac{\rho_w}{2} \dot{z}^2 C_D + \frac{\pi}{6} D^3 \rho_a g - \frac{\pi}{6} D^3 \rho_w g$$

where $\ddot{z}$ is the acceleration of the particle, $\dot{z}$ is the velocity of the particle, C_D is the drag coefficient, and g is the acceleration of gravity ($g > 0$). The first term on the right of (2) is the drag force exerted on the surface of the sphere by the fluid. The Reynolds number for the falling particle is

$$(3) \quad R_e = \dot{z} D/\nu$$

where ν is the kinematic viscosity of the fluid. The drag coefficient, C_D, is a function of the Reynolds number as follows:

$$(4) \quad C_D = \begin{cases} 24/R_e & R_e \leq 1.92 \\ 18.5/R_e^{3/5} & 1.92 < R_e \leq 508.39 \\ 0.44 & 508.39 < R_e \leq 200{,}000 \\ 0.22 & R > 200{,}000 \end{cases}$$

(Bird, Stewart, and Lightfoot, 1960). The second term on the right of equation (2) is the gravitational force and the third term is the buoyant force.

2. Dividing both sides of (2) by the mass of the particle and rearranging,

$$(5) \quad \ddot{z} = - \frac{3}{4} \frac{\rho_w}{\rho_a} \dot{z}^2 \times \frac{C_D}{D} + g\left(1 - \frac{\rho_w}{\rho_a}\right).$$

If the particle starts from rest in the fluid ($\dot{z} = 0$ at $t = 0$)

$$(6) \quad \ddot{z} = - 18 \nu \rho_w \dot{z}/(\rho_a D^2) + g\left(1 - \frac{\rho_w}{\rho_a}\right).$$

Let $A_s = 18 \nu \rho_w/(\rho_a D^2)$ and $B = g\left(1 - \frac{\rho_w}{\rho_a}\right)$ so that

(7) $\ddot{z} = B - A_s \dot{z}$

This may be rewritten as,

(8) $\frac{d\dot{z}}{dt} = B - A_s \dot{z}$

from which, separating the variables,

(9) $d\dot{z} / \left(\frac{B}{A_s} - \dot{z} \right) = A_s dt.$

This last expression may now be integrated to yield

(10) $\ln \left(\frac{B}{A_s} - \dot{z} \right) = -A_s t + \ln C_1$

where C_1 is a constant of the integration. Taking the antilogarithm, and noting that since $\dot{z} = 0$ at $t = 0$, $C_1 = B/A_s$, we find

(11) $\dot{z} = B(1 - e^{-A_s t})/A_s.$

Integrating once again, we have,

(12) $z = \frac{B}{A_s} t + \frac{B}{A_s^2} e^{-A_s t} + C_2$

where C_2 is a constant of the integration. Since $z = 0$ at $t = 0$, $C_2 = - B/A_s^2$, hence,

(13) $z = \frac{B}{A_s} t - \frac{B}{A_s^2} (1 - e^{-A_s t})$

Equations (11) and (13) apply only until $R_e = 1.92$. At this point the dependence of the drag coefficient upon the Reynolds number changes form and a new equation of motion must be written and solved. This transition occurs at a velocity,

(14) $\dot{z}_1 = 1.92\nu/D$

a time

(15) $t_1 = \frac{1}{A_s} \ln \left(1 - \dot{z}_1 \frac{A_s}{B} \right)^{-1} = \frac{1}{A_s} \ln \left(1 - \frac{1.92\nu A_s}{DB} \right)^{-1}$

and a distance

(16) $z_1 = \frac{B}{A} t_1 - \frac{B}{A_s^2} (1 - e^{-A_s t_1})$

After these values are attained, $C_D = 18.5/R_e^{3/5}$, and the equation of motion for the particle becomes,

(17) $\ddot{z} = - \frac{111}{8} \frac{\rho_w}{\rho_a} \nu^{3/5} \dot{z}^{1.4}/D^{1.6} + g \left(1 - \frac{\rho_w}{\rho_a} \right)$

or

(18) $\ddot{z} = B - A_t \dot{z}^{1.4}$

where $A_t = \frac{111}{8} \frac{\rho_w}{\rho_a} \nu^{3/5}/D^{1.6}$. Separating the variable, we have,

$$(19) \quad d\dot{z}/\left(\frac{B}{A_t} - \dot{z}^{1.4}\right) = A_t dt.$$

Despite the simple appearance of this expression it is not readily integrable and velocities are most easily found by a numerical integration of (19).

3. Noting that,

$$(20) \quad \ddot{z} = \dot{z} \frac{d\dot{z}}{dz}$$

equation (18) may be rewritten as

$$(21) \quad \dot{z} \frac{d\dot{z}}{dz} = B - A_t \dot{z}^{1.4}$$

and the variable separated to express z as a function of $\dot{z}$

$$(22) \quad \dot{z}d\dot{z}/\left(\frac{B}{A_t} - \dot{z}^{1.4}\right) = A_t dz$$

The equation of motion (18) is valid until $R_e = 508.39$. The velocity at which this second transition occurs is

$$(23) \quad \dot{z}_2 = 508.39\nu/D;$$

the time, t_2, is,

$$(24) \quad t_2 = t_1 + \int_{\dot{z}_1}^{\dot{z}_2} d\dot{z}/A_t\left(\frac{B}{A_t} - \dot{z}^{1.4}\right)$$

and the distance,

$$(25) \quad z_2 = z_1 + \int_{\dot{z}_1}^{\dot{z}_2} \dot{z}d\dot{z}/A_t\left(\frac{B}{A_t} - \dot{z}^{1.4}\right)$$

4. After time t_2, $C_D = 0.44$ and the equation of motion becomes

$$(26) \quad \ddot{z} = -0.33 \frac{\rho_w}{\rho_a} \dot{z}^2/D + g\left(1 - \frac{\rho_w}{\rho_a}\right)$$

or

$$(27) \quad \ddot{z} = B - A_u \dot{z}^2$$

where $A_u = 0.33 \frac{\rho_w}{\rho_a}/D$. We may again rewrite this as

$$(28) \quad d\dot{z}/\left(\frac{B}{A_u} - \dot{z}^2\right) = A_u dt$$

and integrate to obtain

$$(29)\quad \sqrt{\frac{A_u}{B}}\tanh^{-1}\left(\sqrt{\frac{A_u}{B}}\,\dot{z}\right) = A_u t + C_3$$

where C_3 is a constant of integration. At $t = t_2$, $\dot{z} = \dot{z}_2$ so that

$$(30)\quad C_3 = \sqrt{\frac{A_u}{B}}\tanh^{-1}\left(\sqrt{\frac{A_u}{B}}\,\dot{z}_2\right) - A_u t_2$$

For brevity we shall continue to use "C_3" instead of this more lengthy expression. Rearranging (29) yields

$$(31)\quad \dot{z} = \sqrt{\frac{B}{A_u}}\tanh\left(\sqrt{A_u B}\,t + \sqrt{\frac{B}{A_u}}\,C_3\right).$$

To generate an expression for z, let us again integrate (27) in terms of dz instead of dt. Equation (28) may then be written as

$$(32)\quad \dot{z}d\dot{z}/\left(\frac{B}{A_u} - \dot{z}^2\right) = A dz$$

and this expression integrates to

$$(33)\quad -\frac{1}{2}\ln\left(\frac{B}{A_u} - \dot{z}^2\right) = A_u z + C_4$$

where C_4 is a constant of integration given by

$$(34)\quad C_4 = -\frac{1}{2}\ln\left(\frac{B}{A_u} - \dot{z}_2^2\right) - A_u z_2$$

Equations (31) and (33) are valid until $R_e = 2 \times 10^5$ at which point $C_D = 0.22$. This transition occurs at velocity $\dot{z}_3 = 2 \times 10^5\ \nu/D$, time t_3, and distance z_3, which for convenience we will leave unspecified. The equation of motion and its integration are the same as for equation (27) except that $A_v = A_u/2$ and, of course, a new constant of integration must be determined.

Evaluation of Fall Velocities

5. For spherical particles with a density $\rho_{a_2} = 1.5\ Mg/m^3$ falling through still water ($\rho_w = 1.0\ Mg/m^3$, $\nu = 0.001\ Ns/m^2$), we find that if the particle diameter is 1 cm or greater

$$(35)\quad \dot{z}_2 < 5\ cm/sec$$

$$(36)\quad t_2 < 0.16\ sec$$

and,

$$(37)\quad z_2 < 0.8\ cm$$

Therefore for practical purposes no large error is made by assuming that $\dot{z}_2 = 0$, $t_2 = 0$ and $z_2 = 0$. These assumptions greatly simplify the calculation because then

$$(38) \quad \dot{z} = \sqrt{\frac{B}{A_u}} \tanh \left(\sqrt{BA_u}\, t\right)$$

and,

$$(39) \quad z = \frac{1}{2} \left(\ln \frac{B}{A_u} - \ln \left(\frac{B}{A_u} - \dot{z}^2\right)\right)/A_u$$

These particles have a terminal velocity of

$$(40) \quad \dot{z}_t = \sqrt{\frac{B}{A_u}} \quad \text{if } \dot{z}\, D/\nu < 2.0 \times 10^5$$

and achieve 99 percent of their terminal velocity in a time

$$t_{99} = 2.65/\sqrt{BA_u} \quad \text{if } \dot{z}\, D/\nu < 2.0 \times 10^5$$

If $\dot{z}\, D/\nu > 2.0 \times 10^5$, the calculation must be performed in two steps to allow for the change in the drag coefficient at $R_e = 2 \times 10^5$. The Reynolds number exceeds 2×10^5 for all particles greater than about 15 cm in diameter ($\rho = 1.5$ Mg/m^3).

APPENDIX H: IMPACT PROPERTIES OF DREDGED MATERIAL

1. A series of tests was conducted to define the mechanical properties of dredged material from the Saybrook site at high rates of deformation, such as are encountered in the impact of clods with the bottom. The tests were preliminary in character and were intended to demonstrate the type of laboratory study useful in characterizing the properties of dredged material important in placement operations. The samples tested were taken from the bucket of the clamshell dredge used at Saybrook.

2. The Saybrook disposal site has a hard bottom and is not expected to absorb any of the impact energy of descending clods. If there is to be no dispersion of the impacting material, all of the kinetic energy of impact will have to be absorbed in plastic deformation of the clods. The tests were designed to measure the magnitude of this energy dissipation in plastic deformation.

3. The first measurement done was a drained triaxial test. The deformation rate was chosen to allow dissipation of 95 percent of the pore pressure and was calculated by the method of Bishop and Henkel (1957) from consolidation curves measured in the laboratory. The strain rate used was 2×10^{-4} min^{-1}. The change in pore water volume during compression of the sample was measured during the test and is shown in Figure H1; the pore volume decreases by 8 percent for a 25 percent compression. It is expected, therefore, that rapid compression will result in a rise in pore water pressure and in liquifaction of the soil. Since impact occurs under water, liquifaction will result in dispersion and is therefore considered to be soil failure for purposes of this study.

4. Unconfined compression tests were done over a wide range of strain rates to find the amount of energy used in plastic deformation of the soil before failure. The unconfined compression test approximates the deformation that occurs during impact with a hard bottom. Two test procedures were used:

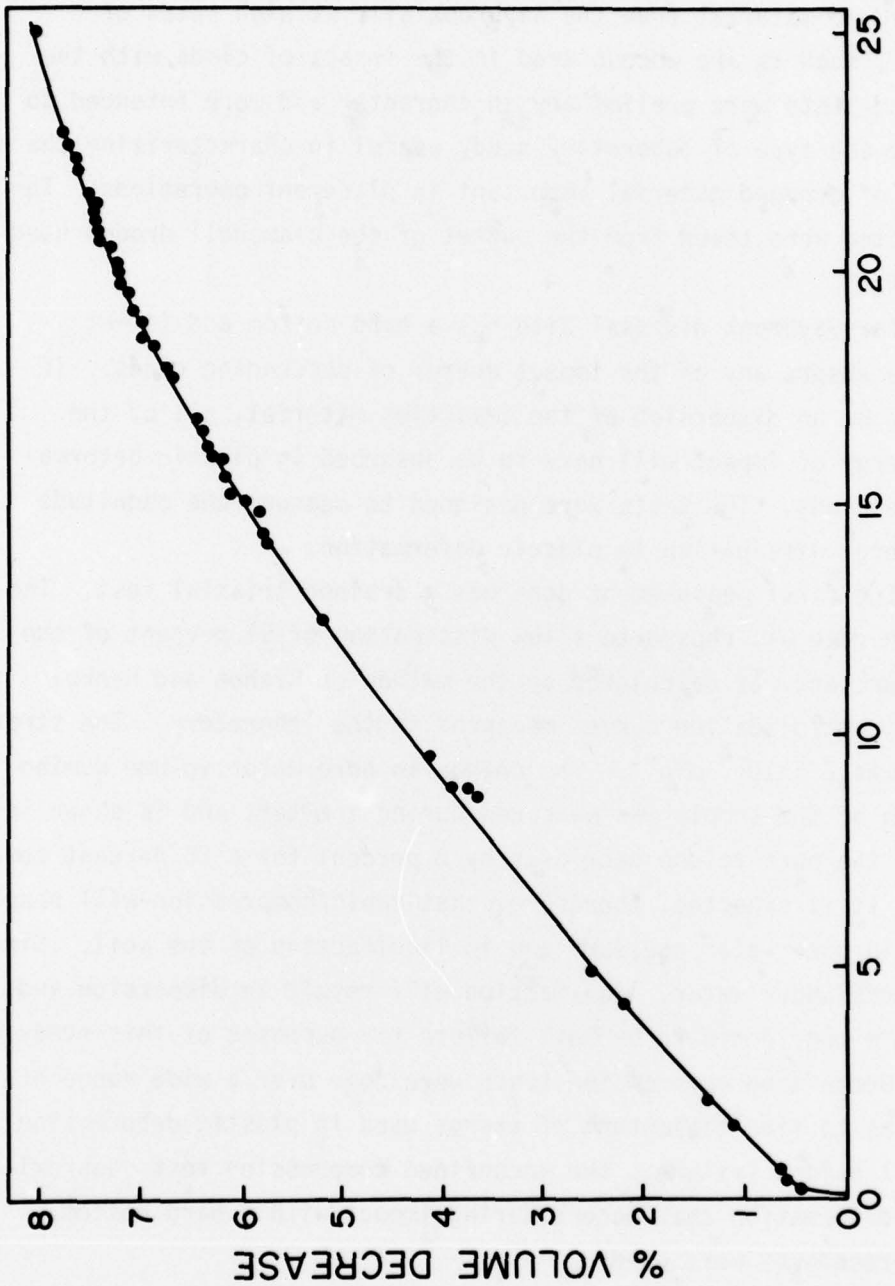

Figure H1. Change in pore volume during compression: drained triaxial test, North Cove clay.

a. Samples were immersed in water and tested in compression in an Instron testing machine at strain rates ranging from 0.085%/sec to 1%/sec.

b. For higher strain rates a special test fixture was designed. Piston displacement was indicated by the voltage output from a slide wire potentiometer attached to the piston while the force on the sample was measured with a WES soil pressure cell. The signals from the WES cell and from the potentiometer were displayed on a dual trace oscilloscope. A schematic diagram of the setup is shown in Figure H2. It was intended to do the tests in this fixture with the sample immersed in water but there has not yet been an opportunity to complete this aspect of the work. The strain rates attained ranged from 15%/sec to 150%/sec.

5. The force-displacement curves measured in the unconfined compression tests were found to pass through a maximum. The decreasing part of the curve is identified with failure of the sample by liquifaction. A typical curve is shown in Figure H3, where nominal stress and average strain are plotted. The maximum in the force-displacement curve is taken to be a lower bound to the onset of failure and, in the submerged state, to dispersion. Both the magnitude of the stress, σ_{max}, and the strain at the maximum, ε_{max}, were found to increase as the deformation rate was increased; σ_{max} by a factor of 12 and ε_{max} by 7 as the strain rate was increased from 0.08 to 150%/sec, Figures H4 and H5. It is thought that the decrease of the interstitial volume and the rise in pore pressure are less at the high strain rates. The mechanical work done to failure of the soil is the area under the force-displacement curve up to its maximum. This also increases as the deformation rate increases, as shown in Figure H6.

6. It is necessary to know the deformation rates attained during impact to apply the above results to clods of dredged material impacting with the bottom. The impact speed is known from the results presented in Figure 9 of text. The deformation rate can be estimated from a measurement of the amount of deformation that occurs and the duration of the impact. These were measured in the laboratory for samples of the dredged material falling in air at speeds equivalent to the terminal speed of the clods. The samples were allowed to fall on a WES soil

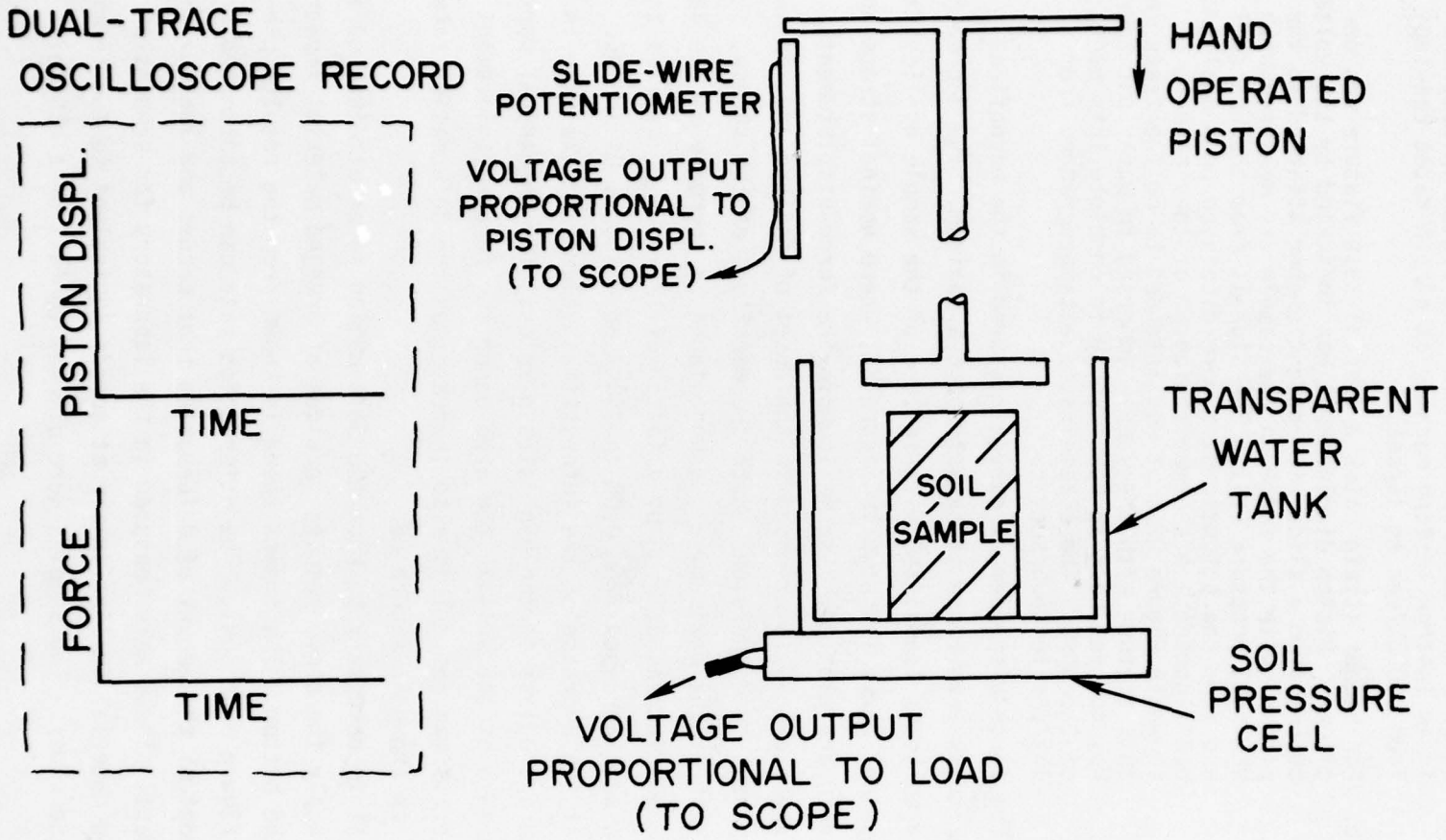

Figure H2. Schematic of setup for rapid unconfined compression tests.

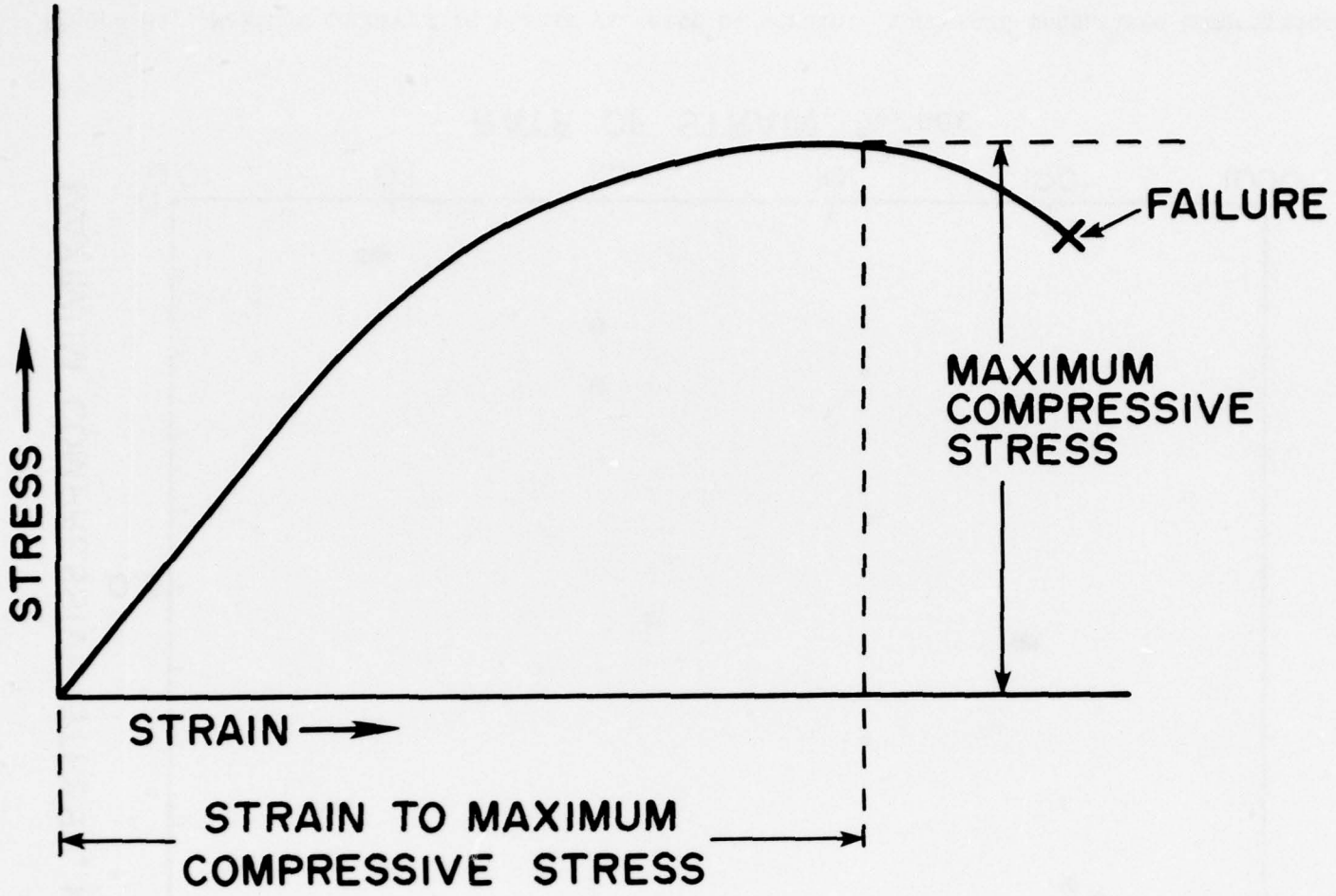

Figure H3. Typical stress-strain curve.

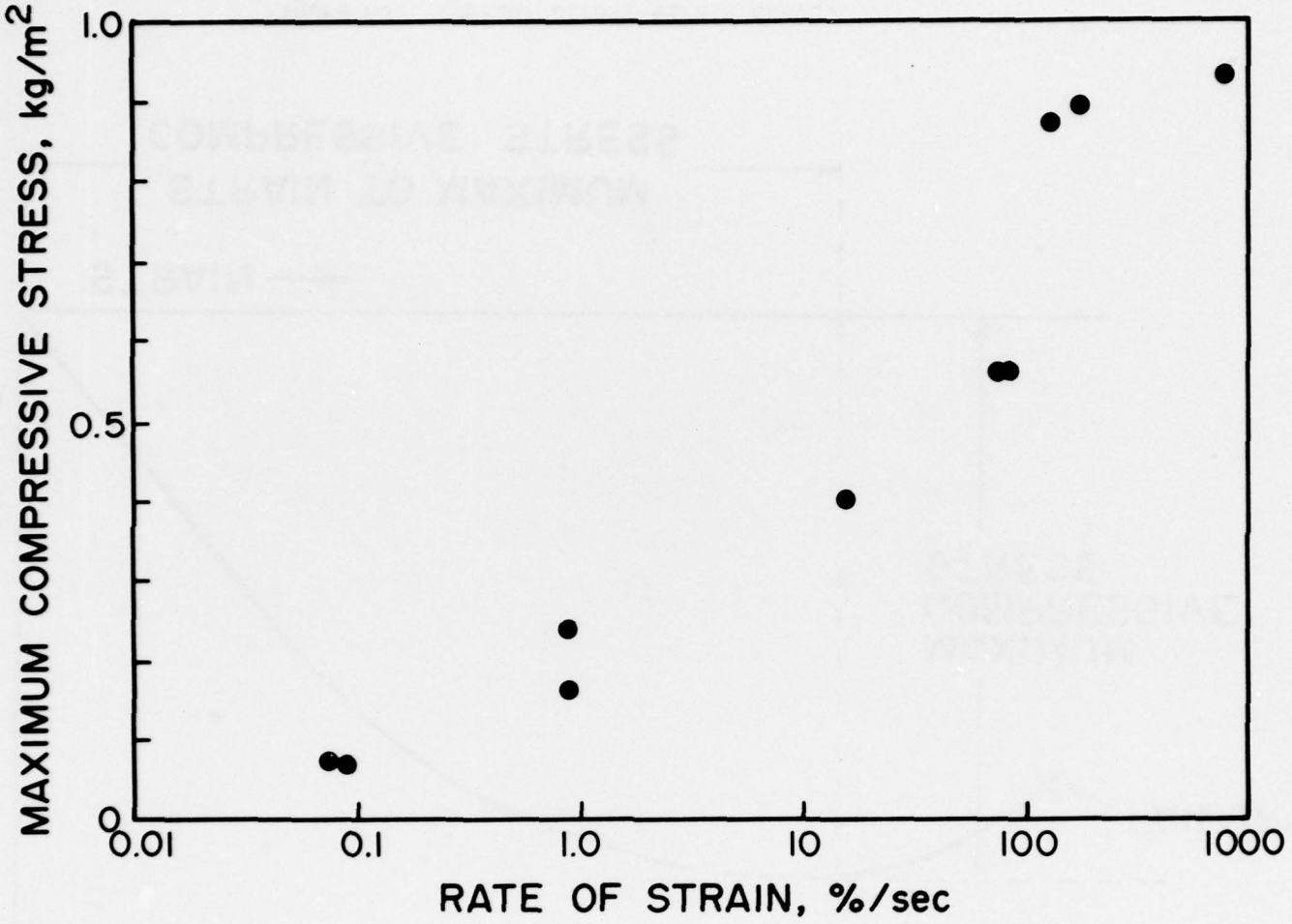

H6

Figure H4. Maximum compressive stress vs. rate of strain: submerged unconfined compression.

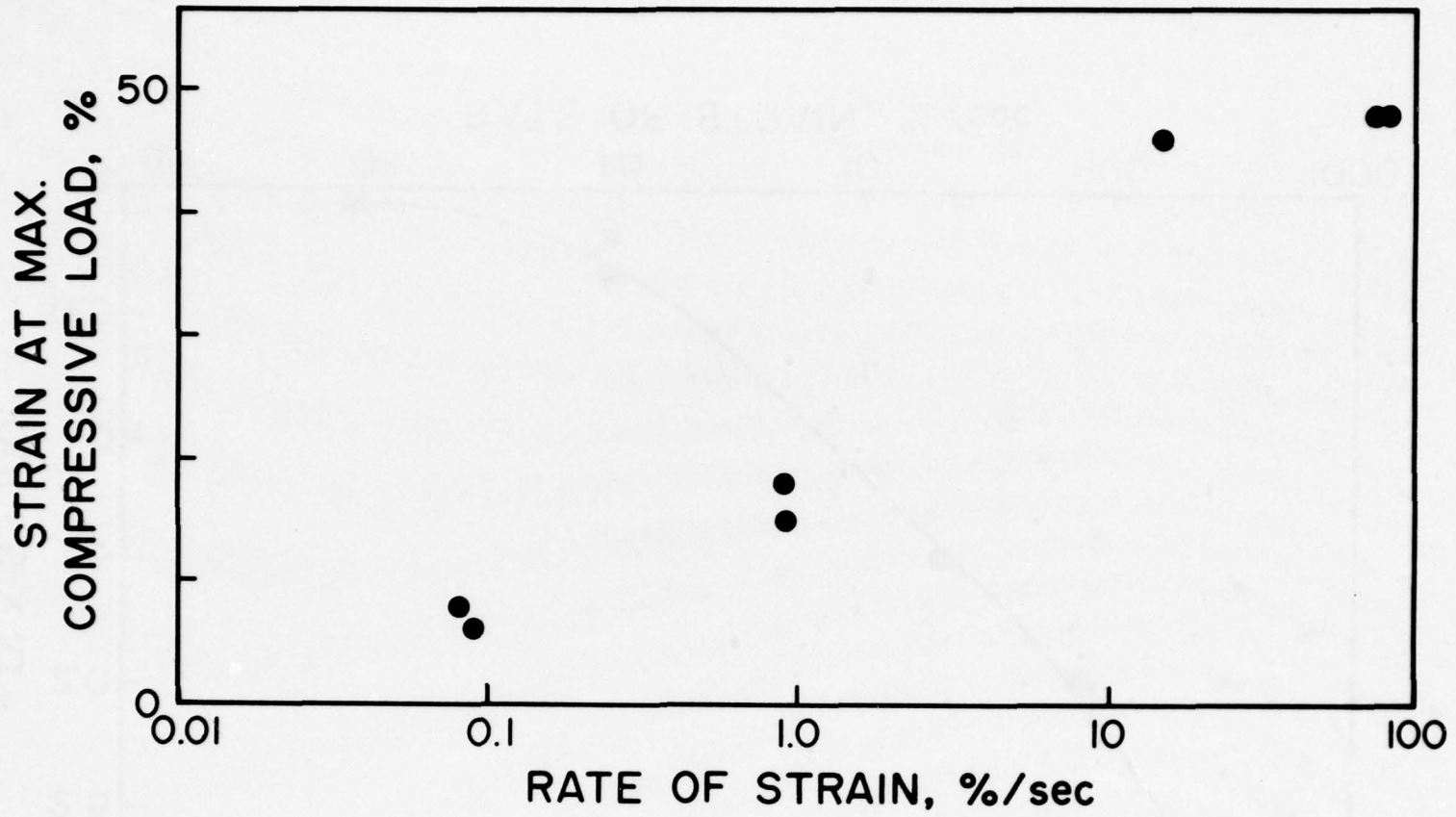

Figure H5. Percent strain at maximum compressive load vs. rate of strain.

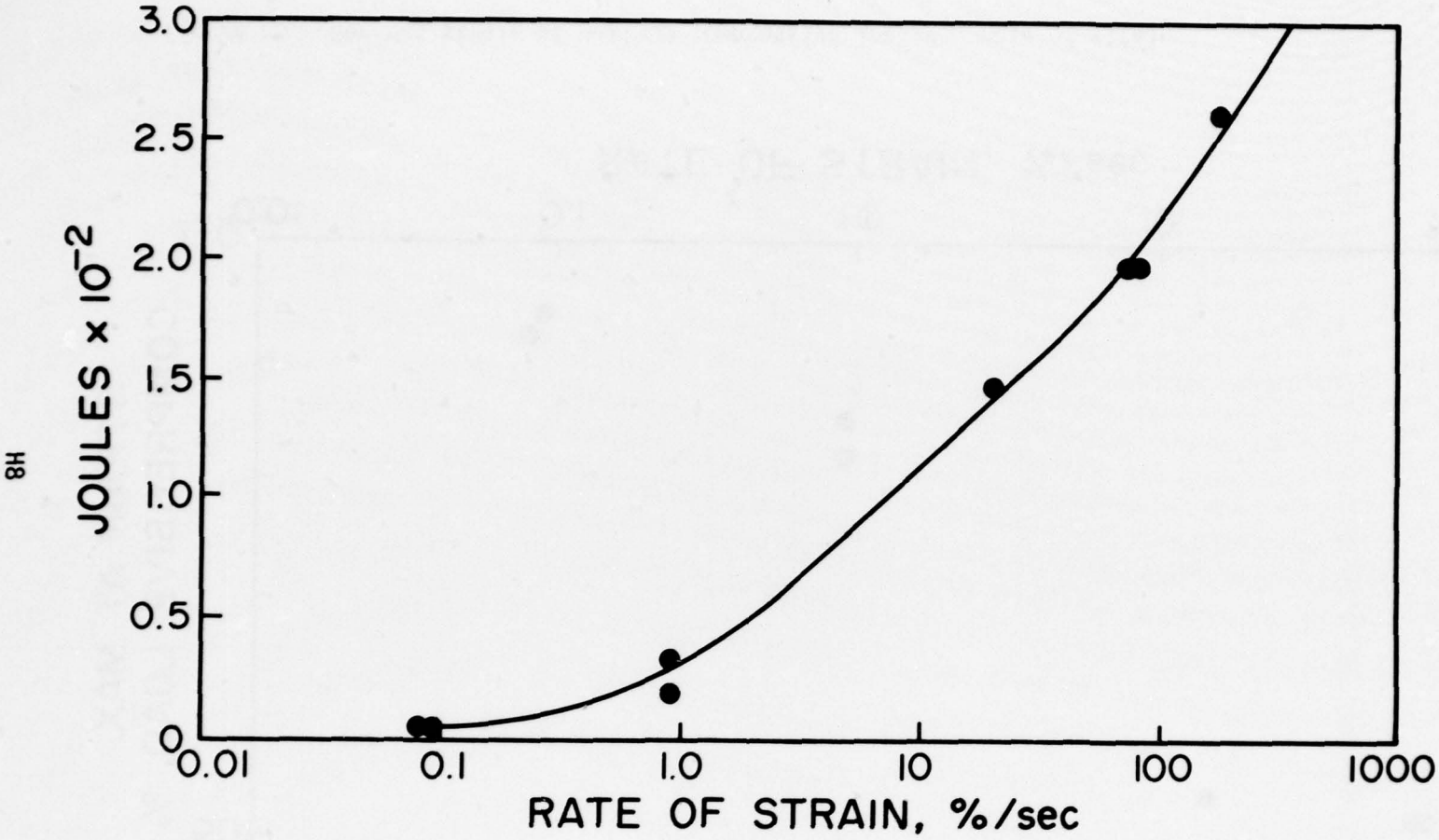

H8

Figure H6. Energy of deformation to maximum compressive stress vs. $\log_{10}$ strain rate.

pressure cell. A photograph of one sample is shown in Figure H7; failure of the bottom of the sample by liquifaction is evident. The impact force was displayed on an oscilloscope and photographed. The duration of impact was read from the oscilloscope record. It was found that the deformation rate was in all cases between $v_t/2$ and $v_t/4$. Once the deformation rate is known, the energy absorbed in plastic work before failure in impact can be computed. The results are shown in Figure 15 of the text.

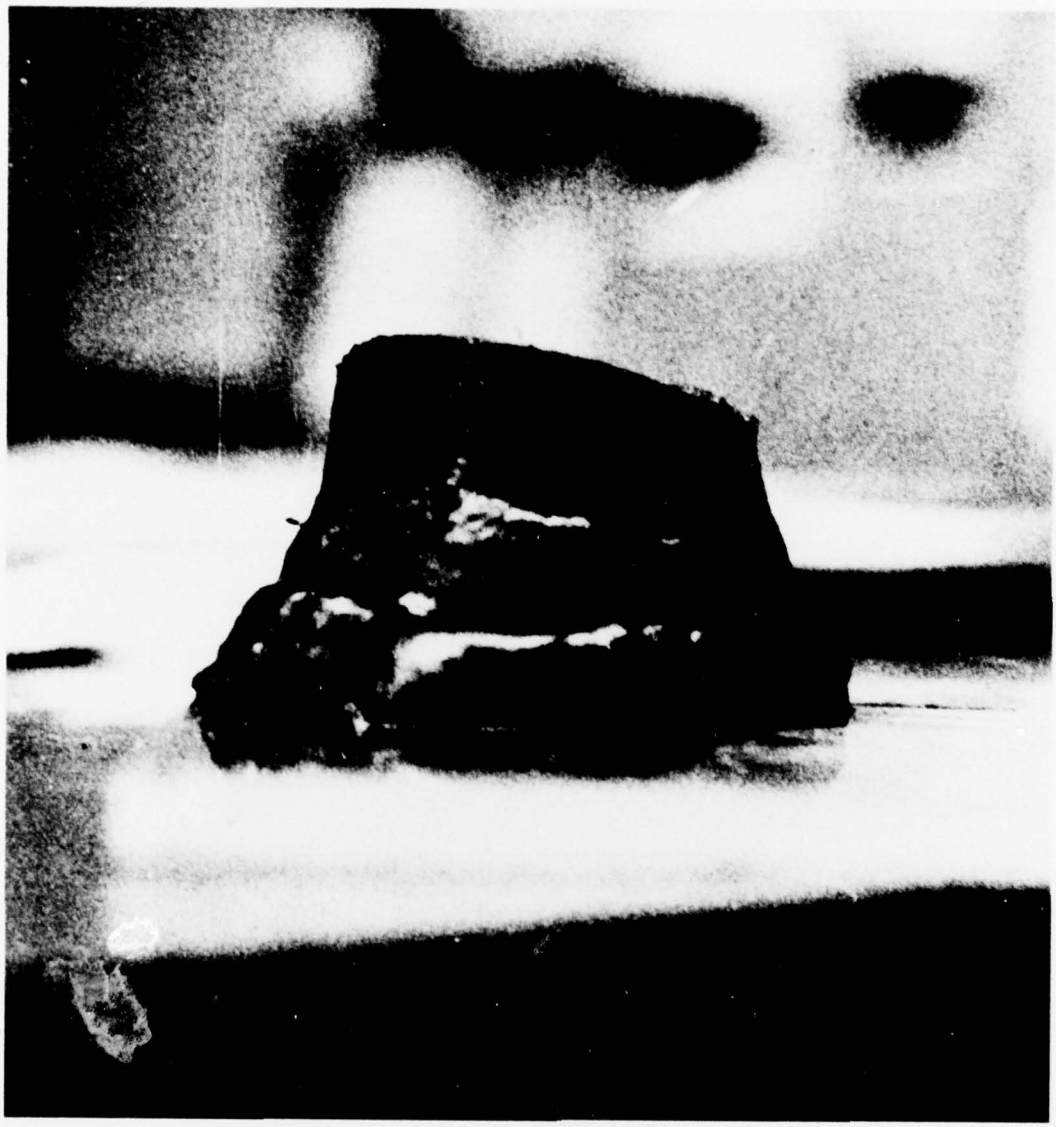

Figure H7. A sample of dredged material after impact on a WES soil pressure cell.

APPENDIX I: FIELD METHODS

1. During the course of this research certain field methods were found to be particularly efficacious and certain difficulties particularly common and troublesome. Some of these are enumerated here.

2. If useful data on the placement of dredged material are to be obtained in the field, it is essential to choose appropriate sensitivity, response time, and recording characteristics for the instruments used. The water speed and the concentrations of solids encountered in a placement operation range over several orders of magnitude. Instruments with high accuracy and precision but with a limited range of response are usually inappropriate. Precise calibration is often not of as much concern as reliability. If expensive, sophisticated instruments are chosen, it may not be possible to deploy them in adequate numbers to define the placement processes, which occur in three dimensions, in a considerable volume of water, and with large gradients of concentration velocities. A larger number of less expensive instruments may be a better use of available resources than deployment of a few, more expensive instruments.

3. It is most desirable to use instruments that record continuously or with a high sampling frequency. Since the placement processes are transient and of short duration, important aspects may be missed completely if the sampling frequency is low. This point is particularly important in taking water samples for subsequent analysis. Large, rapid variations in concentration within the bottom surge are revealed by continuously recording instruments; individual water samples can be quite misleading unless a continuous record of transmittance or some other parameter related to solids concentration is recorded simultaneously. Because the placement processes proceed very rapidly, accurate timing of all records and samples is of the utmost importance. Particular care is required to establish the time of release of dredged material from the hoppers of the transporting vessel.

4. Large lateral gradients of concentration and velocity occur in the disposal area. Consequently, high accuracy in the location of all instruments is required. Secure moorings are required for equipment placed on the bottom to prevent displacement during passage of the bottom surge. The exact position of the dredge or scow at the moment of discharge must be determined to good accuracy.

5. If it is desired to know the actual quantity of dredged material released, the volume and density of the material in the hoppers before discharge must be measured. Alternatively, careful draft measurements before and after discharge can be used to calculate these quantities by the methods presented in this report. Corrections for the change in trim of the vessel in filled and empty condition may be required.

6. If more than one discharge operation is to be studied, precise navigational control over the positioning of the vessel carrying the dredged material is required. In two of the localities studied, movement of disposal site buoys occurred and was not detected by dredging contractors. This vitiated the results of detailed disposal site surveys.

In accordance with letter from DAEN-RDC, DAEN-ASI dated 22 July 1977, Subject: Facsimile Catalog Cards for Laboratory Technical Publications, a facsimile catalog card in Library of Congress MARC format is reproduced below.

Bokuniewicz, Henry Joseph
Field study of the mechanics of the placement of dredged material at open-water disposal sites / by Henry J. Bokuniewicz ... [et al.], Department of Geology and Geophysics, Yale University, New Haven, Connecticut. Vicksburg, Miss. : U. S. Waterways Experiment Station ; Springfield, Va. : available from National Technical Information Service, 1978.
2 v. : ill. ; 27 cm. (Technical report - U. S. Army Engineer Waterways Experiment Station ; D-78-7)
Prepared for Office, Chief of Engineers, U. S. Army, Washington, D. C., under Contract No. DACW-39-76-C-0105-Mod. P001 (DMRP Work Unit No. 1B09)
References: v. 1, p. 93-94.
Contents: v. 1. Main text and Appendices A-I.-v. 2. Appendices J-O.
1. Dredged material. 2. Dredged material disposal. 3. Dredging. 4. Waste disposal sites. I. United States. Army. Corps of Engineers. II. Yale University. Dept. of Geology and Geophysics. III. Series: United States. Waterways Experiment Station, Vicksburg, Miss. Technical report ; D-78-7.
TA7.W34 no.D-78-7